12

Office of Naval Research

Contract N00014-75-C-0848 NR-372-012

ELECTRICALLY SMALL LOOP ANTENNA LOADED BY A HOMOGENEOUS AND ISOTROPIC FERRITE CYLINDER-PART II

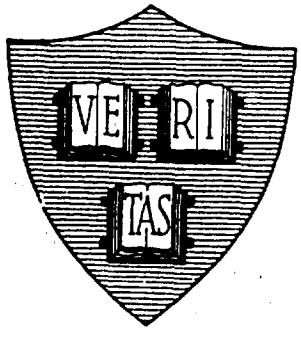

By

D.V. Giri and R.W.P. King

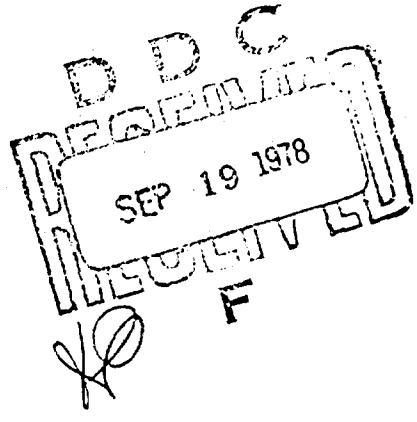

July 1978

Technical Report No. 668

Division of Applied Sciences

Harvard University Cambridge, Massachusetts

Unclassified

SECURITY CLASSIFICATION OF THIS PAGE (When Data Entered)

REPORT DOCUMENTATION PAGE

READ INSTRUCTIONS BEFORE COMPLETING FORM

1. REPORT NUMBER: Technical Report No. 668 ✓ (14)
2. GOVT ACCESSION NO.: TR-668
3. RECIPIENT'S CATALOG NUMBER:

4. TITLE (and Subtitle): (6) ELECTRICALLY SMALL LOOP ANTENNA LOADED BY A HOMOGENEOUS AND ISOTROPIC FERRITE CYLINDER, PART II,
5. TYPE OF REPORT & PERIOD COVERED: (9) Interim Report
6. PERFORMING ORG. REPORT NUMBER:

7. AUTHOR(s): (10) D. V. Giri [redacted] R. W. P. King
8. CONTRACT OR GRANT NUMBER(s): (15) N00014-75-C-0648, N00014-67-A-0298-0008

9. PERFORMING ORGANIZATION NAME AND ADDRESS:
Division of Applied Sciences
Harvard University
Cambridge, Massachusetts

10. PROGRAM ELEMENT, PROJECT, TASK AREA & WORK UNIT NUMBERS: (12) 124p.

11. CONTROLLING OFFICE NAME AND ADDRESS: (11)

12. REPORT DATE: July [redacted]978
13. NUMBER OF PAGES: 125

14. MONITORING AGENCY NAME & ADDRESS (if different from Controlling Office):

15. SECURITY CLASS. (of this report): Unclassified
15a. DECLASSIFICATION/DOWNGRADING SCHEDULE:

16. DISTRIBUTION STATEMENT (of this Report)

This document has been approved for public release and sale; its distribution is unlimited. Reproduction in whole or in part is permitted by the U.S. Government.

17. DISTRIBUTION STATEMENT (of the abstract entered in Block 20, if different from Report)

18. SUPPLEMENTARY NOTES

19. KEY WORDS (Continue on reverse side if necessary and identify by block number)

magnetic current on finite ferrite-rod antenna
approximate 3-term solution
numerical solution of coupled integral equations
experimental verification

20. ABSTRACT (Continue on reverse side if necessary and identify by block number)

Two theoretical approaches are developed to determine the magnetic current distribution on a ferrite cylinder of finite length that is center-driven by an electrically small loop antenna carrying a constant current. The first method makes use of the analogy between the ferrite rod antenna and the conducting cylindrical dipole antenna to derive an integral equation for the magnetic current on an infinitely permeable ($\mu_r = \infty$) ferrite antenna that corresponds to the integral equation for the electric current on a perfectly conducting electric di-

(Continued)

DD FORM 1 JAN 73 1473 EDITION OF 1 NOV 65 IS OBSOLETE

Unclassified

SECURITY CLASSIFICATION OF THIS PAGE (When Data Entered)

20. Abstract (Continued)

pole antenna. In the limit $h \to \infty$, this integral equation is shown to agree with that obtained previously in Part I for the infinite ferrite rod antenna. Continuing to parallel the treatment of the electric dipole antenna, the integral equation is modified by the introduction of an internal impedance per unit length of the magnetic conductor to account for values of μ_r that are large but not infinite, and finally an approximate, three-term expression is derived for the current on an 'imperfectly conducting' magnetic conductor. The second, more rigorous theoretical approach obtains two coupled integral equations in terms of the tangential electric field and the tangential electric surface current from independent treatments of the interior (ferrite) and exterior (free space) problems. The coupled equations are then solved numerically by means of the moment method. Finally the results of the two theories are compared with experimental measurements made on eleven different antenna configurations. The agreement is good.

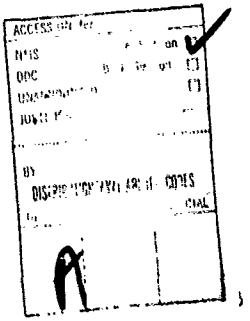

Office of Naval Research

N00014-75-C-0648 NR-372-012

ELECTRICALLY SMALL LOOP ANTENNA LOADED BY A HOMOGENEOUS AND ISOTROPIC FERRITE CYLINDER - PART II

By

D. V. Giri and R. W. P. King

Technical Report No. 668

July 1978

The research reported in this document was made possible through support extended the Division of Engineering and Applied Physics, Harvard University by the U.S. Army Research Office, the U.S. Air Force Office of Scientific Research, and the U.S. Office of Naval Research under the Joint Services Electronics Program by Contracts N00014-67-A-0298-0005 and N00014-75-C-0648.

Division of Applied Sciences

Harvard University • Cambridge, Massachusetts

TABLE OF CONTENTS

ELECTRICALLY SMALL LOOP ANTENNA LOADED BY A HOMOGENEOUS AND ISOTROPIC FERRITE CYLINDER - PART II

By

D. V. Giri and R. W. P. King

Division of Applied Sciences
Harvard University, Cambridge, Massachusetts 02138

ABSTRACT

The problem of a finite, ferrite-rod antenna has been treated theoretically by recognizing an analogy between the ferrite antenna and the conducting cylindrical dipole antenna which has been studied extensively. Initially the ferrite is idealized to be a perfect magnetic conductor and an Hallén type of integral equation [1] is obtained for the magnetic current. By allowing the antenna height to approach infinity, the formulation is shown to be consistent with previously obtained results for the infinitely long ferrite antenna [2]. Subsequently, the integral equation is modified appropriately to treat the ferrite as an imperfect magnetic conductor, and the current is obtained in the three-term form of King and Wu [3]. Because this treatment relies rather heavily on a mathematical equivalence of the two problems under idealized driving conditions, an alternative, more rigorous formulation is presented. The result is a pair of coupled integral equations in the tangential electric field (or magnetic current) and the circumferential electric current. The coupled integral equations are solved numerically. An experimental apparatus was fabricated to verify the solutions. Good agreement is obtained for a range of parameters. The experiments were performed for three values of $\Omega = 2 \ln(2h/a) = 8.5534$, 7.4754 and 6.089. The electrical radius ak_0 ranged from .00132 to .01662.

1. INTRODUCTION

In an earlier report on this subject [2] the magnetic current on a ferrite-rod antenna was derived explicitly in the form of an inverse Fourier integral. The driving loop loaded by an infinitely long, homogeneous and isotropic ferrite rod was assumed to be electrically small so that it carried an essentially constant current I_0^e. When the ferrite rod is assumed to be of infinite length, the magnetic current is equal to a definite integral which is suitable for numerical evaluation. Two values of electrical radii, viz., $ak_0 = 0.05$ and 0.1, were considered and for one of the cases the magnetic current was plotted [2] for several values of the permeability of the ferrite rod ranging from 10 to 200. The total magnetic current can be interpreted in terms of a sum of transmission and radiation currents. If μ_r and ϵ_r of the ferrite rod are assumed to be real, the transmission current can be associated with an unattenuated, rotationally symmetric TE surface wave. It was further found that the cutoff condition for this wave is that the electrical radius ak_1 be greater than 2.405.

In a practical situation, however, the antenna is of necessity finite and electrically short as well, so that a new mathematical formulation along with an experimental investigation is needed for the problem of a finite ferrite-rod antenna. Sections 2 through 8 present the two different theoretical approaches used to determine the magnetic current distribution on the finite ferrite antenna; Section 9 describes the experimental apparatus and results.

2. PROBLEM OF A FINITE FERRITE-ROD ANTENNA

The present formulation is based on the analogy between the cylindrical dipole antenna and the ferrite-rod antenna. The dipole antenna is made up of a wire, rod or tube of high electrical conductivity and may be driven by a

two-wire line. Equivalently, a monopole antenna fed by a coaxial line corresponds to a dipole antenna through its image in a ground plane. In either configuration, the driving source is represented by an idealized voltage or electric field generator which mathematically takes the form of a delta function. Similarly, the ferrite rod antenna is fabricated from a material of high magnetic permeability and is driven by an electrically small loop antenna carrying a constant current. The loop is, correspondingly, represented by an idealized current or magnetic field generator and takes the form of a delta function. These similarities suggest approaching the problem of the ferrite antenna by treating the ferrite rod as a good magnetic conductor. Initially, however, the ferrite is idealized to be a perfect magnetic conductor ($\mu_r = \infty$) and, later, appropriate changes are made to account for the finiteness of the value of the permeability of the ferrite material.

3. FERRITE AS A PERFECT MAGNETIC CONDUCTOR

The analogy between the ferrite antenna and the dipole antenna is based on the dual property of electric and magnetic field vectors in Maxwell's equations

$$\begin{aligned} \nabla \times \vec{E} &= -\vec{B} \\ \nabla \times \vec{H} &= \vec{J} + \vec{D} \\ \nabla \cdot \vec{B} &= 0 \\ \nabla \cdot \vec{D} &= \rho \end{aligned} \tag{1}$$

Figure 1(a) shows an electrically small loop antenna of diameter 2a. The loop carries a constant current and is assumed to be made up of a wire of infinitesimally small radius. The wire loop is loaded by a ferrite cylinder of height 2h. The ferrite is assumed to have an infinite permeability, in which

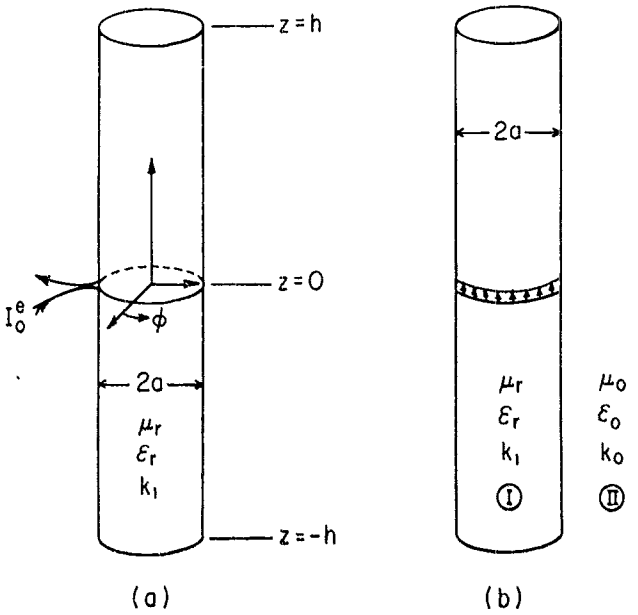

FIG. 1 (a) ELECTRICALLY SMALL LOOP ANTENNA OF DIAMETER '2a' LOADED BY A FERRITE CYLINDER OF HALF HEIGHT 'h' AND SURROUNDED BY FREE SPACE.

(b) MATHEMATICALLY EQUIVALENT BUT PHYSICALLY UNAVAILABLE MODEL FOR THE ANTENNA SHOWING THE IDEALIZED CURRENT GENERATOR $\hat{\phi}\, I_0^e\, \delta(\rho-a)\, \delta(z)$.

case the value of its dielectric constant ϵ_r is immaterial in view of the nature of the driving source. Figure 1(b) shows the mathematical model of the antenna. Region I is the ferrite with parameters μ_r, ϵ_r, k_1 and region II is free space with constitutive parameters μ_0, ϵ_0 and wave number k_0. Because of the nature of the driving source and azimuthal symmetry, the non-zero components of the fields are H_z, H_ρ and E_ϕ. A time dependence of the form $\exp(-i\omega t)$ is assumed. Because of the assumption $\mu_r = \infty$, H_z and H_ρ vanish in region I. The ferrite is also assumed to be homogeneous and isotropic. Thus the idealized driving source is taken into account by setting

$$H_z = -I_0^e \delta(z) \qquad \text{(for } \rho = a \text{ and } |z| \leq h\text{)} \tag{2}$$

Since both regions I and II have vanishing electrical conductivity and there is no free charge, Maxwell's equations reduce to

$$\nabla \times \vec{E} = -\vec{B} \tag{3a}$$

$$\nabla \times \vec{H} = \vec{D} \tag{3b}$$

$$\nabla \cdot \vec{B} = 0 \tag{3c}$$

$$\nabla \cdot \vec{D} = 0 \tag{3d}$$

It is required to solve (3a-d) for the fields subject to the condition (2) which states that the tangential component of $\vec{H}$ is discontinuous by the true electric surface current at $\rho = a$ and for $|z| \leq h$. In order to obtain an integral equation for the magnetic current on the antenna, an electric vector potential $\vec{A}^e$ and a magnetic scalar potential ϕ^* are defined and used.

$$\vec{D} = -\nabla \times \vec{A}^e \tag{4}$$

The definition of $\vec{A}^e$ is incomplete unless its divergence is also specified. Using (4) in (3b) gives $\nabla \times (\vec{H} + \vec{A}^e) = 0$, from which the scalar magnetic

potential is defined by setting

$$\vec{H} + \vec{A}^e = -\nabla\phi^* \tag{5}$$

In terms of the potentials, the fields are now given by

$$\vec{E} = (-1/\varepsilon)\nabla \times \vec{A}^e \tag{6a}$$

$$\vec{H} = -\nabla\phi^* - \dot{\vec{A}}^e \tag{6b}$$

Substitution of (6a,b) into Maxwell's equations (3c) and (3a) gives

$$\nabla^2\phi^* + \nabla \cdot \dot{\vec{A}}^e = 0 \tag{7a}$$

$$\nabla^2\vec{A}^e - \mu\varepsilon\ddot{\vec{A}}^e = \nabla[\nabla \cdot \vec{A}^e + \mu\varepsilon\dot{\phi}^*] \tag{7b}$$

Equation (7) is a set of coupled equations for the potentials which may be decoupled by defining the dual Lorentz gauge

$$\nabla \cdot \vec{A}^e + \mu\varepsilon\dot{\phi}^* = 0 \tag{8}$$

Upon using (8), (7) becomes

$$\nabla^2\phi^* - \mu\varepsilon\ddot{\phi}^* = 0 \tag{9a}$$

$$\nabla^2\vec{A}^e - \mu\varepsilon\ddot{\vec{A}}^e = 0 \tag{9b}$$

If (9) is solved for the potentials, subject to suitable boundary conditions, then the electromagnetic field is known everywhere by making use of (6). However, for the problem at hand, a $\hat{z}$-component of electric vector potential is adequate for a complete solution so that $\vec{A}^e = \hat{z}A_z^e$. On the surface ($\rho = a$, $|z| \leq h$) of the antenna, (6b) then becomes

$$H_z = -I_0^e\delta(z) = -(\partial\phi^*/\partial z) + i\omega A_z^e \tag{10}$$

Using (8), one can rewrite (10) as

$$\left(\frac{d^2A_z^e}{dz^2} + k_0^2 A_z^e\right) = i(k_0/v_0)I_0^e\delta(z) \tag{11}$$

where k_0 is the free space wave number and v_0 the velocity of light in free space. This equation is identical to that for the z-component of the magnetic vector potential in the case of the dipole antenna [1, eq.(3.2.4)] and, therefore, has a complete solution - like [1, eq.(3.2.12)] - which is given by

$$A_z^e(z) = (i/v_0)[C \cos k_0 z + (I_0^e/2)\sin k_0|z|] \tag{12}$$

Equation (12) is an expression for the z-component of electric vector potential in terms of the driving current I_0^e. However, the general formula for $\vec{A}^e(\vec{r})$ due to an arbitrary distribution of magnetic surface current $\vec{K}^*(\vec{r})$ can be written as

$$\vec{A}^e(\vec{r}) = (\epsilon_0/4\pi)\int_{S_i} \vec{K}^*(\vec{r}')(e^{ik_0R}/R)\, dS_i'$$

In general, $\vec{K}^*(\vec{r}) = \vec{K}^*(\vec{r}) + \hat{n} \times \vec{P}(\vec{r})$, but because of the nature of the driving source $\vec{P}(\vec{r}) = 0$, so that $\vec{K}^*(\vec{r}) = \vec{K}^*(\vec{r}) = (\hat{n} \times \vec{E})$ = magnetic surface current. Since rotational symmetry obtains, the total axial magnetic current can be introduced with thin antenna approximation so that $I_z^*(z) = 2\pi a K_z^*(\vec{r})$

$$A_z^e(z) = A_z^e(\vec{r}) = (\epsilon_0/4\pi)\int_{-h}^{h} I_z^*(z')\, dz' \int_{-\pi}^{\pi} (e^{ik_0R_s}/R_s)\, d\theta'/2\pi$$

where

$$R_s = [(z - z')^2 + (2a \sin \theta'/2)^2]^{1/2}$$

Letting

$$K_s(z,z') = \int_{-\pi}^{\pi} (e^{ik_0R_s}/R_s)\, d\theta'/2\pi$$

gives

$$A_z^e(z) = (\epsilon_0/4\pi)\int_{-h}^{h} I_z^*(z')K_s(z,z')\, dz' \tag{13}$$

$A_z^e(z)$ was previously obtained in (12). Equations (12) and (13) together lead to the required integral equation,

$$\int_{-h}^{h} I_z^*(z')K_s(z,z')\,dz' = i4\pi\zeta_0[C\cos k_0 z + (I_0^e/2)\sin k_0|z|] \qquad (14)$$

with $\zeta_0 = (\mu_0/\varepsilon_0)^{1/2}$ = the free space characteristic impedance.

The integral equation (14) for the magnetic current on a finite, infinitely permeable, ferrite rod antenna can be identified formally with the similar integral equation [1, eq.(3.2.23)] for the electric current on a finite dipole antenna made up of a perfect metallic conductor. Comparing the integral equations for the two cases, one finds that the driving voltage V_0^e and the free space characteristic impedance ζ_0 in the electric dipole case are replaced by the driving current I_0^e and the free space characteristic admittance $(1/\zeta_0)$ in the magnetic case. Commonly used metals like copper and brass are found to have sufficiently large electrical conductivities to justify the assumption of vanishing electric field inside the material of the dipole antenna so that an integral equation of the form (14) is adequate and has been used to obtain the electric current distributions. Furthermore, if more accuracy is required, theories do exist for imperfectly conducting cylindrical transmitting antennas. However, it is questionable whether the integral equation (14) is directly applicable to the practical ferrite rod antenna due to the relative permeability ranges of available ferrites. Whereas the treatment of the imperfectly conducting dipole antenna is done for reasons of improved accuracy, a similar treatment (μ_r large but not infinite) for the ferrite antenna appears to be a necessity. This forms the subject of Section 5.

4. MAGNETIC CURRENT ON AN INFINITE ANTENNA

The magnetic current $I_z^*(z)$ obtained by solving the integral equation (14) may be called a zeroth-order solution because of the assumption $\mu_r = \infty$. The integral equation (14) is for a finite antenna from which the zeroth-order solution $I_\infty^*(z)$ for an antenna of infinite length may be obtained. For the sake of convenience, the integral equation is rewritten as

$$\int_{-h}^{h} I_z^*(z')K_s(|z - z'|)\, dz' = (4\pi/\zeta_0)A_z^e(z) = i4\pi\zeta_0[C \cos k_0 z + \frac{I_0^e}{2} \sin k_0|z|]$$

As $h \to \infty$, the vector potential $A_z^e(z)$ is a traveling wave which may be obtained by setting $C = I_0^e/2i$. In this case,

$$\int_{-\infty}^{\infty} I_\infty^*(z')K_s(|z - z'|)\, dz' = 2\pi\zeta_0 I_0^e e^{ik_0|z|} \tag{15}$$

Taking Fourier transforms of both sides of (15), one obtains

$$\int_{-\infty}^{\infty} e^{-i\xi z}\, dz \int_{-\infty}^{\infty} I_\infty^*(z')K_s(|z - z'|)\, dz' = 2\pi\zeta_0 I_0^e \int_{-\infty}^{\infty} e^{-i\xi z} e^{ik_0|z|}\, dz$$

The left side of the above equation is a convolution integral and on the right side, the integration may be performed to obtain

$$\bar{K}(\xi)\bar{I}_\infty^*(\xi) = 2\pi\zeta_0 I_0^e[2ik_0/(k_0^2 - \xi^2)]$$

With $\gamma_0^2 = k_0^2 - \xi^2$

$$\bar{I}_\infty^*(\xi) = 4i\pi\zeta_0 I_0^e k_0/\gamma_0^2\bar{K}(\xi) \tag{16}$$

By recalling

$$K_s(|z - z'|) = \int_{-\pi}^{\pi} (e^{ik_0 R_s}/R_s)\, d\theta'/2\pi$$

with $R_s = [(z - z')^2 + (2a \sin \theta'/2)^2]^{1/2}$, it can be shown [3] that the Fourier transform $\bar{K}(\xi)$ of the kernel $K_s(z,z')$ is given by

$$\bar{K}(\xi) = \int_{-\infty}^{\infty} e^{-i\xi z} K_s(z)\, dz = i\pi J_0(a\gamma_0)H_0^{(1)}(a\gamma_0) \tag{17}$$

Using (17) in (16), one obtains

$$\bar{I}_\infty^*(\xi) = 4\zeta_0 I_0^e k_0/\gamma_0^2 J_0(a\gamma_0)H_0^{(1)}(a\gamma_0)$$

The inverse Fourier transform may now be taken.

$$I_\infty^*(z) = \frac{1}{2\pi}\int_{-\infty}^{\infty} \bar{I}_\infty^*(\xi)e^{i\xi z}\, d\xi$$

$$I_\infty^*(z) = \frac{2}{\pi} I_0^e \zeta_0 k_0 \int_{-\infty}^{\infty} \frac{e^{i\xi z}\, d\xi}{\gamma_0 J_0(a\gamma_0)H_0^{(1)}(a\gamma_0)} \quad \text{volts} \tag{18}$$

Equation (18) is thus an explicit expression in the form of an infinite integral for the current on an infinitely long, infinitely permeable, ferrite rod antenna.

The problem of infinitely long ferrite rod antennas was formulated previously [2] in terms of differential equations and the Fourier transform of this current was obtained, from [2, eq.(23)], to be

$$\bar{I}_\infty^*(\xi) = \frac{-i\omega a(\mu_r - 1)I_0^e \mu_0 2\pi a H_1^{(1)}(a\gamma_0)J_1(a\gamma_1)}{a[\gamma_1 J_0(a\gamma_1)H_1^{(1)}(a\gamma_0) - \gamma_0 \mu_r J_1(a\gamma_1)H_0^{(1)}(a\gamma_0)]} \tag{19}$$

where $\gamma_1^2 = k_1^2 - \xi^2$ and $\gamma_0^2 = k_0^2 - \xi^2$, ξ is the Fourier transform variable, and k_1 and k_0 are the wave numbers in the ferrite and the surrounding free space medium, respectively. The zeroth-order current on the infinite antenna may be obtained from (19) by taking the limit $\mu_r \to \infty$.

First, (19) may be rewritten as

$$\bar{I}_\infty^*(\xi) = (-i\omega a I_0^e \mu_0 2\pi)\left[\frac{\gamma_1 J_0(a\gamma_1)}{(\mu_r - 1)J_1(a\gamma_1)} - \frac{\gamma_0 \mu_r H_0^{(1)}(a\gamma_0)}{(\mu_r - 1)H_1^{(1)}(a\gamma_0)}\right]^{-1}$$

As $\mu_r \to \infty$, the ratio $[J_0(a\gamma_1)/J_1(a\gamma_1)]$ is finite so that the first term within the brackets approaches zero. In this case

$$\bar{I}^*_\infty(\xi) = \frac{4\zeta_0 I_0^e k_0}{\gamma_0^2 J_0(a\gamma_0) H_0^{(1)}(a\gamma_0)} \left[a\gamma_0 \frac{\pi i}{2} H_1^{(1)}(a\gamma_0) J_0(a\gamma_0)\right]$$

Furthermore, for a thin antenna, a small argument approximation may be used for the Bessel functions in the numerator so that $\bar{I}^*_\infty(\xi)$ reduces to

$$\bar{I}^*_\infty(\xi) = \frac{4\zeta_0 I_0^e k_0}{\gamma_0^2 J_0(a\gamma_0) H_0^{(1)}(a\gamma_0)}$$

from which

$$I^*_\infty(z) = \frac{2}{\pi} I_0^e \zeta_0 k_0 \int_{-\infty}^{\infty} \frac{e^{i\xi z}\, d\xi}{\gamma_0^2 J_0(a\gamma_0) H_0^{(1)}(a\gamma_0)} \quad \text{volts} \tag{20}$$

Thus, equations (20) and (18) are both independently derived explicit expressions for the zeroth-order ($\mu_r = \infty$) magnetic currents on an infinitely long ferrite rod antenna. In the limit of infinite permeability the two formulations give the same result. This limit is, however, physically unrealizable since a magnetic material with $\mu_r = \infty$ does not exist and, hence, a modification of the formulation which treats the ferrite as an imperfect magnetic conductor is required. This modification has, once again, an analogue in the electric case in the treatment of the imperfectly conducting cylindrical transmitting antenna [3], [4].

5. FERRITE AS AN IMPERFECT MAGNETIC CONDUCTOR

In order to account for the fact that the relative permeability is large but not infinite, the concept of 'internal impedance' is useful and suffi-

cient. With reference to Fig. 2, the internal impedance per unit length of a cylindrical magnetic conductor of circular cross section of radius a with its axis along the z-axis of a system of cylindrical coordinates (ρ,ϕ,z) may be defined by

$$z_m^i = (r_m^i - ix_m^i) = H_z(\rho = a)/I_z^* \tag{21}$$

where $H_z(\rho = a)$ is the tangential magnetic field at the surface, $\rho = a$, of the conductor and I_z^* is the total axial magnetic current. Recalling the expressions of electric and magnetic fields in terms of the potentials

$$\vec{H} = -\nabla\phi^* - \vec{A}^e \tag{22a}$$

$$\vec{D} = -\nabla \times \vec{A}^e \tag{22b}$$

$$\nabla \cdot \vec{A}^e + \mu\varepsilon\dot{\phi}^* = 0 \tag{22c}$$

the electric vector potential satisfies

$$(\nabla^2 + k^2)\vec{A}^e = 0 \tag{23}$$

where k is replaced by k_1 and k_0 for the two regions I and II shown in Fig. 2. For the problem of a thin cylindrical conductor, the axial component of electric potential is sufficient to satisfy Maxwell's equations and the relevant boundary conditions. Thus, the electromagnetic fields everywhere can be obtained by setting $\vec{A}^e = \hat{z}A_z^e$. With the vector potential being entirely axial and also because of azimuthal symmetry, (23) becomes

$$\left[\frac{\partial^2}{\partial z^2} + \frac{1}{\rho}\frac{\partial}{\partial\rho}\left(\rho\frac{\partial}{\partial\rho}\right) + k^2\right]A_z^e(\rho,z) = 0 \tag{24}$$

A product solution to (24) is sought in the following form:

$$A_z^e(\rho,z) = f_z(z)R_z(\rho) \tag{25}$$

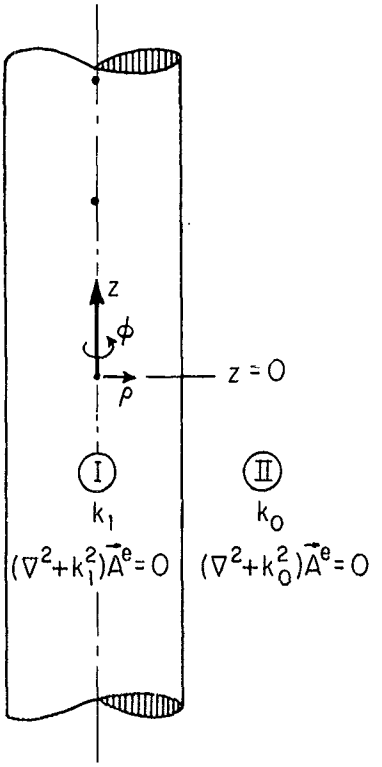

FIG. 2 A CYLINDRICAL MAGNETIC CONDUCTOR CARRYING A TOTAL AXIAL MAGNETIC CURRENT OF I_z^* AND IMMERSED IN FREE SPACE.

Substitution of (25) into (24) leads to

$$R_z \frac{d^2 f_z}{dz^2} + f_z \frac{1}{\rho} \frac{d}{d\rho} \left(\rho \frac{dR_z}{d\rho}\right) + k^2 f_z R_z = 0 \tag{26}$$

Equation (26) may be rewritten as

$$\frac{1}{f_z} \frac{d^2 f_z}{dz^2} + k^2 = -\frac{1}{R_z} \frac{1}{\rho} \frac{d}{d\rho} \left(\rho \frac{dR_z}{d\rho}\right) \tag{27}$$

The left side of (27) is a function of z alone, while the right side is a function of ρ alone. Hence, they can be equal to each other for all possible values of ρ and z only if they are both equal to a constant (say ζ^2) which may, however, be multivalued. Therefore,

$$\frac{d^2 f_z}{dz^2} + (k^2 - \zeta^2) f_z = 0 \quad \text{and} \quad \frac{1}{\rho} \frac{d}{d\rho} \left(\rho \frac{dR_z}{d\rho}\right) + \zeta^2 R_z = 0$$

After solving the foregoing differential equations for f_z and R_z, the axial vector potential in the two regions can be written down as

$$A^e_{z1}(\rho, z) = C_1 J_0(\zeta_1 \rho) \exp(i\sqrt{k_1^2 - \zeta_1^2}\, z) \qquad \text{in region I}$$

$$A^e_{z2}(\rho, z) = C_2 H_0^{(1)}(\zeta_0 \rho) \exp(i\sqrt{k_0^2 - \zeta_0^2}\, z) \qquad \text{in region II}$$

Boundary conditions that are useful in determining the unknown constants in the solution require the continuity of tangential $\vec{E}$ and $\vec{H}$ across the surface $\rho = a$; that is

$$E_{\phi 1}\Big|(\rho = a) = E_{\phi 2}\Big|(\rho = a)$$

$$\nu_1 B_{z1}\Big|(\rho = a) = \nu_2 B_{z2}\Big|(\rho = a)$$

In terms of the vector potential, the boundary conditions at the surface $\rho = a$ are

$$\frac{1}{\varepsilon_1}\frac{\partial A^e_{z1}}{\partial \rho} = \frac{1}{\varepsilon_0}\frac{\partial A^e_{z2}}{\partial \rho}$$

$$\frac{i\omega}{\mu_1}\frac{\zeta_1^2}{k_1^2}A^e_{z1} = \frac{i\omega}{\mu_0}\frac{\zeta_0^2}{k_0^2}A^e_{z2}$$

Application of the boundary conditions yields

$$\frac{1}{\varepsilon_1}C_1\zeta_1 J_0'(\zeta_1 a)\exp(i\sqrt{k_1^2-\zeta_1^2}\,z) = \frac{1}{\varepsilon_0}C_2\zeta_0 H_0^{(1)\prime}(\zeta_0 a)\exp(i\sqrt{k_0^2-\zeta_0^2}\,z) \qquad (28)$$

$$\frac{i\omega}{\mu_1}\frac{\zeta_1^2}{k_1^2}C_1 J_0(\zeta_1 a)\exp(i\sqrt{k_1^2-\zeta_1^2}\,z) = \frac{i\omega}{\mu_0}\frac{\zeta_0^2}{k_0^2}C_2 H_0^{(1)}(\zeta_0 a)\exp(i\sqrt{k_0^2-\zeta_0^2}\,z) \qquad (29)$$

Since (28) and (29) are valid for all values of z at all times, it follows that

$$\sqrt{k_1^2-\zeta_1^2} = \sqrt{k_0^2-\zeta_0^2} = q \text{ (say)} \qquad (30)$$

so that $\zeta_1 = \sqrt{k_1^2-q^2}$ and $\zeta_0 = \sqrt{k_0^2-q^2}$. Dividing (29) by (28) and rearranging, one obtains

$$\zeta_0 a\frac{H_0^{(1)}(\zeta_0 a)}{H_0^{(1)\prime}(\zeta_0 a)} = \frac{\varepsilon_1\mu_0}{\varepsilon_0\mu_1}\frac{k_0^2}{k_1^2}\zeta_1 a\frac{J_0(\zeta_1 a)}{J_0'(\zeta_1 a)} \qquad (31)$$

Although, in general, an explicit solution is not possible, equations (30) and (31) are theoretically sufficient to determine the unknowns ζ_1 and ζ_0. The two unknowns will be determined here by two methods.

Method 1:

An approximate solution is possible by allowing k_1 to become very large. Since q is finite, $\zeta_1 \to k_1$ and, therefore, ζ_1 is also large. Using this on the right side of (31) gives

$$i \frac{\varepsilon_1 \mu_0}{\varepsilon_0 \mu_1} \frac{k_0^2}{k_1^2} \zeta_1 a \to 0$$

Therefore,

$$\zeta_0 a \frac{H_0^{(1)}(\zeta_0 a)}{H_0^{(1)\prime}(\zeta_0 a)} \simeq 0 \tag{32}$$

Equation (32) is satisfied by $\zeta_0 = 0$ since it can be shown that the ratio $H_0^{(1)}(\zeta_0 a)/H_0^{(1)\prime}(\zeta_0 a)$ remains finite as ζ_0 approaches the value of zero. It then follows from (30) that

$$\zeta_1 = \sqrt{k_1^2 - k_0^2} = k_1 \sqrt{1 - (1/\mu_r \varepsilon_r)} \simeq k_1$$

Thus the solutions are $\zeta_1 \simeq k_1$ and $\zeta_0 \simeq 0$.

Method 2:

Method 1 may seem to be an oversimplification and, hence, a slightly more rigorous method may be needed in some cases. It is observed that (31) may be identified with a similar equation obtained by Sommerfeld [5] in the problem on 'waves on wires.' Sommerfeld has developed an iterative form of solution which may be used here.

In the limit of large ζ_1, the right side of (31) becomes

$$i \frac{\varepsilon_1 \mu_0}{\varepsilon_0 \mu_1} \frac{k_0^2}{k_1^2} \zeta_1 a = i \frac{\varepsilon_r}{\mu_r} \frac{k_0^2}{k_1^2} a \sqrt{k_1^2 - q^2} \simeq i \frac{\varepsilon_r}{\mu_r} \frac{k_0^2}{k_1} a = i \frac{a k_0}{\mu_r} \sqrt{\varepsilon_r / \mu_r}$$

and is small. Since the left side of (31) also has to be small, we have

$$(\zeta_0 a)^2 \ln(\gamma \zeta_0 a/2i) = -\frac{2}{\gamma^2} u \ln u \quad \text{with} \quad u = (\gamma \zeta_0 a/2i)^2$$

where $\gamma = 1.781$.

Equation (31) finally becomes

$$u \ln u = v \quad \text{with} \quad v = -\frac{i\gamma^2}{2}\frac{ak_0}{\mu_r}\sqrt{\epsilon_r/\mu_r}$$

Since $\ln u$ varies slowly in comparison with u, it is possible to write

$$u_{n+1} \ln u_n = v$$

where u_n is the n^{th} approximation to u. The method is best illustrated by an example. In the later part of this report, eleven different antenna configurations were used in the experimental determination of the magnetic current. The example chosen here (antenna #1) corresponds to the lowest value of the $|\mu_r\epsilon_r|$ product for the eleven cases.

Example: $ak_0 = 0.00166$, $\mu_r = (18 + i.036)$, $\epsilon_r = 11.0$.

$$\text{Let } u_0 = v = -\frac{i\gamma^2}{2}\frac{ak_0}{\mu_r}\sqrt{\epsilon_r/\mu_r} \simeq -i(1.1 \times 10^{-4})$$

This gives

$$u_1 = \frac{v}{\ln u_0} = \frac{-i1.1 \times 10^{-4}}{(-9.115 + i4.712)} = -10^{-4}(.049 - i.095)$$

$$u_2 = \frac{v}{\ln u_1} = \frac{-i1.1 \times 10^{-4}}{(-11.445 + i2.047)} = -10^{-4}(.0167 - i.0931)$$

Continuing the iteration

$$u_3 = \frac{v}{\ln u_2} = \frac{-i1.1 \times 10^{-4}}{(-11.5684 + i1.7478)} = -10^{-4}(.0140 - i.0930)$$

$$u_4 = \frac{v}{\ln u_3} = \frac{-i1.1 \times 10^{-4}}{(-11.5748 + i1.7208)} = -10^{-4}(.0138 - i.0930)$$

and finally

$$u_5 = \frac{v}{\ln u_4} = \frac{-i1.1 \times 10^{-4}}{(-11.5748 + i1.7184)} = -10^{-4}(.0138 - i.0930)$$

It is seen that this iterative procedure is rapidly converging and using the above value of u,

$$(\zeta_0 a)^2 = -\frac{4}{\gamma^2} u^2 = 10^{-10}(1.062 + i.3225)$$

Furthermore, from (30)

$$(aq)^2 = (ak_0)^2 - (a\zeta_0)^2$$

$$= 2.7556 \times 10^{-6} - 10^{-10}(1.062 + i.3225)$$

from which $a\zeta_1$ may be calculated using

$$(a\zeta_1)^2 = (ak_1)^2 - (aq)^2 = (ak_1)^2 - (ak_0)^2 + (a\zeta_0)^2$$

$$= ak_1^2\left[1 - \frac{1}{\mu_r \epsilon_r} + \left(\frac{a\zeta_0}{ak_1}\right)^2\right]$$

$$= ak_1^2[1 - (.0056 - i.00001) + 10^{-7}(2.159 + i.651)]$$

From the calculated values of $(a\zeta_0)^2$ and $(a\zeta_1)^2$, it is seen that the approximate solutions, i.e., $\zeta_0 = 0$ and $\zeta_1 \simeq k_1$, are quite satisfactory even when $|\mu_r \epsilon_r|$ is as low as 180.

Therefore, the vector potential in the interior of the conductor is given by

$$A_{z1}^e(\rho,z) = A_{z1}^e(\rho)A_{z1}^e(z) = C_1 J_0(k_1\rho)\exp(i\sqrt{k_1^2 - \zeta_1^2}\, z)$$

where ζ_1 in the argument of the Bessel function is replaced by k_1 in view of the calculations of "Method 2." The constant C_1 can be written in terms of the potential on the surface so that

$$A_{z1}^e(\rho) = A_{z1}^e(a)J_0(k_1\rho)/J_0(k_1 a)$$

Since H_z is proportional to A_z,

$$H_{z1}(\rho) = H_{z1}(a)J_0(k_1\rho)/J_0(k_1a)$$

The magnetization is then given by

$$\dot{M}_z(\rho) = (\mu_r - 1)\dot{H}_{z1}(\rho) = (\mu_r - 1)\dot{H}_{z1}(a)J_0(k_1\rho)/J_0(k_1a)$$

from which the magnetic current can be obtained as

$$I_z^*(\rho) = 2\pi \int_0^\rho \mu_0 \dot{M}_z(\rho')\rho' \, d\rho'$$

$$= 2\pi\mu_0(\mu_r - 1) \frac{\dot{H}_{z1}(a)}{J_0(k_1a)} \int_0^\rho J_0(k_1\rho') \, \rho' \, d\rho'$$

Performing the integration gives

$$I_z^*(\rho) = \frac{2\pi\mu_0(\mu_r - 1)\dot{H}_{z1}(a)}{J_0(k_1a)} \frac{\rho}{k_1} J_1(k_1\rho) \tag{33}$$

The total magnetic current carried by the conductor is, however, given by

$$I_z^*(a) = 2\pi \int_0^a \mu_0 \dot{M}_z(\rho) \, \rho \, d\rho$$

which becomes

$$I_z^*(a) = \frac{2\pi\mu_0(\mu_r - 1)\dot{H}_{z1}(a)}{J_0(k_1a)} \frac{a}{k_1} J_1(k_1a) \tag{34}$$

From (33) and (34) the radial distribution of the magnetic current in the interior of the conductor is given by

$$I_z^*(\rho) = I_z^*(a) \frac{\rho}{a} \frac{J_1(k_1\rho)}{J_1(k_1a)} \tag{35}$$

Furthermore, having obtained the total axial magnetic current of (34), the

internal impedance per unit length defined in (21) can be written as

$$z_m^i = r_m^i - ix_m^i = H_{z1}(\rho = a)/I_z^*(a)$$

$$= \left[\frac{i}{2\omega} \frac{1}{\mu_0 \chi^m} \frac{1}{\pi a^2} k_1 a \frac{J_0(k_1 a)}{J_1(k_1 a)} \right] \Omega/m \qquad (36)$$

where $\chi^m = (\mu_r - 1)$ = magnetic susceptibility;

ω = radian frequency;

$\mu_0 = 4\pi \times 10^{-7}$ h/m = permeability of free space;

πa^2 = cross-sectional area of the conductor;

$k_1 = \beta_1 + i\alpha_1 = k_0(\beta_{1N} + i\alpha_{1N})$ = wave number in the material of the conductor.

With $\mu_r = (\mu_r' + i\mu_r'') = |\mu_r| e^{i\theta_\mu}$ and $\epsilon_r = (\epsilon_r' + i\epsilon_r'') = |\epsilon_r| e^{i\theta_\epsilon}$,

$$k_1 = k_0 |\mu_r \epsilon_r|^{1/2} \exp[i(\theta_\mu + \theta_\epsilon)/2]$$

so that

$$\beta_1 = k_0 |\mu_r \epsilon_r|^{1/2} \cos[(\theta_\mu + \theta_\epsilon)/2] \qquad (37a)$$

and

$$\alpha_1 = k_0 |\mu_r \epsilon_r|^{1/2} \sin[(\theta_\mu + \theta_\epsilon)/2] \qquad (37b)$$

One may now use the internal impedance per unit length of a magnetic conductor carrying an axial magnetic current to find an integral equation for the magnetic current on a finite ferrite rod antenna. The axial component $A_z^e(z)$ on the surface of a cylindrical antenna that has an internal impedance per unit length z_m^i, carries an axial current $I_z^*(z)$, and is driven at $z = 0$ by a delta-function generator with an mmf of I_0^e, satisfies the following differential equation:

$$\left(\frac{d^2}{dz^2} + k_0^2\right) A_z^e(z) = -\frac{ik_0^2}{\omega}\left[z_m^i I_z^*(z) - I_0^e \delta(z)\right] \tag{38}$$

If the antenna were made of a perfect magnetic conductor, $z_m^i = 0$ because $\chi^m =$ infinity so that (38) will reduce to (11). If the radius a of the antenna and the free-space wave number $k_0 = \omega/v_0 = 2\pi/\lambda_0$ satisfy the inequality

$$ak_0 << 1$$

then the vector potential is given approximately by

$$A_z^e(z) \simeq \frac{\varepsilon_0}{4\pi} \int_{-h}^{h} I_z^*(z') K(z,z')\, dz' \tag{39}$$

If the equations (38) and (39) are formally identified with those for the imperfectly conducting, electric dipole antenna [3, eqs. (7) and (9)], it is observed that μ_0 and I_0^e play the roles of ε_0 and V_0^e. King and Wu [3] have developed a three-term solution for the electric current on the imperfectly conducting dipole antenna which can be well applied to the present problem of the ferrite as an imperfect magnetic conductor. The procedure used to obtain the three-term solution will be described here briefly; for a detailed analysis the reader is referred to [3].

The approximate kernel in (39) may be separated into real and imaginary parts,

$$K(z,z') = K_R(z,z') - iK_I(z,z') = e^{ik_0 r}/r$$

so that

$$K_R(z,z') = \frac{\cos k_0 r}{r} \qquad , \qquad K_I(z,z') = -\frac{\sin k_0 r}{r}$$

with $r = [(z - z')^2 + a^2]^{1/2}$. The vector potential may also be divided into two parts,

$$A_z^e(z) = A_R^e(z) - iA_I^e(z)$$

where

$$A_R^e(z) = \frac{k_0 \epsilon_0}{4\pi} \int_{-h}^{h} I_z^*(z') \frac{\cos k_0 r}{k_0 r} dz' \tag{40}$$

$$A_I^e(z) = -\frac{k_0 \epsilon_0}{4\pi} \int_{-h}^{h} I_z^*(z') \frac{\sin k_0 r}{k_0 r} dz' \tag{41}$$

The properties of the two integrals are quite different. The kernel in (40) has a sharp peak at $k_0|z - z'| = 0$ and thus greatly magnifies the contribution to the integral due to current elements near $z = z'$. The current vanishes at the end but the vector potential $A_R^e(h)$ has a small finite value so that the difference in vector potential should vary closely like $I_z^*(z)$. Therefore,

$$(4\pi/\epsilon_0)[A_R^e(z) - A_R^e(h)] = \Psi(z) I_z^*(z) \doteq \Psi I_z^*(z) \tag{42}$$

where Ψ is the approximately constant value of $\Psi(z)$ defined at a suitable reference value of z. However, in the second integral in (41) the rather flat behavior of $(\sin k_0 r)/k_0 r$ with $k_0 r$ allows the following approximation:

$$\frac{\sin k_0 r}{k_0 r} = \frac{2 \sin \frac{k_0 r}{2} \cos \frac{k_0 r}{2}}{k_0 r} \doteq \cos \frac{k_0 r}{2}$$

which is useful over a range $k_0 r \leq \pi$. This approximation leads to

$$A_I^e(z) = A_I^e(0) \cos \frac{k_0 z}{2} \tag{43}$$

where $A_I^e(0)$ is a constant given by

$$A_I^e(0) = \frac{k_0 \epsilon_0}{4\pi} \int_{-h}^{h} I_z^*(z') \cos \frac{k_0 z'}{2} dz' \tag{44}$$

If equation (42), rearranged in the form $I_z^*(z) = (4\pi/\Psi\epsilon_0)[A_R^e(z) - A_R^e(h)]$, is substituted in the differential equation (38), one obtains:

$$\left(\frac{d^2}{dz^2} + k_0^2\right)\,[A_z^e(z) - A_z^e(h)] = -\,i4\pi\zeta_0 k_0 z_m^{i\psi-1}[A_R^e(z) - A_R^e(h)] - k_0^2 A_z^e(h) + \frac{i}{\omega}\,k_0^2 I_0^e \delta(z) \tag{45}$$

A complex constant k may now be defined by

$$k^2 = (\beta + i\alpha)^2 = k_0^2\left(1 + \frac{i4\pi z_m^{i\psi}\zeta_0}{k_0^{\psi}}\right) \tag{46}$$

Using (43) and (46), (45) becomes

$$\left(\frac{d^2}{dz^2} + k^2\right)\,[A_z^e(z) - A_z^e(h)] = -i(k^2 - k_0^2)A_I^e(z) - [k_0^2 A_R^e(h) - ik^2 A_I^e(h)] + \frac{i}{\omega}\,k_0^2 I_0^e \delta(z)$$

$$= -i(k^2 - k_0^2)A_I^e(0)\,\cos\frac{k_0 z}{2} - [k_0^2 A_R^e(h) - ik^2 A_I^e(h)] + \frac{i}{\omega}\,k_0^2 I_0^e \delta(z) \tag{47}$$

The integral equation of (39) may now be written in the form

$$[A_z^e(z) - A_z^e(h)] = \frac{\epsilon_0}{4\pi}\int_{-h}^{h} I_z^*(z')K_d(z,z')\,dz' \tag{48}$$

where the difference kernel K_d is given by

$$K_d(z,z') = K(z,z') - K(h,z') = \frac{e^{ik_0 r}}{r} - \frac{e^{ik_0 r_h}}{r_h}$$

with $r = [(z - z')^2 + a^2]^{1/2}$ and $r_h = [(h - z')^2 + a^2]^{1/2}$. If the differential equation (47) is solved for the vector potential difference and the solution is substituted for the left-hand side of (48), an integral equation for the magnetic current on the ferrite antenna is obtained, viz.,

$$\int_{-h}^{h} I_z^*(z')K_d(z,z')\,dz' = \frac{-i4\pi k_0\zeta_0}{k\cos kh}\,[(1/2)I_0^e M_{kz} + U_k' F_{kz} - D\cos kh\,F_{0z}'] \tag{49}$$

where for ease of reference, the same notation as in King and Wu [3] is employed and the various factors on the right side are given by

$$M_{kz} = \sin k(h - |z|)$$

$$U_k' = U_k + D \cos \frac{k_0 h}{2}$$

$$U_k = (i\omega k/k_0^2)[(k_0^2/k^2)A_R^e(h) - iA_I^e(h)]$$

$$D = -\frac{\omega k}{k_0^2}\left[\frac{k^2 - k_0^2}{k^2 - k_0^2/4}\right] A_I^e(0)$$

$$F_{kz} = \cos kz - \cos kh$$

$$F_{0z}' = \cos \frac{k_0 z}{2} - \cos \frac{k_0 h}{2}$$

Following the procedure as in [3], an approximate formal solution to the integral equation may be written in the form

$$I_z^*(z) = I_V^* M_{kz} + I_U^* F_{kz} + I_D^* F_{0z}' \tag{50}$$

where the coefficients I_V^*, I_U^* and I_D^* are obtained by a numerical procedure.

Letting $T_U^* = I_U^*/I_V^*$, $T_D^* = I_D^*/I_V^*$ and evaluating I_V^*, one may write (50) as

$$I_z^*(z) = \frac{-i2\pi k_0 \zeta_0 I_0^e}{k \Psi_{dR} \cos kh}\left[\sin k(h - |z|) + T_U^*(\cos kz - \cos kh) + T_D^*(\cos \frac{k_0 z}{2} - \cos \frac{k_0 h}{2})\right] \tag{51}$$

where k is redefined by

$$k^2 = (\beta + i\alpha)^2 = k_0^2\left(1 + \frac{i4\pi z_m^i \zeta_0}{k_0 \Psi_{dR}}\right) \tag{52}$$

and Ψ_{dR} is given by the integral expression

$$\int_{-h}^{h} \sin k(h - |z'|) K_{dR}(z,z')\, dz' = \sin k(h - |z|)\Psi_{dR} \tag{53}$$

Thus, equation (51) is the required expression for the total magnetic current on the antenna from which the admittance can be obtained to be

$$Y = G - iB = I_z^*(0)/I_0^e \quad \text{ohms}$$

$$= \frac{-i2\pi k_0 \zeta_0}{k\Psi_{dR} \cos kh} [\sin kh + T_U^*(1 - \cos kh) + T_D^*(1 - \cos \frac{k_0 h}{2})] \qquad (54)$$

Note that, because of an earlier approximation of the imaginary part of the kernel, equations (51) and (54) are valid representations for the magnetic current and admittance only when $k_0 h \leq 5\pi/4$.

The existing computer programs for the imperfectly conducting dipole antenna due to King, Harrison and Aronson [4] have been modified for use on the IBM 370/155 computer system of the Joint Harvard/M.I.T. Ratch Processing Center. Appendix B includes a listing of the Fortran IV programs that compute the magnetic current distribution and the admittance of the finite ferrite-rod antenna when the ferrite is treated as an imperfect magnetic conductor.

6. THE LIMITATIONS OF THE THEORETICAL FORMULATION

The present formulation is based on an analogy between the ferrite-rod antenna and the conducting cylindrical dipole antenna. Because of the symmetry in Maxwell's equations, a set of scalar magnetic (ϕ^*) and electric vector ($\vec{A}^e$) potentials was defined and used in formulating the finite ferrite-rod antenna problem. It is considered useful to determine the existence of these potentials for the infinite antenna and thus provide some justification for their use in the finite antenna problem.

The electromagnetic fields in both regions for the case of the infinitely long antenna were determined previously [2] to be:

Region I, $0 \leq \rho \leq a$:

$$\bar{E}_{\phi 1}(\rho,\xi) = i\omega\mu_1 a I_0^e H_1^{(1)}(\gamma_0 a) J_1(\gamma_1 \rho)/D(\xi)$$

$$\bar{H}_{z1}(\rho,\xi) = \frac{1}{i\omega\mu_1}\left[\partial\bar{E}_{\phi 1}(\rho,\xi)/\partial\rho + \bar{E}_{\phi 1}(\rho,\xi)/\rho\right] = aI_0^e\gamma_1 H_1^{(1)}(\gamma_0 a)J_0(\gamma_1\rho)/D(\xi)$$

$$\bar{H}_{\rho 1}(\rho,\xi) = (\xi/\omega\mu_1)\bar{E}_{\phi 1}(\rho,\xi) = iaI_0^e\xi H_1^{(1)}(\gamma_0 a)J_1(\gamma_1\rho)/D(\xi)$$

$$\bar{H}_{\phi 1}(\rho,\xi) = \bar{E}_{\rho 1}(\rho,\xi) = \bar{E}_{z1}(\rho,\xi) = 0 \tag{55}$$

Region II, $\rho \geq a$:

$$\bar{E}_{\phi 2}(\rho,\xi) = i\omega\mu_1 aI_0^e J_1(\gamma_1 a)H_1^{(1)}(\gamma_0\rho)/D(\xi)$$

$$\bar{H}_{z2}(\rho,\xi) = aI_0^e\gamma_0\mu_r J_1(\gamma_1 a)H_0^{(1)}(\gamma_0\rho)/D(\xi)$$

$$\bar{H}_{\rho 2}(\rho,\xi) = iaI_0^e\mu_r\xi J_1(\gamma_1 a)H_1^{(1)}(\gamma_0\rho)/D(\xi)$$

$$\bar{H}_{\phi 2}(\rho,\xi) = \bar{E}_{\rho 2}(\rho,\xi) = \bar{E}_{z2}(\rho,\xi) = 0 \tag{56}$$

where

$$D(\xi) = a[\gamma_1 J_0(\gamma_1 a)H_1^{(1)}(\gamma_0 a) - \gamma_0\mu_r J_1(\gamma_1 a)H_0^{(1)}(\gamma_0 a)]$$

The actual field quantities may be obtained by applying the Fourier inverse formula to the above transformed fields. It can be verified easily that the above field quantities satisfy the following transformed boundary conditions:

i) Tangential $\vec{E}$: $\bar{E}_{\phi 2}(a^+,\xi) = \bar{E}_{\phi 1}(a^-,\xi)$ (57a)

ii) Tangential $\vec{H}$: $\bar{H}_{z2}(a^+,\xi) - \bar{H}_{z1}(a^-,\xi) = -I_0^e$ (57b)

iii) Normal $\vec{B}$: $\bar{B}_{\rho 2}(a^+,\xi) = \bar{B}_{\rho 1}(a^-,\xi)$ (57c)

iv) Normal $\vec{D}$: Zero in both regions

ϕ^* is a scalar magnetic potential and has a non-zero value in both regions. For the infinitely long antenna, the only non-zero component of $\vec{A}^e$ is

the z-component so that $\vec{A}^e = \hat{z}A_z^e$. The potentials may be derived either from the already known electromagnetic fields or from an independent solution of the following wave equations with suitable boundary conditions:

$$(\nabla^2 + k^2)\vec{A}^e(\rho,z) = 0 \quad , \quad (\nabla^2 + k^2)\phi^*(\rho,z) = 0$$

The equations reduce to

Region I, $0 \leq \rho \leq a$:

$$\left[\frac{\partial^2}{\partial z^2} + \frac{1}{\rho}\frac{\partial}{\partial \rho}\rho\frac{\partial}{\partial \rho} + k_1^2\right] A_{z1}^e(\rho,z) = 0$$

Region II, $\rho \geq a$:

$$\left[\frac{\partial^2}{\partial z^2} + \frac{1}{\rho}\frac{\partial}{\partial \rho}\rho\frac{\partial}{\partial \rho} + k_0^2\right] A_{z2}^e(\rho,z) = 0$$

Using a Fourier transform pair, the above equations become

$$\left[\frac{\partial^2}{\partial \rho^2} + \frac{1}{\rho}\frac{\partial}{\partial \rho} + (k_1^2 - \xi^2)\right] \bar{A}_{z1}^e(\rho,\xi) = 0$$

$$\left[\frac{\partial^2}{\partial \rho^2} + \frac{1}{\rho}\frac{\partial}{\partial \rho} + (k_0^2 - \xi^2)\right] \bar{A}_{z2}^e(\rho,\xi) = 0$$

With a change of variable the above equations can be recognized as Bessel equations with the following solutions,

$$\bar{A}_{z1}^e(\rho,\xi) = PJ_0(\gamma_1\rho) \qquad \text{for } 0 \leq \rho \leq a$$

$$\bar{A}_{z2}^e(\rho,\xi) = QH_0^{(1)}(\gamma_0\rho) \qquad \text{for } \rho \geq a$$

where $\gamma_0 = (k_0^2 - \xi^2)^{1/2}$ and $\gamma_1 = (k_1^2 - \xi^2)^{1/2}$

The boundary conditions (57a,b), expressed in terms of the electric vector potential, become

$$(1/\varepsilon_1)\partial\bar{A}^e_{z1}(a^-,\xi)/\partial\rho = (1/\varepsilon_0)\partial\bar{A}^e_{z2}(a^+,\xi)/\partial\rho \tag{58a}$$

$$(i\omega\gamma_0^2/k_0^2)\bar{A}^e_{z2}(a^+,\xi) - (i\omega\gamma_1^2/k_1^2)\bar{A}^e_{z1}(a^-,\xi) = -I^e_0 \tag{58b}$$

By applying the boundary conditions and determining P and Q, the electric vector potential can be written as:

$$\begin{aligned}
\bar{A}^e_{z1}(\rho,\xi) &= -i\omega\mu_1\varepsilon_1 a I^e_0 H_1^{(1)}(\gamma_0 a) J_0(\gamma_1\rho)/\gamma_1 D(\xi) && \text{for } 0 \le \rho \le a \\
\bar{A}^e_{z2}(\rho,\xi) &= -i\omega\mu_1\varepsilon_0 a I^e_0 J_1(\gamma_1 a) H_0^{(1)}(\gamma_0\rho)/\gamma_0 D(\xi) && \text{for } \rho \ge a
\end{aligned} \tag{59}$$

Similarly, by solving the wave equation for the scalar magnetic potential ϕ^*, the solution can be obtained as:

$$\begin{aligned}
\bar{\phi}^*_1(\rho,\xi) &= ia\xi I^e_0 H_1^{(1)}(\gamma_0 a) J_0(\gamma_1\rho)/\gamma_1 D(\xi) && \text{for } 0 \le \rho \le a \\
\bar{\phi}^*_2(\rho,\xi) &= ia\xi I^e_0 \mu_r J_1(\gamma_1 a) H_0^{(1)}(\gamma_0\rho)/\gamma_0 D(\xi) && \text{for } \rho \ge a
\end{aligned} \tag{60}$$

The boundary conditions satisfied by $\bar{\phi}^*(\rho,\xi)$ at the surface $\rho = a$ are:

$$(\omega\mu_1/\xi)\partial\bar{\phi}^*_1(a^-,\xi)/\partial\rho = (\omega\mu_0/\xi)\partial\bar{\phi}^*_2(a^+,\xi)/\partial\rho \tag{61a}$$

$$\gamma_0^2\bar{\phi}^*_2(a^+,\xi) - \gamma_1^2\bar{\phi}^*_1(a^-,\xi) = -i\xi I^e_0 \tag{61b}$$

It can also be verified that the potentials satisfy the gauge condition,

$$\partial A^e_z(\rho,z)/\partial z - i\omega\mu\varepsilon\phi^*(\rho,z) = 0 \qquad \text{in both regions}$$

The potentials of (59) and (60) can also be obtained from the electromagnetic fields of (55) and (56) by making use of the following relationships in both regions:

$$E_\phi(\rho,z) = (1/\varepsilon)\partial A_z^e(\rho,z)/\partial z \quad ; \quad H_z(\rho,z) = -\partial\phi^*(\rho,z)/\partial z + i\omega A_z^e(\rho,z)$$

and

$$\partial A_z^e(\rho,z)/\partial z - i\omega\mu\varepsilon\phi^*(\rho,z) = 0$$

The above analysis verifies that when the antenna is infinitely long, both the scalar magnetic and electric vector potentials exist. They are both discontinuous across the antenna surface and satisfy respective wave equations, appropriate boundary conditions, and the gauge condition.

In the case of the finite antenna, however, a precise knowledge of the vector potential in the two regions is not necessary to derive an approximate integral equation for the magnetic current. What is required is the electric vector potential on the surface of the antenna. To determine this, an internal impedance per unit length is defined and used to obtain the three-term solution for the magnetic current. Using the computer programs described and listed in Appendix B, the magnetic current was evaluated for a range of parameters. The current distribution was studied as a function of the four independent parameters, viz., μ_r'; μ_r'' or $Q = \mu_r'/\mu_r''$; h/λ_0 or $k_0 h$; and ak_0 or $\Omega = 2\ln(2h/a)$. In this study the value of the dielectric constant of the ferrite was fixed at 10.

The ranges of the four parameters were as follows: $\mu_r' = 10, 100, 1000$; $Q = 1$ to $Q = 100$; $h/\lambda_0 = .1$ to $h/\lambda_0 = .5$; and $ak_0 = .001$ to $ak_0 = .1$. Typical results of the computations are shown plotted in Fig. 3. The quantities μ_r', ak_0, h/λ_0 and Q are varied, respectively, in Fig. 3a-d, while in each case the remaining three parameters are kept constant.

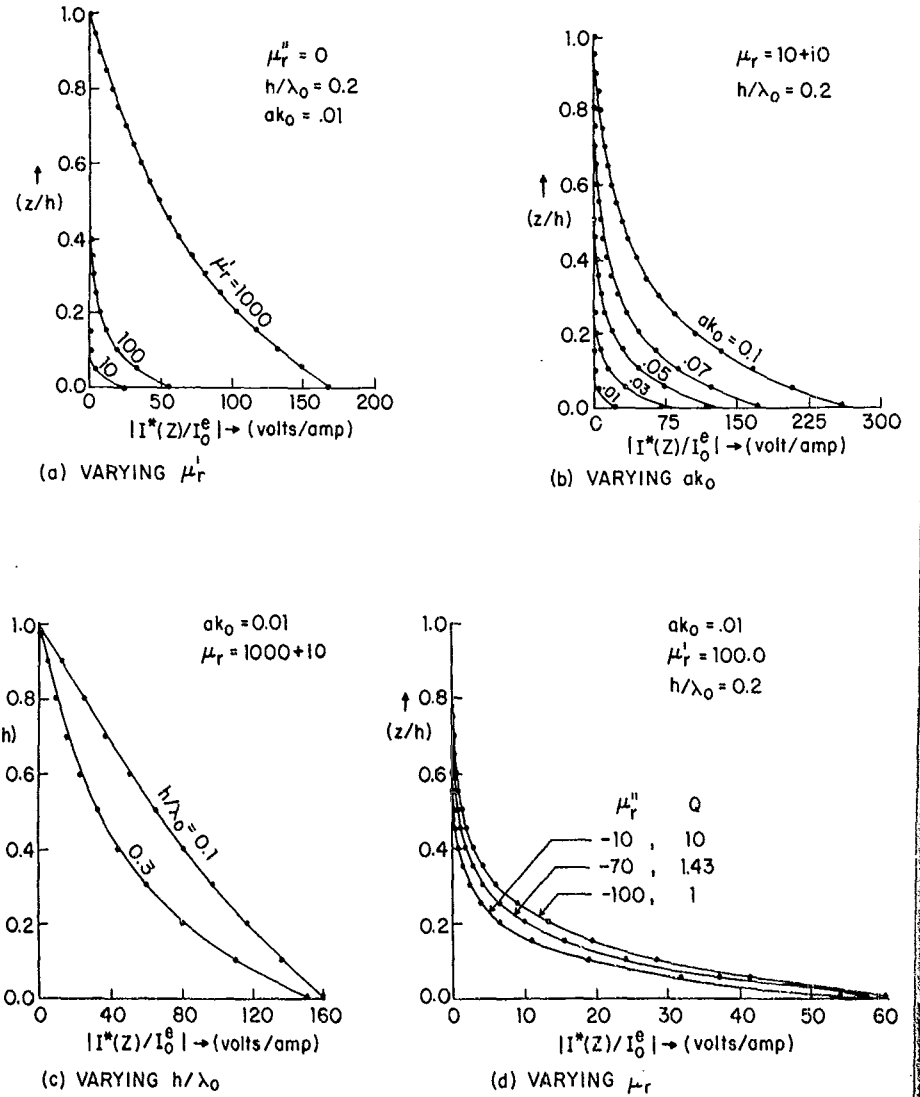

FIG. 3 PLOT OF THE MAGNITUDE OF NORMALIZED MAGNETIC CURRENT ($|I^*(Z)/I_0^e|$) AS A FUNCTION OF NORMALIZED DISTANCE (z/h) FOR VARIOUS PARAMETER RANGES. ($\varepsilon_r = 10+i0$ FOR ALL THE CASES)

In Fig. 3a for fixed height, radius, and ratio Q, the magnetic current on the antenna is seen to increase with the real part of the relative permeability. A similar behavior is observed in Fig. 3b for increasing antenna radius and fixed height, permeability and Q. A comparison between Fig. 3a and Fig. 3d shows that a large value of μ_r' produces a greater increase in the magnetic current than a high Q ratio; in fact, an increase in Q for $Q < 50$ is seen to reduce the magnitude of the magnetic current. To interpret Fig. 3c, it is useful to examine the behavior of the propagation constant k on the antenna, given by

$$k = \beta + i\alpha = k_0[1 + i(4\pi z_m^i \zeta_0/k_0 \Psi_{dR})]^{1/2}$$

If the dimensionless parameter $\Phi_i = (4\pi z_m^i \zeta_0/k_0)$ is introduced, this expression becomes

$$k = \beta + i\alpha = k_0(1 + i\Phi_i/\Psi_{dR})^{1/2}$$

Despite the fact that Ψ_{dR} is itself a function of k, an efficient iterative method can be used to determine the value of the propagation constant. By substituting for z_m^i from (36) the following expression for Φ_i is obtained:

$$\Phi_i = \frac{2iak_1}{(ak_0)^2 \chi_m} \frac{J_0(ak_1)}{J_1(ak_1)}$$

Φ_i becomes positive imaginary for the cases plotted in Fig. 3c where ak_1 is real. This makes the propagation constant k on the antenna pure imaginary which leads to an exponentially decreasing magnetic current. For most practical ferrites the positive imaginary part of Φ_i dominates, which makes the attenuation constant α significantly larger than the phase constant β. This can also be seen in the experimental results reported in Section 9.

At this stage it is considered useful to summarize all the approximations and assumptions involved in the derivation of the integral equation in (38) with (39). The ferrite was first treated as a perfect magnetic conductor (μ_r = infinity) and the integral equation in (14) was obtained. This expression was later modified by adding an intrinsic impedance per unit length for a practical ferrite that is an imperfect magnetic conductor and finite. The basic assumption that the radius be small, i.e., $ak_0 << 1$, was made. An implied approximation was introduced when the impedance per unit length z_m^i, derived originally for the infinitely long magnetic conductor, was used for the finite antenna. Its use can be justified as follows. For an infinitely long magnetic conductor, the transverse distribution of electric vector potential is independent of the axial distribution. It is reasonable to assume that this remains the case when the conductor length is large compared to the radius, so that the intrinsic impedance per unit length derived for the infinitely long conductor can be used directly for antennas of finite length. A further question arises concerning the discontinuity of the electric vector potential across the antenna surface. It has been established that the electric vector potential is discontinuous across the antenna surface when the antenna is infinitely long. It is reasonable to conclude that the discontinuity exists even when the length of the antenna is finite. The derivation of the integral equation for the magnetic current or the tangential electric field requires a knowledge of the electric vector potential on the surface $\rho = a$, which has apparently two values. This problem is not peculiar to the ferrite-rod antenna but also exists in the analogous resistive electric dipole antenna. In either case, the value of the vector potential used is that obtained by approaching the antenna surface from the surrounding medium. It is believed, however, that the discontinuity in the vector potential is a

consequence of the way in which the vector potential was defined and can be overcome with the introduction of a suitable scale factor in the definition.

The approach of treating the ferrite as an imperfect magnetic conductor relies on the mathematical equivalence of the two analogous problems. One cannot escape the fact, however, that while there are two pieces of conductor separated by a slice voltage or electric field generator in the case of an electric dipole, the magnetic conductor in the ferrite problem is a single continuous rod driven on the outside surface. A delta function, although unphysical, is a mathematical convenience in either case.

In view of the above discussion, a more rigorous analysis which does not invoke the analogy with the electric dipole is developed and presented in the following section.

7. A MORE RIGOROUS TREATMENT OF THE FINITE ANTENNA

Since the total magnetic current $I_z^*(z)$ is linearly related to the tangential electric field $E_\phi(a,z)$ by the relation

$$I_z^*(z) = -2\pi a E_\phi(a,z) \quad ,$$

the following procedure seeks to derive an integral equation for $E_\phi(a,z)$ by solving the ferrite-interior and free space-exterior problems.

Interior Problem. The interior problem consists of a ferrite cylinder of height 2h driven at the center by a constant-current loop. The driving condition will be accounted for after the interior and exterior problems are solved. The diameter of the rod and of the loop is 2a and the restriction $ak_0 << 1$ is satisfied in order to maintain a constant current I_0^e in the driving loop. Given a cylindrical coordinate system (ρ,ϕ,z) and after eliminating $\vec{H}$ from Maxwell's curl equation and imposing azimuthal symmetry, one obtains

for the electric field

$$\left[\frac{\partial^2}{\partial\rho^2} + \frac{1}{\rho}\frac{\partial}{\partial\rho} + (k_1^2 - \frac{1}{\rho^2}) + \frac{\partial^2}{\partial z^2}\right] E_\phi(\rho,z) = 0 \tag{62}$$

with $k_1 = k_0(\mu_r\epsilon_r)^{1/2}$, $|z| \leq h$, $0 \leq \rho \leq a$, and $E_\phi(\rho,z) = E_\phi(\rho,-z)$.

Solving (62) by a separation-of-variables technique gives

$$E_\phi(\rho,z) = \sum_{n=-\infty}^{\infty} A_n \cos[(n + 1/2)\pi z/h] J_1\{\rho[k_1^2 - (n + 1/2)^2\pi^2/h^2]^{1/2}\} \tag{63}$$

with the coefficients A_n given by

$$A_n = \frac{1}{hJ_1\{a[(n+1/2)^2\pi^2/h^2]^{1/2}\}} \int_{-h}^{h} E_\phi(a,z') \cos[(n+1/2)\pi z'/h]\, dz'$$

This procedure aims to determine the tangential magnetic field $H_z(a,z)$ from independent treatments of both the interior and exterior problems and then to require that their difference equal $-I_0^e\delta(z)$, the true electric surface current. Thus, $H_z(a^-,z)$ can be obtained from the above by using

$$H_z(\rho,z) = (1/i\omega\mu_1)[\partial E_\phi(\rho,z)/\partial\rho + E_\phi(\rho,z)/\rho]$$

$$= (1/i\omega\mu_1 h)\left[\sum_{n=-\infty}^{\infty}\left(\int_{-h}^{h} dz'\, E_\phi(a,z') \cos[(n + 1/2)\pi z'/h]\right)\right.$$

$$\times \cos[(n + 1/2)\pi z/h]\, \frac{J_0\{\rho[k_1^2 - (n + 1/2)^2\pi^2/h^2]^{1/2}\}}{J_1\{a[k_1^2 - (n + 1/2)^2\pi^2/h^2]^{1/2}\}}$$

$$\left.\times [k_1^2 - (n + 1/2)^2\pi^2/h^2]^{1/2}\right] \tag{64}$$

It should be pointed out that, as a first approximation, $E_\phi(a,z)$ is made

to vanish on the top and bottom surfaces defined by $|z| = h$ and $0 \leq \rho \leq a$, thus neglecting all the fringing fields at the ends of the antenna. In practice, this condition nearly prevails for antennas with heights large compared to the radius ($h >> a$).

Exterior Problem. The exterior problem is concerned with the free space surrounding the ferrite rod which extends from ($0 \leq \rho \leq a$) and ($-h \leq z \leq h$) for all ϕ. It is equivalent to solving the problem with the ferrite removed but with the tangential electric field on the surface $E_\phi(a,z)$ for $|z| \leq h$ required to be the same as that used in the interior problem. With an assumed $e^{-i\omega t}$ time dependence, the governing equations are:

$$\nabla \times \vec{H} = -i\omega\varepsilon_0 \vec{E} \tag{65a}$$

$$\nabla \times \vec{E} = i\omega\mu_0 \vec{H} \tag{65b}$$

$$\nabla \cdot \vec{H} = 0 \tag{65c}$$

$$\nabla \cdot \vec{D} = 0 \tag{65d}$$

From (65d) in free space, one may define an electric vector potential

$$\vec{D} = -\nabla \times \vec{A}^e$$

so that

$$\vec{E} = -(1/\varepsilon_0)\nabla \times \vec{A}^e$$

This leads to

$$\vec{H} = -\nabla\phi^* + i\omega\vec{A}^e$$

The exterior problem may be modeled by a cylindrical surface of radius a

that extends from z = -h to z = h. This surface, when immersed in free space, has the following boundary conditions valid for $|z| \leq h$:

$$E_\phi(a^+,z) = f^+(z) = E_\phi(a,z) \tag{66a}$$

$$E_\phi(a^-,z) = f^-(z) = 0 \tag{66b}$$

Substituting for $\vec{E}$ and $\vec{H}$ in (65b), one obtains

$$-\nabla \times \nabla \times \vec{A}^e + i\omega\mu_0\varepsilon_0\nabla\phi^* + k_0^2\vec{A}^e = 0 \tag{67a}$$

$$(\nabla^2 + k_0^2)\vec{A}^e = \nabla(\nabla \cdot \vec{A}^e + \mu_0\varepsilon_0\dot{\phi}^*) = \nabla\chi \tag{67b}$$

If the Lorentz gauge is satisfied, the Lorentz factor χ [and the right-hand side of (67b)] is zero. The equations may now be specialized to the problem at hand. There is rotational symmetry in the problem and the non-zero quantities are E_ϕ, H_ρ, H_z, A_z^e and ϕ^*. Equations (65a,b) for the different components become

$$(\partial H_\rho/\partial z - \partial H_z/\partial\rho) = -i\omega\varepsilon_0 E_\phi \tag{68a}$$

$$i\omega\mu_0 H_\rho = -\partial E_\phi/\partial z \tag{68b}$$

$$i\omega\mu_0 H_z = \frac{1}{\rho}\frac{\partial}{\partial\rho}(\rho E_\phi) \tag{68c}$$

These three equations are true everywhere except on the surface $\rho = a$ and $|z| \leq h$. To make the equations valid on the surface, one has to introduce the surface conditions into the above equations. In addition to the conditions in (66a,b), there is an electric current $K_\phi(z)$ on the surface as well as a large axial magnetic field. Thus, (68a-c) become

$$(\partial H_\rho/\partial z - \partial H_z/\partial \rho) + \delta(\rho - a)K_\phi(z) = -i\omega\varepsilon_0 E_\phi \tag{69a}$$

$$i\omega\mu_0 H_\rho = -\partial E_\phi/\partial z \tag{69b}$$

$$i\omega\mu_0 H_z + \delta(\rho - a)E_\phi = (\partial E_\phi/\partial \rho + E_\phi/\rho) \tag{69c}$$

In terms of the potentials, the fields are given by

$$H_\rho = -\partial\phi^*/\partial\rho$$

$$H_z = -\partial\phi^*/\partial z + i\omega A_z^e$$

$$E_\phi = (1/\varepsilon_0)\partial A_z^e/\partial\rho$$

From the preceding equation,

$$A_z^e(\rho,z) = \varepsilon_0 \int_\rho^\infty E_\phi(\rho',z)\, d\rho' \tag{70}$$

It is now required to set up an equation for $A_z^e(\rho,z)$.

$$(\nu^2 + k_0^2)A_z^e(\rho,z) = \left[\frac{\partial^2}{\partial\rho^2} + \frac{1}{\rho}\frac{\partial}{\partial\rho} + \frac{\partial^2}{\partial z^2} + k_0^2\right]\varepsilon_0 \int_\rho^\infty E_\phi(\rho',z)\, d\rho'$$

$$= \varepsilon_0[\partial E_\phi(\rho,z)/\partial\rho + E_\phi(\rho,z)/\rho] + \varepsilon_0 \frac{\partial}{\partial z}\int_\rho^\infty \partial E_\phi(\rho',z)/\partial z\, d\rho'$$

$$+ \varepsilon_0 k_0^2 \int_\rho^\infty E_\phi(\rho',z)\, d\rho'$$

With (69b,c) this becomes

$$(\nu^2 + k_0^2)A_z^e(\rho,z) = \varepsilon_0[i\omega\mu_0 H_z(\rho,z) + \delta(\rho - a)E_\phi(\rho,z)]$$

$$- i\omega\mu_0\varepsilon_0 \int_\rho^\infty \partial H_\rho(\rho',z)/\partial z\, d\rho' + \varepsilon_0 k_0^2 \int_\rho^\infty E_\phi(\rho',z)\, d\rho'$$

Using (69a) gives

$$(\nabla^2 + k_0^2)A_z^e(\rho,z)$$

$$= i\omega\mu_0\varepsilon_0 H_z(\rho,z) + \varepsilon_0\delta(\rho - a)E_\phi(\rho,z) - i\omega\mu_0\varepsilon_0 \int_\rho^\infty \left[-i\omega\varepsilon_0 E_\phi(\rho',z) + \frac{\partial H_z(\rho',z)}{\partial\rho}\right.$$

$$\left. - \delta(\rho' - a)K_\phi(z)\right] d\rho' + \varepsilon_0 k_0^2 \int_\rho^\infty E_\phi(\rho',z)\, d\rho'$$

$$= i\omega\mu_0\varepsilon_0 H_z(\rho,z) + \varepsilon_0\delta(\rho - a)E_\phi(\rho,z) - \varepsilon_0 k_0^2 \int_\rho^\infty E_\phi(\rho',z)\, d\rho'$$

$$+ i\omega\mu_0\varepsilon_0 K_\phi(z) \int_\rho^\infty \delta(\rho' - a)\, d\rho' - i\omega\mu_0\varepsilon_0 H_z(\rho,z) + \varepsilon_0 k_0^2 \int_\rho^\infty E_\phi(\rho',z)\, d\rho'$$

$$= \varepsilon_0\delta(\rho - a)E_\phi(\rho,z) + i\omega\mu_0\varepsilon_0 K_\phi(z) \int_\rho^\infty \delta(\rho' - a)\, d\rho'$$

The ρ' integral may be performed:

$$\int_\rho^\infty \delta(\rho' - a)\, d\rho' = H(a - \rho) = \begin{cases} 1 & \text{if } 0 \le \rho \le a^- \\ 0 & \text{if } \rho \ge a^+ \end{cases}$$

Therefore, finally

$$(\nabla^2 + k_0^2)A_z^e(\rho,z) = \varepsilon_0\delta(\rho - a)E_\phi(\rho,z) + i\omega\mu_0\varepsilon_0 K_\phi(z)H(a - \rho) \tag{71}$$

If (71) is formally identified with (67b), it is seen that the second term on the right in (71) corresponds to the Lorentz factor term. The Lorentz gauge is satisfied ($\chi = 0$) in the exterior region ($\rho > a$) but is not satisfied in the interior region. Furthermore, by differentiating with respect to ρ

$$\chi = \nabla \cdot \vec{A}^e + \mu_0\varepsilon_0\phi^* = \partial A_z^e(\rho,z)/\partial z - i\omega\mu_0\varepsilon_0\phi^*(\rho,z) \quad ,$$

it can be shown that χ is independent of ρ and a function of z only, i.e., $\chi = \chi(z)$, which leads to:

$$\chi(z) = \partial A_z^e(\rho,z)/\partial z - i\omega\mu_0\varepsilon_0\phi^*(\rho,z) = \begin{cases} i\omega\mu_0\varepsilon_0 \int_0^z K_\phi(z')\,dz' & \text{if } 0 \le \rho \le a^- \\ 0 & \text{if } \rho \ge a^+ \end{cases}$$

It is thus seen that the Lorentz condition is satisfied on the exterior but not in the interior. This is because of the presence of the transverse electric current in the ferrite medium. This situation can be contrasted to an electric dipole antenna (thin or thick), where there are no magnetic currents to make the Lorentz condition invalid.

It is now required to solve (71) for the electric vector potential. The equation becomes

$$\left(\frac{\partial^2}{\partial\rho^2} + \frac{1}{\rho}\frac{\partial}{\partial\rho} + \frac{\partial^2}{\partial z^2} + k_0^2\right) A_z^e(\rho,z) = \varepsilon_0\delta(\rho - a)E_\phi(\rho,z) + i\omega\mu_0\varepsilon_0 K_\phi(z)H(a - \rho)$$

This equation can be solved with the use of Green's theorem and the principle of superposition. Thus,

$$A_z^e(\rho,z) = A_{zE}^e(\rho,z) + A_{zK}^e(\rho,z)$$

where

$$A_{zE}^e(\rho,z) = -(\varepsilon_0/4\pi)\int_{-\pi}^{\pi} d\phi'/2\pi \int_0^\infty d\rho'\, 2\pi\rho' \int_{-\infty}^{\infty} dz'\, E_\phi(\rho,z')\delta(\rho' - a)(e^{ik_0R}/R)$$

$$= -(a\varepsilon_0/2)\int_{-h}^{h} dz'\, E_\phi(a,z')K(z - z',\rho)$$

with

$$K(z - z',\rho) = \int_{-\pi}^{\pi} \frac{d\phi'}{2\pi}\,\frac{e^{ik_0R}}{R} \tag{72}$$

and $R = [(z - z')^2 + \rho^2 + a^2 - 2\rho a\cos\phi']^{1/2}$. $A_{zE}^e(\rho,z)$ will be used later

to obtain $A^e_{z1}(a,z)$. Similarly,

$$A^e_{zK}(\rho,z) = -(i\omega\mu_0\varepsilon_0/4\pi) \int_{-\pi}^{\pi} d\phi'/2\pi \int_0^{\infty} d\rho' \, 2\pi\rho' \int_{-\infty}^{\infty} dz' \, K_\phi(z')H(a-\rho)(e^{ik_0R_1}/R_1)$$

$$= -(i\omega\mu_0\varepsilon_0/2) \int_{-h}^{h} dz' \, K_\phi(z')M_1(z-z',\rho)$$

where

$$M_1(z-z',\rho) = \int_{-\pi}^{\pi} \frac{d\phi'}{2\pi} \int_0^a d\rho' \, \rho' \, \frac{e^{ik_0R_1}}{R_1} \tag{73}$$

and $R_1 = [(z-z')^2 + \rho^2 + \rho'^2 - 2\rho\rho' \cos\phi']^{1/2}$.

Thus, the total electric vector potential is

$$A^e_z(\rho,z) = -(a\varepsilon_0/2) \int_{-h}^{h} dz' \, E_\phi(a,z')K(z-z',\rho)$$

$$-(i\omega\mu_0\varepsilon_0/2) \int_{-h}^{h} dz' \, K_\phi(z')M_1(z-z',\rho) \tag{74}$$

By specializing (74) for $\rho = a^+$ and $\rho = a^-$ and by making use of (70) and (66a,b), one obtains

$$\varepsilon_0 E_\phi(a,z) = -(a\varepsilon_0/2) \int_{-h}^{h} dz' \, E_\phi(a,z') \, \partial K(z-z',\rho)/\partial\rho\Big|_{\rho=a^+}$$

$$- (i\omega\mu_0\varepsilon_0/2) \int_{-h}^{h} dz' \, K_\phi(z') \, \partial M_1(z-z',\rho)/\partial\rho\Big|_{\rho=a^-} \tag{75}$$

Returning to (74), one may now obtain for the tangential magnetic field

$$H_z(\rho,z) = (i\omega/k_0^2)\left(\frac{\partial^2}{\partial z^2} + k_0^2 \right) A^e_z(\rho,z)$$

Thus,

$$H_z(\rho,z) = (a/2)(1/i\omega\mu_0)\left(\frac{\partial^2}{\partial z^2} + k_0^2\right)\int_{-h}^{h} dz'\ E_\phi(a,z')K(z - z',\rho)$$

$$+ (1/2)\left(\frac{\partial^2}{\partial z^2} + k_0^2\right)\int_{-h}^{h} dz'\ K_\phi(z')M_1(z - z',\rho) \qquad (76)$$

Once again, on the exterior surface $\rho = a^+$,

$$H_z(a^+,z) = (a/2)(1/i\omega\mu_0)\left(\frac{\partial^2}{\partial z^2} + k_0^2\right)\int_{-h}^{h} dz'\ E_\phi(a,z')\ K(z - z',a^+)$$

$$+ (1/2)\left(\frac{\partial^2}{\partial z^2} + k_0^2\right)\int_{-h}^{h} dz'\ K_\phi(z')M_1(z - z',a^+) \qquad (77)$$

It now remains to use (77) and (64) to obtain the integral equation.

Integral Equation for $E_\phi(a,z)$ and $K_\phi(z)$. The required integral equations for the unknown quantities may be obtained from the results of (64) and (77) for the interior and exterior problems by requiring that

$$H_z(a^+,z) - H_z(a^-,z) = -I_0^e\delta(z)$$

This gives

$$\left\{(a/2)(1/i\omega\mu_0)\left(\frac{\partial^2}{\partial z^2} + k_0^2\right)\int_{-h}^{h} dz'\ E_\phi(a,z')K(z - z',a) + (1/2)\left(\frac{\partial^2}{\partial z^2} + k_0^2\right)\right.$$

$$\left.\times \int_{-h}^{h} dz'\ K_\phi(z')M_1(z - z',a)\right\} + \left\{(i/\omega\mu_1 ah)\left(\sum_{n=-\infty}^{\infty}\left[\int_{-h}^{h} dz'\ E_\phi(a,z')\right.\right.\right.$$

$$\left.\left.\left.\times \cos(pz')\right]\cos(pz)\ \frac{J_0[a(k_1^2 - p^2)^{1/2}]}{J_1[a(k_1^2 - p^2)^{1/2}]}\ [a(k_1^2 - p^2)^{1/2}]\right)\right\} = -I_0^e\delta(z) \qquad (78a)$$

with $p = (n + 1/2)\pi/h$.

The other equation to be satisfied simultaneously is (75), which is reproduced here for convenience:

$$\varepsilon_0 E_\phi(a,z) = -(a\varepsilon_0/2) \int_{-h}^{h} dz'\, E_\phi(a,z')\, \partial K(z - z',\rho)/\partial\rho\Big|_{\rho=a^+} - (i\omega\mu_0\varepsilon_0/2) \int_{-h}^{h} dz'\, K_\phi(z')\, \partial M_1(z - z',\rho)/\partial\rho\Big|_{\rho=a^-} \qquad (78b)$$

The two kernels $K(z - z',\rho)$ and $M_1(z - z',\rho)$ appearing in the coupled integral equations above are defined by (72) and (73) respectively.

It can be verified easily that in the limit $h \to \infty$ the integrals in (78a,b) become convolution integrals, that the two equations decouple and that the expression for $F_\phi(\rho,z)$ on the surface $\rho = a$ is in complete agreement with the results presented in Part I [2, Eqs. (17) or (18)].

Returning to the coupled integral equations in (78a,b), it is seen that there are three kernels. First of all, the kernel on the right-hand side of (78a) will be examined carefully. The kernel is made up of an infinite series which is clearly divergent since, for large values of n, it behaves like n. Although strictly not valid, the operations of summation and integration will be interchanged for the purpose of examining the series. The interchange is reversed at a later stage so that, in effect, all the steps are valid.

It is convenient to define the kernel $M(z,z')$ on the left-hand side of (78a) as:

$$M(z,z') = \sum_{n=-\infty}^{\infty} \cos(pz')\cos(pz)\, \frac{J_0[a(k_1^2 - p^2)^{1/2}]}{J_1[a(k_1^2 - p^2)^{1/2}]}\, [a(k_1^2 - p^2)^{1/2}]$$

where $p = (n + 1/2)\pi/h$.

As was pointed out earlier, this series is divergent and, hence, it is useful to write it as the sum of two series, using the first two terms in the

asymptotic form. For large values of n, the series behaves like

$$\sum \cos(pz')\,\cos(pz)\,\frac{J_0(iap)}{J_1(iap)}\,(iap) \simeq \sum \cos(pz')\,\cos(pz)\,\frac{I_0(ap)}{I_1(ap)}\,(ap)$$

$$\simeq \sum \cos(pz')\,\cos(pz)\,\frac{1+\frac{1}{8ap}}{1-\frac{3}{8ap}}\,(ap) \simeq \sum \cos(pz')\,\cos(pz)\,\left[1+\frac{1}{2ap}\right](ap)$$

We now write

$$M(z,z') = P(z,z') + Q(z,z') \tag{79}$$

with

$$P(z,z') = \sum_{n=-\infty}^{\infty}\left[\frac{J_0[a(k_1^2-p^2)^{1/2}]}{J_1[a(k_1^2-p^2)^{1/2}]}\,[a(k_1^2-p^2)^{1/2}] - ap - \frac{1}{2}\right]\cos(pz')\,\cos(pz) \tag{80}$$

and

$$Q(z,z') = \sum_{n=-\infty}^{\infty}(ap+1/2)\,\cos(pz')\,\cos(pz) \tag{81}$$

Equation (79) along with (80) and (81) is exact because it only adds and subtracts the first two terms in the asymptotic form. Now $P(z,z')$ can be written as:

$$P(z,z') = \sum_{n=-\infty}^{\infty} A_n \cos(pz')\,\cos(pz)$$

with A_n given by the term in the square brackets in (80).

If all the coefficients A_n were equal, $P(z,z')$ would be a delta function; but this is not the case. In view of the differential operator on the left-hand side of (78a), it is helpful to remove a similar factor from $P(z,z')$. This is easily accomplished by solving an equation of the form:

$$(\partial^2/\partial z^2 + k_0^2)f(z) = \cos(pz)$$

Through the use of Green's function (or by any other method), one can obtain:

$$f(z) = a_1 \cos(k_0 z) + a_2 \sin(k_0 z) + (1/k_0) \int_0^z \sin[k_0(z - z')]\cos(pz')\, dz'$$

Note that, without any loss of generality, the constants a_1 and a_2 can be set equal to zero and the integral on the right performed to obtain:

$$f(z) = [\cos(pz) - \cos(k_0 z)]/(k_0^2 - p^2)$$

so that

$$P(z,z') = \left(\frac{\partial^2}{\partial z^2} + k_0^2\right) \sum_{n=-\infty}^{\infty} A_n \left[\frac{\cos(pz) - \cos(k_0 z)}{k_0^2 - p^2}\right] \cos(pz') \qquad (82)$$

In (82) it appears that one of the terms in the series will be equal to infinity if $p = k_0$. This condition is equivalent to $h/\lambda = 1/4,\ 3/4,\ 5/4, \ldots,$. This is not the case, however, because of the numerator and the fact that, as $p \to k_0$, the term in the square brackets in (82) approaches $[z \sin(k_0 z)]/2k_0$.

Returning to (81), it is found that, since $Q(z,z')$ is an odd series, its most divergent part is identically equal to zero, so that

$$Q(z,z') = (1/2) \sum_{n=-\infty}^{\infty} \cos(pz') \cos(pz) = (h/2)\delta(z - z') \qquad (83)$$

Using (82) and (83) with (79) in the integral equation (78a), one obtains

$$\left(\frac{\partial^2}{\partial z^2} + k_0^2\right)\left[\int_{-h}^{h} dz'\, E_\phi(a,z')K(z - z',a) + \frac{i\omega\mu_0}{a}\int_{-h}^{h} K_\phi(z')M_1(z - z',a)\, dz'\right]$$

$$= -\frac{2}{a}\left\{i\omega\mu_0 I_0^e \delta(z) - \frac{1}{a\mu_r}\frac{1}{2} E_\phi(a,z) - \frac{1}{a\mu_r}\frac{1}{h}\left(\frac{\partial^2}{\partial z^2} + k_0^2\right)\int_{-h}^{h} dz'\, E_\phi(a,z')\right.$$

(Continued)

$$\times \left(\sum_{n=-\infty}^{\infty} A_n \left[\frac{\cos(pz) - \cos(k_0 z)}{k_0^2 - p^2} \right] \cos(pz') \right) \Bigg\}$$

Rearranging terms gives

$$\left(\frac{\partial^2}{\partial z^2} + k_0^2 \right) \left[\int_{-h}^{h} dz' \, E_\phi(a,z') K_1(z - z') + \frac{i\omega\mu_0}{a} \int_{-h}^{h} K_\phi(z') M_1(z - z', a) \, dz' \right]$$

$$= - \frac{2}{a} \left[i\omega\mu_0 I_0^e \delta(z) - \frac{1}{a\mu_r} \frac{1}{2} E_\phi(a,z) \right] \tag{84}$$

where the combined kernel $K_1(z - z')$ is defined as

$$K_1(z - z') = \int_{-\pi}^{\pi} \frac{d\phi'}{2\pi} \frac{e^{ik_0 R_s}}{R_s} - \frac{2}{a^2 \mu_r h} \sum_{n=-\infty}^{\infty} A_n \left[\frac{\cos(pz) - \cos(k_0 z)}{k_0^2 - p^2} \right] \cos(pz') \tag{85}$$

with the coefficients A_n given by

$$A_n = \frac{J_0[a(k_1^2 - p^2)^{1/2}]}{J_1[a(k_1^2 - p^2)^{1/2}]} [a(k_1^2 - p^2)^{1/2}] - ap - \frac{1}{2}$$

and $p = (n + 1/2)\pi/h$.

The second integral equation from (78b) is:

$$- \frac{a}{2} \int_{-h}^{h} dz' \, E_\phi(a,z') \frac{\partial}{\partial \rho} K(z - z', \rho) \Big|_{\rho=a^+} - \frac{i\omega\mu_0}{2} \int_{-h}^{h} dz' \, K_\phi(z') \frac{\partial}{\partial \rho} M_1(z - z', \rho) \Big|_{\rho=a^-}$$

$$= E_\phi(a,z)$$

The coupled integral equations can now be written in a short-hand notation suitable for numerical evaluation:

$$\left(\frac{\partial^2}{\partial z^2} + k_0^2 \right) \left[\int_{-h}^{h} dz' \, E_\phi(z') K_1(z - z') + C_1 \int_{-h}^{h} dz' \, I_\phi(z') M_1(z - z') \right] = C_2 \delta(z) + C_3 E_\phi(z) \tag{86a}$$

$$C_4 \int_{-h}^{h} dz'\ E_\phi(z')K_2(z-z') + C_5 \int_{-h}^{h} dz'\ I_\phi(z')M_2(z-z') = \frac{1}{2} E_\phi(z) \qquad (86b)$$

where the electric surface current $I_\phi(z) = 2\pi a K_\phi(z)$. Also, the kernel $K_1(z - z')$ has been defined previously in (85), and

$$C_1 = i\omega\mu_0/2\pi a^2 \quad ; \quad C_2 = -2i\omega\mu_0 I_0^e/a \quad ; \quad C_3 = 1/a^2\mu_r \quad ;$$

$$C_4 = -a/2 \quad ; \quad C_5 = -i\omega\mu_0/4\pi a$$

The factor (1/2) on the right-hand side of (86b) comes from the discontinuity in the derivative of the $K_2(z - z')$ kernel, viz.,

$$K_2(z - z') = \frac{\partial}{\partial\rho} K(z - z',\rho)\Big|_{\rho=a^+} \neq \frac{\partial}{\partial\rho} K(z - z',\rho)\Big|_{\rho=a^-}$$

$$M_2(z - z') = \frac{\partial}{\partial\rho} M_1(z - z',\rho)\Big|_{\rho=a^+} = \frac{\partial}{\partial\rho} M_1(z - z',\rho)\Big|_{\rho=a^-}$$

8. NUMERICAL SOLUTION BY THE MOMENT METHOD OF THE COUPLED INTEGRAL EQUATIONS

The differential equation (86a) can be solved to obtain:

$$\int_{-h}^{h} dz'\ E_\phi(z')K_1(z - z') + C_1 \int_{-h}^{h} dz'\ I_\phi(z')M_1(z - z')$$

$$= C_6 \cos(k_0 z) + C_7 \sin(k_0|z|) + C_8 \int_{0}^{z} dz'\ E_\phi(z')\sin[k_0(z - z')] \qquad (87a)$$

Similarly, from (86b)

$$\int_{-h}^{h} dz'\ E_\phi(z')K_2(z - z') + C_9 \int_{-h}^{h} dz'\ I_\phi(z')M_2(z - z') = C_{10}E_\phi(z) \qquad (87b)$$

where C_6 is unknown and determined numerically by employing the end condition $I_\phi(h) = 0$, and

$$C_1 = i\omega\mu_0/2\pi a^2 \quad ; \quad C_7 = C_2/2k_0 = -i\omega\mu_0 I_0^e/ak_0$$

$$C_8 = C_3/k_0 = 1/a^2\mu_r k_0 \quad ; \quad C_9 = C_5/C_4 = i\omega\mu_0/2\pi a^2 \quad ; \quad C_{10} = 1/2C_4 = -1/a$$

It is now considered useful to examine the four kernels in (87a,b) and to obtain their Fourier transforms. Thus,

$$K_1(z - z') = K(z - z') - \frac{2}{a^2\mu_r h} \sum_{n=-\infty}^{\infty} A_n \left[\frac{\cos(pz) - \cos(k_0 z)}{k_0^2 - p^2} \right] \cos(pz')$$

with $p = (n + 1/2)\pi/h$. The Fourier transform of $K(z - z')$ is given by $\tilde{K}(\xi) = i\pi J_0(a\gamma_0)H_0^{(1)}(a\gamma_0)$ where $\gamma_0^2 = k_0^2 - \xi^2$.

$$M_1(z - z', \rho) = \int_{-\pi}^{\pi} \frac{d\phi'}{2\pi} \int_0^a d\rho' \, \rho' \, \frac{e^{ik_0[(z-z')^2 + \rho^2 + \rho'^2 - 2\rho\rho' \cos\phi']^{1/2}}}{[(z-z')^2 + \rho^2 + \rho'^2 - 2\rho\rho' \cos\phi']^{1/2}}$$

$$\tilde{M}_1(\xi, \rho) = i\pi \int_0^a H_0^{(1)}(\rho_> \gamma_0) J_0(\rho_< \gamma_0) \, \rho' \, d\rho'$$

where

$\rho_>$ = larger of ρ and ρ'

$\rho_<$ = smaller of ρ and ρ'

which leads to

$$\tilde{M}_1(\xi, \rho) = \begin{cases} (i\pi a/\gamma_0) J_0(\rho\gamma_0) H_1^{(1)}(a\gamma_0) & \text{if } \rho > \rho' \\ (i\pi a/\gamma_0) H_0^{(1)}(\rho\gamma_0) J_1(a\gamma_0) & \text{if } \rho < \rho' \end{cases}$$

It is easily seen that

$$\tilde{M}_2(\xi) = \frac{\partial}{\partial\rho} \tilde{M}_1(\xi, \rho)\Big|_{\rho=a^+} = \frac{\partial}{\partial\rho} \tilde{M}_1(\xi, \rho)\Big|_{\rho=a^-} = -i\pi a J_1(a\gamma_0) H_1^{(1)}(a\gamma_0)$$

Finally,

$$\bar{K}_2(\xi) = \frac{\partial}{\partial\rho}\,\bar{K}(\xi,\rho)\Big|_{\rho=a^+}$$

where

$$\bar{K}(\xi,\rho) = i\pi J_0(\rho_< \gamma_0) H_0^{(1)}(\rho_> \gamma_0)$$

with

$\rho_<$ = smaller of ρ and a

$\rho_>$ = larger of ρ and a

so that

$$\bar{K}(\xi,\rho) = \begin{cases} i\pi J_0(\rho\gamma_0) H_0^{(1)}(a\gamma_0) & \text{for } \rho < a \\ i\pi J_0(a\gamma_0) H_0^{(1)}(\rho\gamma_0) & \text{for } \rho > a \end{cases}$$

Therefore,

$$\bar{K}_2(\xi) = -i\pi\gamma_0 J_0(a\gamma_0) H_1^{(1)}(a\gamma_0)$$

To begin the numerical procedure, it is recognized that, because of the evenness of $E_\phi(z)$ and $I_\phi(z)$, the integrals ranging from -h to h may be converted as follows:

$$\int_{-h}^{h} E_\phi(z') K_{1,2}(z - z')\, dz' = \int_0^h E_\phi(z')[K_{1,2}(z - z') + K_{1,2}(z + z')]\, dz'$$

Similarly,

$$\int_{-h}^{h} I_\phi(z') M_{1,2}(z - z')\, dz' = \int_0^h I_\phi(z')[M_{1,2}(z - z') + M_{1,2}(z + z')]\, dz'$$

Now the interval from 0 to h can be subdivided into n+1 panels. Within each panel the unknown quantities $E_\phi(z)$ and $I_\phi(z)$ are approximated by constants and the constant value is assigned to a location z which corresponds to the center of the panel. With the length h = 2nt, each panel is of width 2t except the first and last panels which are of width t.

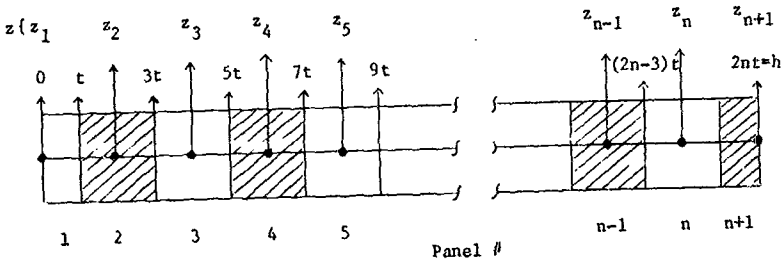

The locations at which the unknown quantities are determined are given by $z_I = (2I - 2)t$ with I = 1, 2, 3, ..., (n+1). Typically,

$$\int_0^h E_\phi(z')[K_1(z - z') + K_1(z + z')]\, dz'$$

$$= \left\{ \int_0^t + \int_t^{3t} + \int_{3t}^{5t} + \ldots + \int_{(2n-3)t}^{(2n-1)t} + \int_{(2n-1)t}^{2nt} \right\} E_\phi(z')[K_1(z - z') + K_1(z + z')]\, dz'$$

In each of these intervals $E_\phi(z)$ is approximated by a constant value so that

$$K_1(I,J) = \int_{\Delta z_J} [K_1(z_I + z') + K_1(z_I - z')]dz' = \int_{(2J-3)t}^{(2J-1)t} dz' \left\{ \frac{1}{2\pi} \int_{-\infty}^{\infty} \bar{K}(\xi) e^{i\xi z_I} \left(e^{i\xi z'} + e^{-i\xi z'} \right) d\xi \right\} - \frac{1}{a^2 \mu_r h} \int_{(2J-3)t}^{(2J-1)t} dz' \left\{ \sum_{n=-\infty}^{\infty} A_n \left[\frac{\cos(pz_I) - \cos(k_0 z_I)}{k_0^2 - p^2} \right] \cos(pz') \right\}$$

By substituting for $\bar{K}(\xi)$ and carrying out the z' integration, one obtains

$$K_1(I,J) = K(I,J) + B(I,J)$$

where

$$K(I,J) = (4/\pi) \int_{-\infty}^{\infty} [i\pi J_0(a\gamma_0)H_0^{(1)}(a\gamma_0)][(\sin \xi t)/\xi]\{\cos[2\xi(I+J-2)t] + \cos[2\xi(I-J)t]\}\, d\xi$$

$$B(I,J) = -\frac{4}{\pi\mu_r} \sum_{n=0}^{\infty} A_n \left[\frac{\cos[2pt(I-1)] - \cos[2k_0 t(I-1)]}{a^2(k_0^2 - p^2)} \right] + \left[\frac{\sin[pt(2J-1)] - \sin[pt(2J-3)]}{(h/\pi)p} \right]$$

The integral in K(I,J) is evaluated by suitably deforming the contour from the real axis to a contour that wraps around the branch cut. When this is done, K(I,J) for I≠J can be written in the form

$$K(I,J) = \int_0^{\infty} f(x)\, e^{-x}\, dx$$

where f(x) is a complex function of a real variable x. The integrals are evaluated using a 10-point Gauss-Laguerre quadrature method. The special case of diagonal elements (I=J) can be written in the form

$$K(I,I) = \frac{1}{\pi} \int_{-\infty}^{\infty} \bar{K}(\xi)[(\sin \xi t)/\xi](e^{2i\xi x_I} + 1)\, d\xi = (1/2)K(1,1) + T(I)$$

where

$$T(I) = \frac{1}{\pi} \int_{-\infty}^{\infty} \bar{K}(\xi)[(\sin \xi t)/\xi]e^{2i\xi z_I}\, d\xi$$

with $z_I = 2(I - 1)t$, $I = 1, 2, \ldots, (n+1)$. $K(1,1)$ is evaluated as an integral on the real axis because of the absence of the exponential decay factor, using 10-point Gauss quadrature routines. $T(I)$ can once again be put in a form suitable for Gauss-Laguerre quadrature by a deformation of the contour that wraps around the branch cut at $\xi = k_0$. Care is taken in evaluating the first and last panels' integrations because of their half normal width. What is discussed for kernel $K(z - z')$ or $\bar{K}(\xi)$ is essentially true with the calculation of the elements corresponding to the three other kernels.

Referring back now to the three terms on the right-hand side of (87a), viz.,

$$C_6 \cos(k_0 z_I) + C_7 \sin(k_0 |z_I|) + C_8 \int_0^{z_I} dz' \, E_\phi(z') \sin[k_0(z_I - z')] ,$$

the first and last terms, containing respectively the unknowns C_6 and $E_\phi(z)$, are moved to the left-hand side. For example,

$$C_6 \cos(k_0 z_I) = C_6 \cos[k_0(2I - 2)t]$$

$$C_8 \int_0^{z_I} dz' \, [\quad] = C_8 \int_0^{(2I-2)t} dz' \, [\quad] = C_8 \left\{ \int_0^{t} + \int_t^{2t} + \ldots + \int_{(2I-3)t}^{(2I-2)t} \right\} dz' \, [\quad]$$

We now define

$$A(I,P) = \int_{(P-1)t}^{Pt} \sin[k_0(z_I - z')\, dz' = (1/k_0)\{\cos[k_0 t(2I - P - 2)] - \cos[k_0 t(2I - P - 1)]\}$$

It is seen that when the term associated with C_8 is moved to the left-hand side, it affects only the lower triangle elements of $K_1(I,J)$ and not the upper triangle elements, thus rendering the $K_1(I,J)$ matrix elements not equal

to $K_1(J,I)$. Extending these calculating principles to (87b), and using the fact that $I_\phi(h) = I_\phi(I=n+1) = 0$, one can finally set up the following matrix equation:

$$\left[\begin{array}{ccc:ccc:c} a_{11} & a_{12} \cdots & a_{1,n+1} & a_{1,n+2} & \cdots & a_{1,2n+1} & a_{1,2n+2} \\ \vdots & \text{I} & \vdots & \vdots & \text{II} & \vdots & \vdots\ \text{V} \\ a_{n+1,1} & \cdots & a_{n+1,n+1} & a_{n+1,n+2} & \cdots & a_{n+1,2n+1} & a_{n+1,2n+2} \\ \hdashline a_{n+2,1} & \cdots & a_{n+2,n+1} & a_{n+2,n+2} & \cdots & a_{n+2,2n+1} & a_{n+2,2n+2} \\ \vdots & \text{III} & \vdots & \vdots & \text{IV} & \vdots & \vdots\ \text{VI} \\ a_{2n+2,1} & \cdots & a_{2n+2,n+1} & a_{2n+2,n+2} & \cdots & a_{2n+2,2n+1} & a_{2n+2,2n+2} \end{array}\right] \left[\begin{array}{c} E_1 \\ \vdots \\ F_{n+1} \\ I_1 \\ \vdots \\ I_n \\ C_6 \end{array}\right] = \left[\begin{array}{c} G_1 \\ \vdots \\ G_{n+1} \\ 0 \\ 0 \\ \vdots \\ 0 \\ 0 \end{array}\right]$$

where the elements on the right-hand side are given by $G(I) = C_7 \sin[k_0(2I-2)t]$ with $I = 1, 2, \ldots, (n+1)$.

The magnetic current $I_z^*(z)$ is easily obtained from the solution of the system of linear equations by using $I_z^*(z) = -2\pi a E_\phi(z)$ volts. The computer programs are included in Appendix C and the results are plotted and discussed in the next section.

9. EXPERIMENTAL MEASUREMENT OF THE MAGNETIC CURRENT

The magnetization current is essentially the time rate of change of the magnetization vector ($\vec{M}$) integrated over the antenna cross section. The experimental procedure, however, determines the total axial magnetic flux with the use of a shielded loop placed coaxially over a driven loop which is loaded by a ferrite cylinder. Suitable modifications to the theory have to be made, therefore, before the computations can be compared with the experimental results. These modifications and the assumption of azimuthal symmetry on which they are based are discussed in detail in Appendix D.

Ferrite materials that are available commercially have been used in this experimental investigation. Table 1 lists the initial permeability μ_r' (i.e., the slope of the B-H curve for small H) and the applicable frequency range for a variety of ferrite materials, grouped under their respective suppliers. Ferrites #C-2050 of Ceramic Magnetics, Inc. and #Q-3 of Indiana General were selected for use in the 5-100 MHz frequency range. Toroidal samples of the #C-2050 material were obtained and its properties (μ_r' and Q) measured as a function of frequency by means of a Q-meter. The quality factor Q of the ferrite material is defined by

$$Q = \frac{1}{\text{loss factor}} = \mu_r'/\mu_r'' = \frac{2\pi \times \text{stored energy}}{\text{energy dissipated per period, } 2\pi/\omega} \tag{88}$$

The measured values of Q and μ_r' for the ferrite material #C-2050 are shown plotted in Fig. 4(a) as a function of frequency together with the values supplied by the manufacturer. Fair agreement is observed between the two. The imaginary part μ_r'' of the relative permeability can be calculated easily using (88) and measured values of μ_r' and Q. The manufacturer-supplied values of μ_r' and Q for the ferrite material #Q-3 are shown in Fig. 4(b). The values of the relative permittivity ϵ_r used in the theoretical calculations were

TABLE 1. List of Commercially Available Ferrite Materials

Source #1: Ceramic Magnetics, Inc., Fairfield, N.J.

Type of Ferrite Material	Manufacturer Code #	Initial Permeability μ_r'	Frequency Range
Mn-Zn	MN-31 DC-10	2800	Up to 10 MHz
Mn-Zn	MN-31 DC-20	3300	Up to 10 MHz
Ni	CN-20	800	300 KHz - 2 MHz
Ni	CM-2002	1500	1 KHz - 1 MHz
Mn	MN-30	4000	Up to 500 KHz
Mn	MN-60	6000	Up to 600 KHz
Mn	MN-100	9500	Below 1 MHz
	C-2010	200-300	Below 15 MHz
	C-2025	150-200	Below 15 MHz
	C-2050	100-150	Below 20 MHz
	C-2075	25-50	Below 50 MHz
	CMD-5005	1400	Up to 10 MHz
	N-40	15-20	Up to 100 MHz

Source #2: Indiana General, Keasbey, N.J.

Ni-Zn	Q-1	125	Up to 10 MHz
Ni-Zn	Q-2	40	Up to 50 MHz
Ni-Zn	Q-3	18	Up to 200 MHz

Source #3: Fair-Rite Products Corp., Wallkill, N.Y.

Ni-Zn	30-61	125	200 KHz - 10 MHz

Source #4: Ferroxcube Corp., Saugertiea, N.Y.

Ni-Zn	4C4	125	Up to 50 MHz
Mn-Zn	3D3	750	Up to 5 MHz
	3B9	1800	Up to 5 MHz
Mn-Zn	3B7	2300	Up to 1 MHz

Source #5: National Moldite Co., Inc., Newark, N.J.

M-Grade	125 @ 1 MHz	Up to 20 MHz

Source #6: Stackpole-Carbon Co., St. Marys, Pa.

Grade 24	2500	Up to 100 KHz
Grade 27A	1000	Up to 800 KHz
Grade 9	190	Up to 2 MHz
Grade 11	125	Up to 6 MHz
Grade 12	35	Up to 80 MHz
Grade 2285A	7.5	Up to 300 MHz

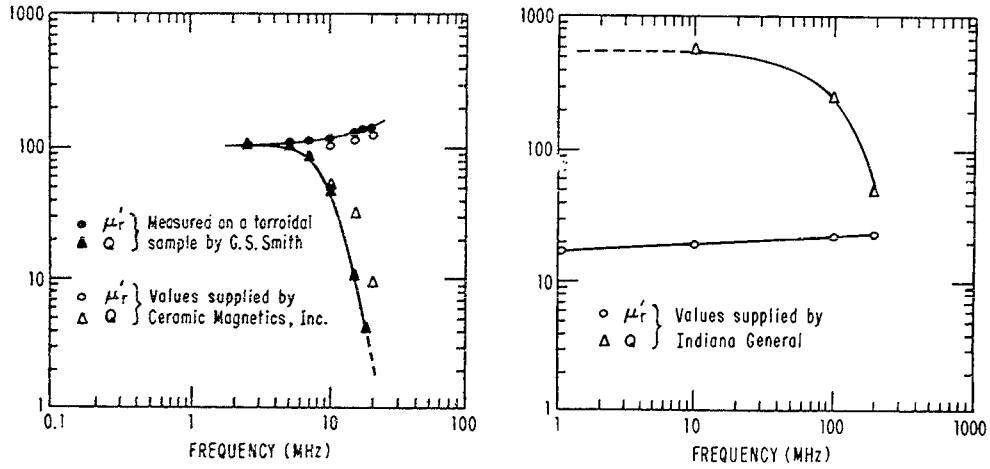

FIG. 4 MAGNETIC PROPERTIES OF FERRITE MATERIAL AS A FUNCTION OF FREQUENCY

(a) MATERIAL #C-2050; SOURCE — CERAMIC MAGNETICS INC.

(b) MATERIAL #Q-3 ; SOURCE — INDIANA GENERAL.

also supplied by the manufacturers. It can be seen from Fig. 4(a) that the value of Q for the ferrite material #C-2050 is nearly constant (≃100) up to about 2 MHz and then falls off rapidly to less than 10% of this value at 20 MHz. Similarly for the material #Q-3, Fig. 4(b) indicates a nearly constant value of Q (≃500) up to about 15 MHz, beyond which it decays to ≃50 at 200 MHz.

Three antenna cores were fabricated, as photographed in Fig. 5(a)-(c). Cores (a) and (b) are made of material #C-2050, while core (c) is made of material #Q-3. Cylindrical rods of 5/16" diameter and 5.25" height were used along with adhesive tape to fabricate core (a) of 2" overall diameter and 21" height. Core (b) has the same height as core (a) but is comprised of five cylindrical rods of 1" diameter and varying lengths. Core (c) is formed from three cylindrical rods of .625" diameter and 7.5" length for a total height of 22.5". As was pointed out earlier, cores (a) and (b) are useful for frequencies up to about 20 MHz, core (c) up to 200 MHz.

The three cores were used in various antenna configurations in which an electrically small loop antenna is loaded by a finite cylindrical ferrite rod. The antenna parameters for the eleven different cases are tabulated in Table 2. For antennas numbered 1 through 3, measurements were made at frequencies of 10, 50 and 100 MHz, respectively. The electrical radius ak_0 of the driven loop ranges from .00166 to .01662. Antennas numbered 4 through 7 were operated at frequencies of 5, 10, 15 and 20 MHz, respectively; the electrical radius ranged from .00132 to .00531. The operating frequencies for antennas numbered 8 through 11 were the same as for the previous set but the radius was doubled.

It can be seen in Table 2 that the value of ak_0 does not exceed 0.017 for any of the eleven antennas. This ensures the validity of the assumption

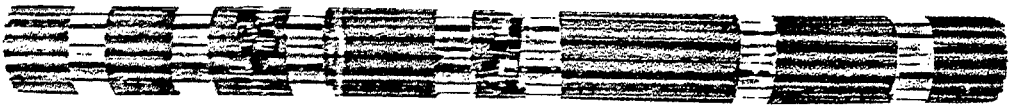

(a)

Dia. 2a = 2", height 2h = 21"

(b)

Dia. 2a = 1", height 2h = 21"

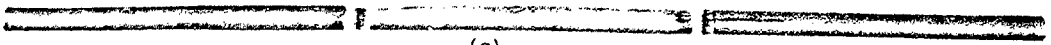

(c)

Dia. 2a = .625", height 2h = 22/5"

FIGURE 5

FERRITE RODS USED IN THE EXPERIMENT

TABLE 2. Antenna Parameters

#Q-3 Material (Supplier: Indiana General)

$2a = 0.625"$, $2h = 22.5"$, $\Omega = 2\,\ell n(2h/a) = 8.5534$

Antenna #	$\mu_r = \mu_r' - j\mu_r''$	h/λ_0	ak_0	$z_m^i = r_m^i + jx_m^i$
1	18 - j.036	.00952	.00166	.00797 - j3.7637
2	19 - j.0544	.04762	.00831	.00214 - j.70979
3	20 - j.0890	.09525	.01662	.001577 - j.33443

#C-2050 Material (Supplier: Ceramic Magnetics, Inc.)

i) $2a = 1"$, $2h = 21"$, $\Omega = 2\,\ell n(2h/a) = 7.4754$

4	100 - j1.0	.00444	.00132	.0051 - j.50479
5	115 - j2.55	.00889	.00265	.0049 - j.21892
6	125 - j12.50	.01333	.00398	.01341 - j.13270
7	135 - j67.5	.01778	.00531	.03747 - j.07394

ii) $2a = 2"$, $2h = 21"$, $\Omega = 2\,\ell n(2h/a) = 6.089$

8	105 - j0.63	.00444	.00265	.001275 - j.12611
9	120 - j2.4	.00889	.005319	.001225 - j.05456
10	150 - j15.	.01333	.007979	.003352 - j.03292
11	140 - j42.	.01778	.01064	.009368 - j.01815

that the driven loop be electrically thin in the theoretical calculation of antenna currents. The height of the monopole antenna (h/λ_0) ranges from .00444 to .09525 so that the longest dipole is nearly (1/5)-wavelength long. The value of the relative permeability $\mu_r = \mu_r' - j\mu_r''$ from Fig. 4 and the internal impedance z_m^i per unit length calculated using equation (36) are also listed in Table 2. In this section an $e^{j\omega t}$ time dependence is implicit and is more convenient. Due account of this change in notation has been taken in using (36) to calculate z_m^i. It is observed that for all antennas considered, the internal impedance is largely reactive.

For each of the three ferrite cylindrical cores described above, a set of driven and measuring loops was fabricated. A photograph and representative line drawing showing the construction of the loops are shown in Fig. 6. The six loops were all constructed from commercially available microcoaxial cables ending in a modified BNC connector. The driven and measuring loops are placed coaxially in the experimental setup, as can be seen in the photograph in Fig. 7 and the block diagram in Fig. 8. The short lengths of microcoaxial transmission lines leading away from the two loops are at right angles to one another in the horizontal plane so that any inductive coupling between the two is minimized. The signal source used in this experiment was either a GR-1001A (5-50 MHz) or an HP-3200B (10-500 MHz) oscillator. When the GR-1001A oscillator was used for measurements with antennas #4 through #11, the power amplifier was not needed. The HP-230B power amplifier was used only in conjunction with the HP-3200B oscillator for measurements on antennas #1 through #3. The source frequency was accurately measured using an HP-5240 electronic counter. A signal proportional to the total axial magnetic field was induced in the receiving loop. An HP-8405A vector voltmeter was used to detect and record this signal (B). The reference signal (A) to the

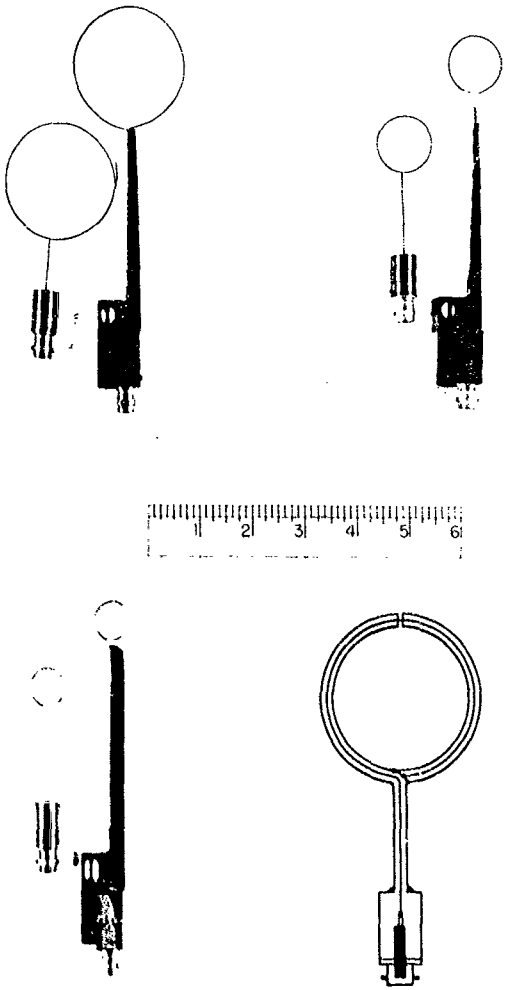

FIGURE 6

THREE PAIRS OF DRIVEN AND MEASURING LOOPS ALONG WITH A LINE DIAGRAM SHOWING THE CONSTRUCTIONAL DETAILS OF A REPRESENTATIVE LOOP.

FIGURE 7

PHOTOGRAPH OF THE EXPERIMENTAL SET-UP

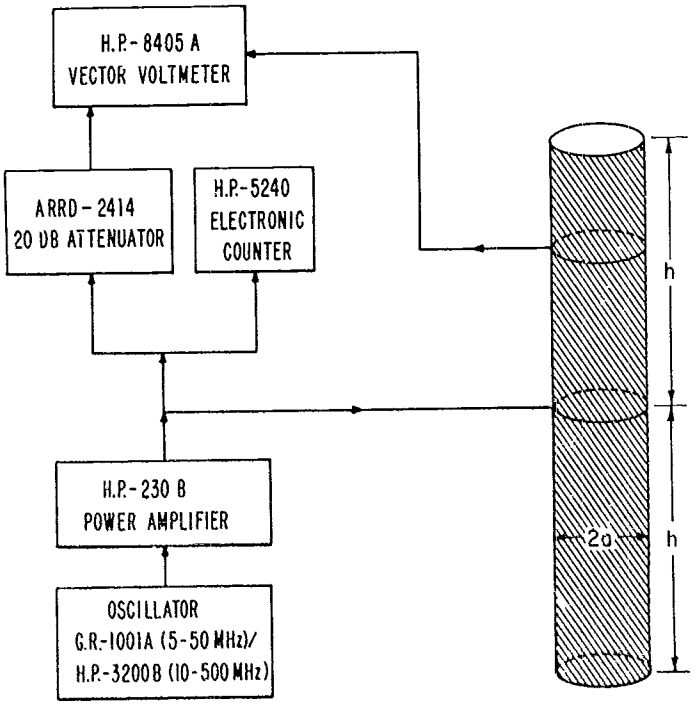

FIG. 8 BLOCK DIAGRAM OF THE EXPERIMENTAL SETUP FOR MEASUREMENT OF MAGNETIC CURRENT ON THE FERRITE ROD ANTENNA.

vector voltmeter was provided from a coaxial T. The vector-voltmeter readings were recorded as a function of the axial distance z from the driving loop. In this manner the amplitude and phase of the magnetic current distribution were obtained for the eleven antenna configurations described in Table 2. The unnormalized data are given in Table C-2 of Appendix C.

Computer programs, described and listed in Appendices A and B, were utilized in calculating the magnetic current distributions for the eleven cases. As discussed earlier, the theoretical calculations are based on a treatment of the ferrite rod as an imperfect magnetic conductor. The theoretical and experimental current distributions are shown graphically in Figs. 9 through 11. Also appearing in Figs. 9 - 11 are Tables 3, 4 and 5, respectively; these show the calculated values of input admittance $Y^* = I_z^*(0)/I_0^e = (G + jB)^*$ ohms and input impedance $Z^* = 1/Y^*$ mhos. The antenna numbering scheme used in the figures and tables corresponds to that given in Table 2. The values of $\Omega = 2\ \&n(2h/a)$ for the antennas in Figs. 9 - 11 are, respectively, 8.5534, 7.4754 and 6.089.

The agreement between the theory and experiment is seen to be good. The antennas used here are relatively short and, consequently, the current distribution is seen to be nearly triangular. As may be expected, the largest deviation of the experimental values from the theoretical computations occurs at either end of the antenna ($z/h = 0, 1$) and especially at the driving point. For this reason the raw experimental data were normalized in most cases to the theoretical calculations at a point nearly a third the distance from the driving point to the end of the antenna. In the case of antennas #1 and #2, there appears to be a kink in the experimental values for the phase of the current distribution. This is believed to be due to the stacking of individual ferrite rods by means of adhesive tape. This is not seen in the magnitude

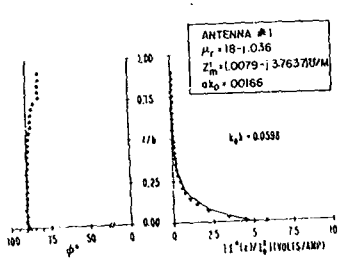

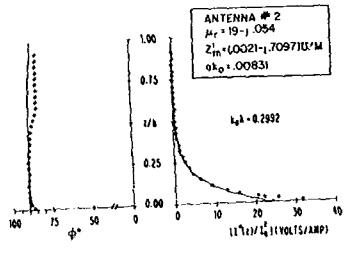

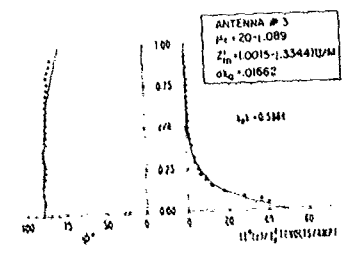

TABLE - 3 CALCULATED (3-TERM THEORY) Y° AND Z° FOR THE THREE ANTENNAS.

ANTENNA #	INPUT ADMITTANCE $Y^\circ = I_0^\circ / V_0^\circ = (G + jB)^\circ \Omega$	INPUT IMPEDANCE $Z^\circ = 1/Y^\circ = (R + jX)^\circ \Omega$
1	.00340 + j .00056	36015 - j .20831
2	.02547 + j .24 66282	.05004 - j .04088
3	.08256 + j .40 79784	.00604 - j .02008

——— THEORETICAL (3-TERM THEORY)

. . . EXPERIMENTAL

(FERRITE SOURCE, MATERIAL Q#3 SUPPLIED BY INDIANA GENERAL)

FIG 9 PLOT OF MAGNITUDE AND PHASE OF THE MAGNETIC CURRENT ALONG THE ANTENNA ($\Omega = 2\ln(2h/a) - 0.5534$)

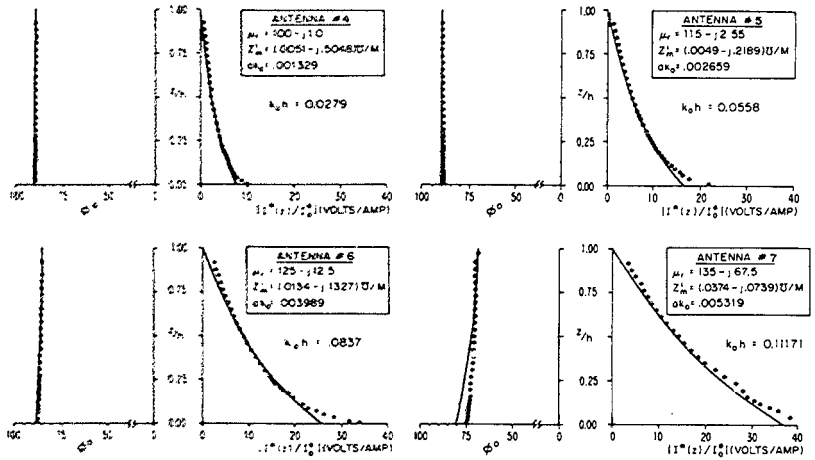

——— THEORETICAL (3-TERM THEORY)

• • • • • EXPERIMENTAL

(FERRITE SOURCE ; MATERIAL C #2050 SUPPLIED BY CERAMIC MAGNETICS)

TABLE 4

Calculated (3-term Theory) Y^m and Z^m for the above four antennas

ANTENNA #	INPUT ADMITTANCE $Y^m = \frac{I^m(o)}{I^m_o} = (G + jB)^m \Omega$	INPUT IMPEDANCE $Z^m = \frac{1}{Y^m} = (R + jX)^m \Omega$
4	.0306 + j 7.831	.00050 - j .12769
5	.1397 + j 16.545	.00051 - j .06043
6	.9560 + j 25.675	.00145 - j .03880
7	6.127 + j 36.637	.00444 - j .02655

FIG 10 PLOT OF MAGNITUDE AND PHASE OF THE MAGNETIC CURRENT ALONG THE ANTENNA.
[$\Omega = 2/\ln(2h/a) = 7.4754$]

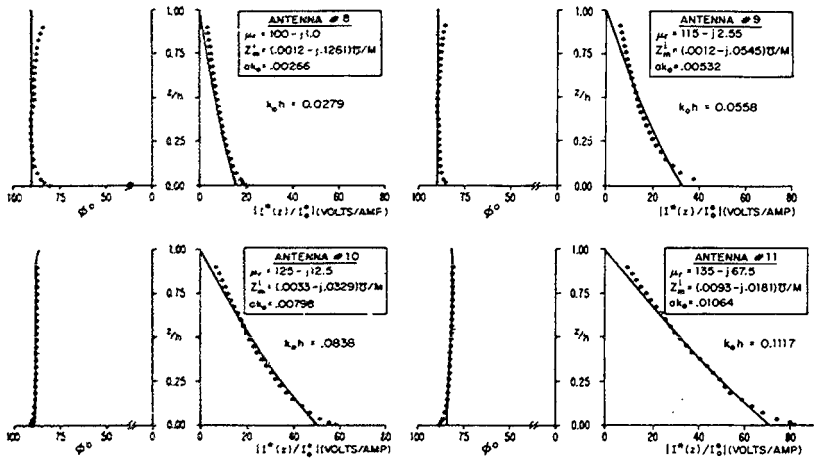

——— THEORETICAL (3-TERM THEORY)

- - - - - EXPERIMENTAL

(FERRITE SOURCE ; MATERIAL C #2050 SUPPLIED BY CERAMIC MAGNETICS)

TABLE 5

Calculated (3-term Theory) Y^m and Z^m for the above four antennas

ANTENNA #	INPUT ADMITTANCE $Y^m = \frac{I^m(o)}{I^m_0} = (G+jB)^m\Omega$	INPUT IMPEDANCE $Z^m = \frac{1}{Y^m} = (R+jX)^m\Omega$
8	.041 + j15.805	.00017 - j.06327
9	.176 + j32.807	.00016 - j.03048
10	1.160 + j50.373	.00046 - j.01984
11	6.749 + j70.870	.00133 - j.01398

FIG. 11 PLOT OF MAGNITUDE AND PHASE OF THE MAGNETIC CURRENT ALONG THE ANTENNA. [$\Omega = 2\ln(2h/a) = 6.089$]

curves because of the relatively low magnitude values. The overall agreement of the theory and experiment was used in deciding the point of normalization.

The coupled integral equations in (86a,b) in the two variables, the tangential electric field $E_\phi(z)$ and circumferential electric current $I_\phi(z)$, were solved numerically by the moment method on a Sigma-7 computer system. The method itself has been discussed in Section 8; the computer programs are listed in Appendix C. Table 6 contains a description of all the subroutines used in this computation. The basic philosophy of this method is to reduce the set of coupled integral equations to a system of linear algebraic equations. The standard routines [6] for solving a system of linear equations were modified to handle complex variables. The results of these computations are plotted in Figs. 12 through 14. As before, the experimental data have been normalized at a point approximately one third the distance from the driving point ($z = 0$) to the end.

The magnetic current $I_z^*(z)$ is easily obtained from the solution for the tangential electric field using the relation $I_z^*(z) = -2\pi a E_\phi(z)$ volts per unit current in the driving loop. The input parameters Y^* and Z^* are also tabulated and the tables are included in the figures showing the magnitude and phase of the magnetic current. In all eleven cases the phase is nearly constant, since the antennas are electrically short in free space, and most of the magnetic current is in phase quadrature. The agreement between the experiment and the theoretical calculations is very good including near the source. This was to be expected because the coupled integral equations (86a,b) in two variables comprise a far more accurate and independent theoretical formulation of the problem than the approximate integral equation (39) which relies rather heavily on an analogy between the ferrite rod antenna and the resistive cylindrical dipole antenna.

TABLE 6

LIST OF SUBROUTINES USED IN SOLVING THE COUPLED INTEGRAL EQUATIONS (86a,b)

PROGRAM NAME	PURPOSE
MAIN	Computes $E_\phi(z)$ and $I_\phi(z)$ by solving the coupled integral equations (86a,b).
BSLSML	Computes Bessel functions $J_0(z)$ and $J_1(z)$ for $\|z\| \leq 10.0$ with 5 figure accuracy.
BESH	Computes Hankel functions $H_0^{(1)}(z)$, $H_0^{(2)}(z)$, $H_1^{(1)}(z)$ and $H_1^{(2)}(z)$.
QGL10	10-point Gauss-Laguerre quadrature routine.
QG10	10-point Gauss quadrature routine.
FCTK	Computes the integrand for $K(z - z')$ for $I \neq J$.
FKI1R, FKI1I	The same, for $I = J = 1$.
FKII	The same, for $I = J \neq 1$.
FCTM1, FM1I1R, FM1III, FM1III	Computes the integrand for $M_1(z - z')$ for $I \neq J$, $I = J = 1$, and $I = J \neq 1$, respectively.
FCTK2, FK2I1R, FK2III, FK2II	Computes the integrand for $K_2(z - z')$ for $I \neq J$, $I = J = 1$, and $I = J \neq 1$, respectively.
FCTM2, FM2I1R, FM2III, FM2II	Computes the integrand for $M_2(z - z')$ for $I \neq J$, $I = J = 1$, and $I = J \neq 1$, respectively.
AUX	Auxiliary function used in computing the above integrands.
SERIES	Computes the infinite series part of the kernel $K_1(z - z')$.
DECOMP, SOLVE, IMPRUV, SING	Programs used in solving the linear system of algebraic equations.
ANGLE	Computes the phase angle of complex variables $I_\phi(z)$ and $E_\phi(z)$.

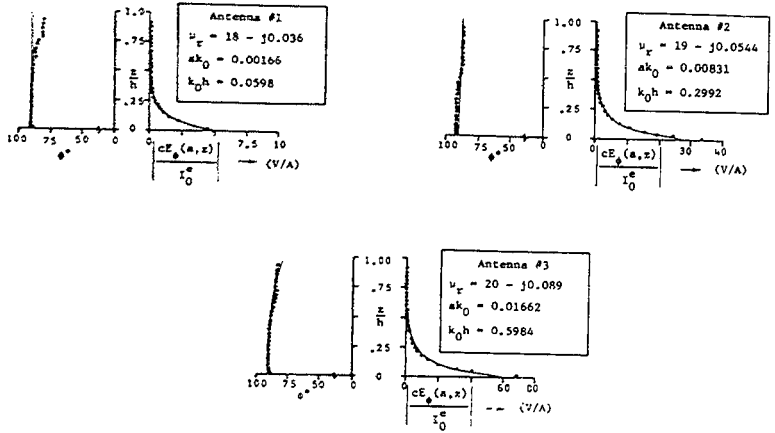

(Ferrite source: Material #3 supplied by Indiana General)

Fig. 12. Plot of magnitude and phase of the magnetic current along the antenna; $\Omega = 2\ln(2h/a) = 8.5534$. (Uncorrected; see Appendix D.)

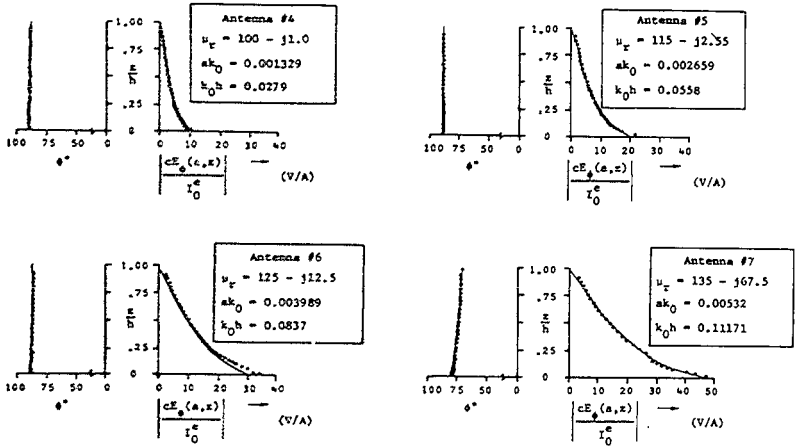

(Ferrite source: Material *CA*2050 supplied by Ceramic Magnetics)

Fig. 13. Plot of magnitude and phase of the magnetic current along the antenna; $\Omega = 2\ \ln(2h/a) = 7.4754$.

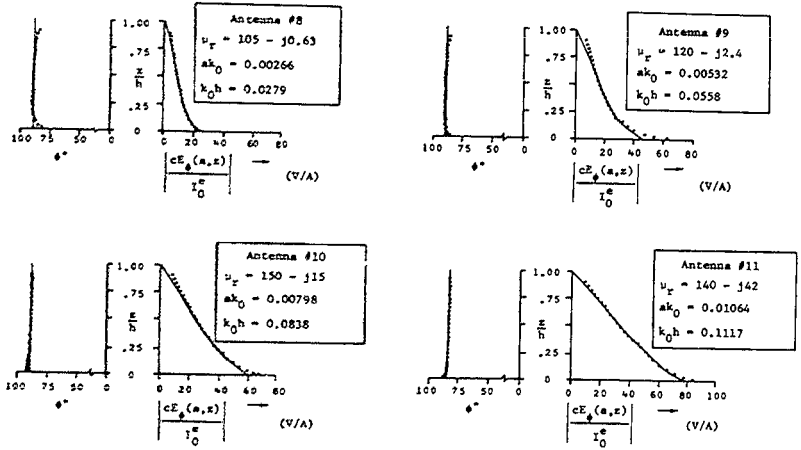

Fig. 14. Plot of magnitude and phase of the magnetic current along the antenna; $\Omega = 2 \ln(2h/a) = 6.089$.

TABLE 7

INPUT ADMITTANCES AND IMPEDANCES OF THE ELEVEN ANTENNAS OBTAINED FROM SOLVING THE COUPLED INTEGRAL EQUATIONS (86a,b)

Antenna #	Input Admittance (ohms)	Input Impedance (mhos)
1	.003 + j 4.99	.00012 - j.20040
2	.03 + j30.22	.00003 - j.03309
3	.10 + j62.32	.00003 - j.01605
4	.03 + j 9.23	.00035 - j.10834
5	.14 + j20.13	.00035 - j.04967
6	.97 + j29.81	.00109 - j.03351
7	6.21 + j45.62	.00293 - j.02152
8	.02 + j23.55	.00004 - j.04246
9	.16 + j44.27	.00008 - j.02259
10	1.06 + j60.02	.00029 - j.01666
11	4.26 + j75.32	.00075 - j.01323

10. SUMMARY

An electrically small loop that carries a constant current and is loaded by a homogeneous and isotropic ferrite rod has been called the ferrite-rod antenna. In Part I [2] of this report the ferrite rod was assumed to be of infinite length and the problem was treated using a boundary-value approach. In a practical situation, however, the antenna is necessarily finite and often electrically short so that a new mathematical formulation was needed, along with an experimental investigation, for the problem of a finite ferrite rod antenna. With this current distribution known precisely, other quantities of interest can be derived from it.

Although, in terms of physical mechanisms, the ferrite-rod antenna can be compared with the dielectric rod antenna, there exists a complete analogy between the ferrite antenna and the conducting cylindrical dipole antenna. This analogy is based on the dual property of electric and magnetic vectors in Maxwell's equations. The electric dipole antenna has received considerable attention from researchers in the past and, therefore, a treatment of the 'magnetic analog' of the dipole antenna is considered useful. Based on this analogy, an integral equation has been derived for the magnetic current on the finite ferrite-rod antenna. As expected, the integral equation is identical in form to the corresponding equation for the electric current on the dipole antenna. This derivation was based on the assumption that the value of the relative permeability μ_r of the ferrite material equals infinity. In effect, the ferrite is treated as a perfect magnetic conductor as when in the 'electric case' the antenna material is assumed to have an infinite electrical conductivity σ. However, in practice, a material with μ_r equal to infinity does not exist and, furthermore, over a useful frequency range the μ_r value is not high enough to justify using the perfect conductor approximation.

For this reason, the integral equation had to be modified. The modification was achieved by defining the internal impedance per unit length of the magnetic conductor to be the ratio of the tangential magnetic field to the total magnetic current flowing in the magnetic conductor. An approximate, 3-term expression for the magnetic current was then obtained in a manner paralleling the procedure used by King and Wu to solve for the electric current on the imperfectly conducting dipole antenna. It was found that for commercially available ferrites the internal impedance per unit length was largely reactive so that the propagation constant k ($= \beta + i\alpha$) on the antenna had a large imaginary part. The predominance of the attenuation constant α makes the magnetic current very small and, thus, one is led to conclude that the practical ferrite-rod antenna is not a very efficient radiator.

The treatment of the ferrite-rod antenna as an analog of the resistive electric dipole antenna relies rather heavily on the mathematical equivalence of the two problems under idealized driving conditions. For this reason, an alternative derivation of the integral equation for the tangential electric field on the ferrite surface was developed. This derivation led to a pair of coupled integral equations in terms of the tangential electric field and tangential electric surface current. The coupled integral equations were solved numerically by the moment method and the magnetic current obtained from the tangential electric field. It was also verified that in the limit $h \to \infty$ the equations decouple and are in complete agreement with the results of the theory for the infinite antenna.

Since the magnetic current is proportional to the total axial magnetic field, a simple experimental apparatus was built to measure the magnetic current distribution on several antenna configurations. A graphical comparison of the theoretical and experimental results has been presented. Although the

three-term solution has been shown to give good results for antenna lengths $k_0 h \leq 5\pi/4$, the antennas used in the experiment were much shorter and the near-triangular distribution of currents was verified. The frequency response of the properties of available ferrite materials and the practical limitations on the size of the ferrite rods made it difficult to construct antennas of longer length.

In conclusion, while ferrites have been used extensively at microwave frequencies and up to several MegaHertz, the fact that ferrites are now becoming commercially available in the range 30 - 300 MHz should lead to useful applications. In situations in which the physical size of the antenna must be kept small, a loop antenna has limited usefulness because of its low efficiency and radiation resistance. The insertion of a suitable ferrite core offers the advantage of both improved efficiency and increased radiation resistance. Although, in theory, an increased radiation resistance should simplify the problem of matching the antenna to its associated circuit, in practice there remains a severe problem. This has been discussed by Dropkin, Metzer and Cacheris [7] who made measurements of the receiving characteristics of a cylindrical ferrite-rod antenna at a frequency of 75 MHz. They conclude that both ferrite-core and air-core loops can be described by similar equivalent circuits. These circuits have resonant properties and each of the lumped circuit elements can be identified with a physical quantity characterizing the antenna. The improved efficiency and the increased radiation resistance which were determined experimentally can be attributed directly to an increased magnetic flux passing through the loop. They also make the interesting observation that with a dielectric cylinder ($\varepsilon_r = 10$, $\mu_r = 1$), the size of the ferrite used had no effect on the air-loop properties. This was because the loop used was small enough to act as a magnetic dipole.

APPENDIX A.

COMPUTATION OF MAGNETIC CURRENT AND ADMITTANCE OF FERRITE ROD ANTENNA

The approximate magnetic current distribution as given by (51) is

$$I_z^*(z) = \frac{-i2\pi k_0 \zeta_0 I_0^e}{k\Psi_{dR} \cos kh} [\sin k(h - |z|) + T_U^*(\cos kz - \cos kh) + T_D^*(\cos \frac{k_0 z}{2} - \cos \frac{k_0 h}{2})]$$

where T_U^* and T_D^* are given by

$$T_U^* = (C_V E_D - C_D E_V)/(C_U E_D - C_D E_U)$$

$$T_D^* = (C_U E_V - C_V E_U)/(C_U E_D - C_D E_U)$$

with

$$C_U = [1 - (k^2/k_0^2)](\Psi_{dUR} - \Psi_{dR})(1 - \cos kh) - (k^2/k_0^2)\Psi_{dUR} \cos kh - i\Psi_{dUI}(\frac{3}{4} - \cos \frac{k_0 h}{2}) + \Psi_U(h)$$

$$C_D = \Psi_{dD}(\frac{3}{4} - \cos \frac{k_0 h}{2}) - [1 - (k^2/k_0^2)]\Psi_{dR}(1 - \cos \frac{k_0 h}{2}) + \Psi_D(h)$$

$$C_V = -[-i\Psi_{dI}(\frac{3}{4} - \cos \frac{k_0 h}{2}) + \Psi_V(h)]$$

$$E_U = -(k^2/k_0^2)\Psi_{dUR} \cos kh + (1/4)\Psi_{dUI} \cos \frac{k_0 h}{2} + \Psi_U(h)$$

$$E_D = -(1/4)\Psi_{dD} \cos \frac{k_0 h}{2} + \Psi_D(h)$$

$$E_V = -(i/4)\Psi_{dI} \cos \frac{k_0 h}{2} - \Psi_V(h)$$

The Ψ functions appearing in the above expressions are defined as follows:

$$\Psi_{dR} = \begin{cases} \Psi_{dR}(0) & k_0 h \leq \pi/2 \\ \Psi_{dR}(h - \lambda/4) & \pi/2 \leq k_0 h \leq 3\pi/2 \end{cases}$$

$$\Psi_{dR}(z) = \csc k(h - |z|) \int_{-h}^{h} \sin k(h - |z'|) \left[\frac{\cos k_0 r}{r} - \frac{\cos k_0 r_h}{r_h} \right] dz'$$

$$\Psi_{dUR} = [1 - \cos kh]^{-1} \int_{-h}^{h} (\cos kz' - \cos kh) \left[\frac{\cos k_0 r_0}{r_0} - \frac{\cos k_0 r_h}{r_h} \right] dz'$$

$$\Psi_{dD} = [1 - \cos \frac{k_0 h}{2}]^{-1} \int_{-h}^{h} (\cos \frac{k_0 z'}{2} - \cos \frac{k_0 h}{2}) \left[\frac{e^{ik_0 r_0}}{r_0} - \frac{e^{ik_0 r_h}}{r_h} \right] dz'$$

$$\Psi_{dI} = -[1 - \cos \frac{k_0 h}{2}]^{-1} \int_{-h}^{h} \sin k(h - |z'|) \left[\frac{\sin k_0 r_0}{r_0} - \frac{\sin k_0 r_h}{r_h} \right] dz'$$

$$\Psi_{dUI} = -[1 - \cos \frac{k_0 h}{2}]^{-1} \int_{-h}^{h} (\cos kz' - \cos kh) \left[\frac{\sin k_0 r_0}{r_0} - \frac{\sin k_0 r_h}{r_h} \right] dz'$$

where the propagation constant k is given by

$$k = k_0[1 + (i4\pi\zeta_0 z_m^i / k_0 \Psi_{dR})]^{1/2}$$

with $\zeta_0 = 376.7\ \Omega$ the characteristic impedance of free space. However, since Ψ_{dR} is dependent on k, an iteration procedure is used. To begin with, k_1 as given by

$$k_1 = k_0[1 + (i4\pi\zeta_0 z_m^i / k_0 \Psi_{dR0})]^{1/2}$$

is determined. With k_1 substituted for k, Ψ_{dR1} is computed and then k is evaluated using

$$k = k_0[1 + (i4\pi\zeta_0 z_m^i / k_0 \Psi_{dR1})]^{1/2}$$

This new value of k is used in evaluating all the Ψ functions and the current distributions.

APPENDIX B

This appendix contains a listing of the main program and all associated subroutines. The main program accepts as inputs h/λ_0, Ω and z_m^i, and computes the input impedance Z^*, admittance Y^*, and magnetic current distribution as a function of distance (z/h) along the antenna. Subroutine NINTG employs Simpson's rule for integration to evaluate the functions. The various integrands are calculated using the subroutines FCTH(Y), FCT0(Y) and FCT1(Y).

```
FORTRAN IV G LEVEL  21              MAIN              DATE = 73325        16/58/48

      C     ******************************************************************
      C     PROGRAM FOR CALCULATION OF MAGNETIC CURRENT AND INPUT ADMITTANCE
      C     OF A FINITE FERRITE ROD ANTENNA
      C
      C     MODIFICATION OF ARONSON'S PROGRAM FOR USE ON THE IBM 370/155 SYSTE
      C     M OF THE 'JOINT HARVARD/MIT COMPUTER CENTER'.
      C
      C
      C
      C
            COMMON A2,H,XXR,Z,COHHR,COHHI,SNHHR,SNHHI,COH2,XKI,
           1V1,V2,V3,V4,V5,V6,V7,V8,V9,V10,V11,V12
            COMPLEX*8 XX,XKH,COHH,SNHH,COHH1,U,SYDR,SYDUR,XX21,SYDO,SYDI, ZI,
           1CU,CO,CV,EU,EO,EV,TU,TO,CGN,YD,ZO,XK2,CUR,SYDU1,SYU,SYV,SYO,DV(10)
            EXTERNAL FCT1,FCTH,FCTO
         10 READ (5,901) HL,OML,ZI
            IF (HL.GT.5.0) GO TO 70
        901 FORMAT (F10.5,4X,F10.5,5X,2F15.5)
            AE=.001
            H=6.28318531*HL
            WRITE (6,950) HL,ZI,OML
        950 FORMAT(1H1,//,30X,'RESULTS OF FERRITE ANTENNA COMPUTATIONS',//,
           110X,'INPUT DATA SUPPLIED',///,10X,'H/LAMBDAO',10X,'=',5X,
           2F10.5,/,10X,'4*PY*ZNI*ZETA/KO  = ',4X,F10.5,' +J ',F12.5,/,10X,
           3'OMEGA',14X,'=',5X,F10.5,//,10X,'USING ABOVE, WE HAVE THE FOLLOWIN
           4G PARAMETERS FOR THE FERRITE ANTENNA',//)
            A2=(2.*H*EXP(-0.5*OML))**2
            COHHR=COS(H)
            SNHHR=SIN(H)
            ZP=0.0
            XKR=1.0
            XKI=0.0
            HP=H-1.57079631
            IF(HP) 12,11,11
         11 ZP=HP
         12 Z=ZP
            HSQHA=H+SQRT(H*H+A2)
            QLH1=ALOG(A2/HSQHA)
            QLH2=0.5*ALOG(A2)
            QLO1=QLH2
            QLO2=ALOG(HSQHA)
            HZ=(H-Z)
            QLZ1=ALOG(A2/(Z+SQRT(Z*Z+A2)))
            QLZ2=ALOG(HZ+SQRT(HZ*HZ+A2))
            CALL NINTG(FCT1,QLZ1,QLZ2,2,AE)
            DV(1)=CMPLX(V1,V2)
            Z=H
            CALL NINTG(FCT1,QLH1,QLH2,2,AE)
            DV(2)=CMPLX(V1,V2)
            Z=ZP
            SYDR=(DV(1)-DV(2))/SIN(HZ)
            XX=1.-(0.,1.)*ZI/SYDR
            XX=CSQRT(XX)
            XXR=REAL(XX)
            XXI=AIMAG(XX)
            CALL NINTG(FCT1,QLZ1,QLZ2,2,AE)
            DV(1)=CMPLX(V1,V2)
            Z=H
            CALL NINTG(FCT1,QLH1,QLH2,2,AE)
            DV(2)=CMPLX(V1,V2)
            Z=ZP
            U=XX*(H-ZP)
            SYDR=(DV(1)-DV(2))/CSIN(U)
            XX=1.-(0.,1.)*ZI/SYDR
            XX=CSQRT(XX)
            XXR=REAL(XX)
            XXI=AIMAG(XX)
            CALL NINTG(FCT1,QLZ1,QLZ2,2,AE)
            DV(1)=CMPLX(V1,V2)
            Z=H
            CALL NINTG(FCT1,QLH1,QLH2,2,AE)
            DV(2)=CMPLX(V1,V2)
            Z=ZP
            XXH=XX*H
            COHH=CCOS(XXH)
            COHH1=1.-COHH
            SNHH=CSIN(XXH)
            COHHR=REAL(COHH)
            COHHI=AIMAG(COHH)
            SNHHR=REAL(SNHH)
            SNHHI=AIMAG(SNHH)
            COH2=COS(0.5*H)
            U=XX*(H-ZP)
            SYDR=(DV(1)-DV(2))/CSIN(U)
            CALL NINTG(FCTO,QLO1,QLO2,8,AE)
            DV(1)=CMPLX(V1,V2)
            DV(2)=CMPLX(V3,V4)
            DV(3)=CMPLX(V5,V6)
            DV(4)=CMPLX(V7,V8)
            CALL NINTG(FCTH,QLH1,QLH2,12,AE)
            DV(5)=CMPLX(V1,V2)
            DV(6)=CMPLX(V3,V4)
            DV(7)=CMPLX(V5,V6)
            DV(8)=CMPLX(V7,V8)
            DV(9)=CMPLX(V9,V10)
            DV(10)=CMPLX(V11,V12)
            SYDR=(DV(1)-DV(5))/COHH1
            COH2O=1.-COH2
            COH2I=1./COH2O
            SYDI=(DV(2)-DV(6))*COH2I
            SYDU=-(DV(3)-DV(7))*COH2I
            SYDO=-(DV(4)-DV(8))*COH2I
            SYV=DV(9)
            SYO=DV(10)
            SYU=DV(6)
            XK2=1.-XKR*XX
            CONTS=0.25-COH2
```

```
      CU=XKZ1*(SYDUR-SYOR)*COHH1-SYDUR*COHH*
     1(0.,1.)*SYDUI*COH75+SYU
      CD=SYDU*COH75-XKZ1*SYDR*COH20+SYU
      CV=-SYV-(0.,1.)*SYDI*COH75
      EU=SYU-XK*XK*SYDUR*COHH-(0.,.25)*SYDUI*COH2
      ED=SYD-0.25*SYDD*COH2
      EV=(0.,0.25)*SYDI *COH2-SYV
      TU=(CV*ED-CD*EV)/(CU*ED-CD*EU)
      TD=(CU*EV-CV*EU)/(CU*ED-CD*EU)
      CON=(0.,1.)*2.*3.1415*120.*3.1415      / (XK*COHH*SYUR)
      WRITE (6,951) XK,SYOR
  951 FORMAT (/,10X,'K/KO  =  ',F15.5,' +J ',F15.5,5X,
     2'SYOR  =  ',F10.5,' + J ',F10.5,//)
      YO=CON*(SNHH+TU*COHH1+TD*COH20)
      ZO=1.0/YO
      WRITE(6,952) YO,ZO
  952 FORMAT(//,10X,'INPUT ADMITTANCE OF THE ANTENNA=  ',F13.5,' +J ',
     1F13.5,' OHMS ',//,10X,'INPUT IMPEDANCE OF THE ANTENNA =  ',
     2F13.5,' +J ',F13.5,' MHOS ',//,10X,'CURRENT DISTRIBUTION ON THE AN
     3TENNA   (VOLTS/AMP)',///  ,12X,'Z/H',11X,'REAL',11X,'IMAG',12X,
     4'MAG',10X,'PHASE',// )
      ZOH=-0.05
      DO 40 N=1,21
      ZOH=ZOH+0.05
      XKZ=XKH*ZOH
      CUR=CON*(SIN(XKH-XKZ)+TU*(COS(XKZ)-COHH)
     1+TD*(COS(0.5* ZOH*H)-COH2))
      CMAG=CABS(CUR)
      CURR=REAL(CUR)
      CURI=AIMAG(CUR)
      CPHAS=ATAN2(CURI,CURR)*180.0/3.14159265
   40 WRITE(6,953) ZOH,CURR,CURI,CMAG,CPHAS
  953 FORMAT (4F15.2,F15.1)
      GO TO 10
   70 CONTINUE
      STOP
      END

C     ****************************************************************
C
C
      SUBROUTINE NINTG(FCT,SL,SU,N,AE)
      DIMENSION VAL(12),VAL2(12),VAL3(12),VAL4(12),VAR(12)
      COMMON XZ,H,XKH,Z,COHH,COHH1,SNHH,SNHH1,COH2,AK1,VAR
      A=AE*1.5
      N1=2
      DX=(SU-SL)*.25
      IF (DX) 15,5,15
    5 DO 10 J=1,N
   10 VAL(J)=0.0
      RETURN
   15 CALL FCT(SL)
      CALL FILL(VAL,N)
      CALL FCT(SU)
      CALL FILL(VAL2,N)
      DO 17 J=1,N
   17 VAL2(J)=0.5*(VAL(J)+VAL2(J))
      SLX=SL+DX
      CALL FCT(SLX)
      CALL FILL(VAL,N)
      SLX=SLX+DX
      CALL FCT(SLX)
      CALL FILL(VAL4,N)
      SLX=SLX+DX
      CALL FCT(SLX)
      CALL FILL(VAL3,N)
      DO 18 J=1,N
   18 VAL3(J)=VAL3(J)+VAL(J)
   20 DO 21 J=1,N
      VAL2(J)=VAL2(J)+VAL4(J)
      VAL4(J)=VAL3(J)
   21 VAL3(J)=0.0
      N1=N1+N1
      SLX=SL+0.5*DX
      DO 22 K=1,N1
      CALL FCT(SLX)
      CALL FILL(VAL,N)
      DO 22 J=1,N
   22 VAL3(J)=VAL(J)+VAL3(J)
   23 SLX=SLX+DX
      DX=0.5*DX
      DO 24 J=1,N
      VAR(J)=DX*(VAL2(J)+VAL4(J)+VAL3(J)+VAL3(J))/1.5
      DIFF=ABS((DX*(VAL2(J)+1.0*VAL4(J)-VAL3(J)-VAL3(J)))/VAR(J))-A
      IF  (DIFF) 24,24,20
   24 CONTINUE
      RETURN
      END

C     ****************************************************************
C
C
      SUBROUTINE FILL(VAL,N)
      DIMENSION VAL(12)
      COMMON XZ,H,XKH,Z,COHH,COHH1,SNHH,SNHH1,COH2,AK1,
     1V1,V2,V3,V4,V5,V6,V7,V8,V9,V10,V11,V12
      GO TO (1,2,3,4,5,6,7,8,9,10,11,12) N
   12 VAL(12)=V12
   11 VAL(11)=V11
   10 VAL(10)=V10
    9 VAL(9)=V9
    8 VAL(8)=V8
    7 VAL(7)=V7
    6 VAL(6)=V6
    5 VAL(5)=V5
    4 VAL(4)=V4
    3 VAL(3)=V3
    2 VAL(2)=V2
    1 VAL(1)=V1
      RETURN
      END
```

```
C     ****************************************************************
C
C
      SUBROUTINE FCTH(Y)
      COMMON A2,H,XKR,Z,COHHR,COHHI,SNHHR,SNHHI,COH2,XK1,
     1V1,V2,V3,V4,V5,V6,V7,V8,V9,V10,V11,V12
      E=EXP(Y)
      E1=1./E
      EA=A2*E1
      R=0.5*(E+EA)
      X=R-EA+H
      R1=SQRT((X+H)**2+A2)
      R11=1./R1
      SV=COS(R)+R11*COS(R1)*R
      SVS=SIN(R)+R11*SIN(R1)*R
      U=XKR*X
      C=COS(U)
      S=SIN(U)
      E=EXP(XK1*X)
      E1=1./E
      CH1=0.5*(E+E1)
      CH2=CH1-E1
      SH1=S*CH1
      SH2=C*CH2
      CH1=C*CH1
      CH2=-S*CH2
      E=SNHHR*CH1-SNHHI*CH2-COHHR*SH1+COHHI*SH2
      SH2=SNHHR*CH2+SNHHI*CH1-COHHR*SH2-COHHI*SH1
      SH1=E
      CH1=CH1-COHHR
      CH2=CH2-COHHI
      U=COS(0.5*X)-COH2
      V1=SV*CH1
      V2=SV*CH2
      V3=U*SV
      V4=-U*SVS
      V5=SVS*SH1
      V6=SVS*SH2
      V7=SVS*CH1
      V8=SVS*CH2
      V9=SH1*SV+SH2*SVS
      V10=SH2*SV-SH1*SVS
      V11=CH1*SV+CH2*SVS
      V12=CH2*SV-CH1*SVS
      RETURN
      END

C     ****************************************************************
C
C
      SUBROUTINE FCTO(Y)
      COMMON A2,H,XKR,Z,COHHR,COHHI,SNHHR,SNHHI,COH2,XK1,
     1V1,V2,V3,V4,V5,V6,V7,V8,V9,V10,V11,V12
      E=EXP(Y)
      E1=1./E
      EA=A2*E1
      R=0.5*(E+EA)
      X=R-EA
      SV=2.*COS(R)
      SVS=2.*SIN(R)
      U=XKR*X
      C=COS(U)
      S=SIN(U)
      E=EXP(XK1*X)
      E1=1./E
      CH1=0.5*(E+E1)
      CH2=CH1-E1
      SH1=S*CH1
      SH2=C*CH2
      CH1=C*CH1
      CH2=-S*CH2
      E=SNHHR*CH1-SNHHI*CH2-COHHR*SH1+COHHI*SH2
      SH2=SNHHR*CH2+SNHHI*CH1-COHHR*SH2-COHHI*SH1
      V5=SVS*E
      V6=SVS*SH2
      CH1=CH1-COHHR
      CH2=CH2-COHHI
      V1=CH1*SV
      V2=CH2*SV
      V7=SVS*CH1
      V8=SVS*CH2
      U=COS(0.5*X)-COH2
      V3=U*SV
      V4=-U*SVS
      RETURN
      END

C     ****************************************************************
C
C
      SUBROUTINE FCT1(Y)
      COMMON A2,H,XKR,Z,COHHR,COHHI,SNHHR,SNHHI,COH2,XK1,
     1V1,V2,V3,V4,V5,V6,V7,V8,V9,V10,V11,V12
      E=EXP(Y)
      E1=1./E
      EA=A2*E1
      R=0.5*(E+EA)
      X=R-EA+Z
      R1=SQRT((X+Z)**2+A2)
      A1=COS(R)+R*COS(R1)/R1
      X=R-X
      R=X*R1
      E=EXP(R*XK1)
      E1=1./E
      CH=0.5*(E+E1)
      SH=CH-E1
      V1=SIN(A)*(CH*A1)
      V2=COS(A)*(SH*A1)
      RETURN
      END
```

APPENDIX C

This appendix opens with two tables containing experimental information. The first, Table C-1, lists the values of the various antenna constants (dimensions, ferrite characteristics, frequency, etc.) for the eleven antenna configurations studied experimentally. Table C-2 gives the raw measured data (unnormalized) for the magnetic current distributions on the eleven antennas as a function of z.

The appendix concludes with a listing of the computer programs used to solve the coupled integral equations in (86a,b). The procedure used, i.e., the moment method, was discussed briefly in Section 8. The coupled integral equations are reduced to a system of linear algebraic equations which are then solved for the unknown variables. An unknown constant in the integral equation is also determined in the numerical procedure by imposing the end condition at $z = h$. The magnetic current $I_z^*(z)$ is easily computed from the solution of the tangential electric field $E_\phi(z)$ by using $I_z^*(z) = -2\pi a E_\phi(z)$ volts per unit current in the driving loop.

#	F MHZ	ϵ_r	μ_r	2a inches	2h inches	h/a	Ω	ak_o	k_1h	ak_1
1	10	11	18-j.036	.625	22.5	36	8.5534	.00166	.80-j.0008	.022-j.0002
2	50	11-j.11	19-j.054	.625	22.5	36	8.5534	.00831	4.12-j.0059	.114-j.0002
3	100	11-j.3	20-j.089	.625	22.5	36	8.5534	.01662	8.46-j.0188	.235-j.0005
4	5	11	100-j.1	1	21	21	7.4754	.00133	.88-j.0044	.042-j.0002
5	10	11	115-j2.55	1	21	21	7.4754	.00266	1.89-j.021	.090-j.001
6	15	10.5	125-j12.5	1	21	21	7.4754	.00399	2.96-j.1479	.141-j.007
7	20	10.25	135-j67.5	1	21	21	7.4754	.00532	4.22-j.9970	.201-j.0475
8	5	11	105-j.63	2	21	10.5	6.089	.00266	.90-j.0027	.086-j.0002
9	10	11	120-j2.4	2	21	10.5	6.089	.00532	1.93-j.0193	.184-j.001
10	15	11	150-j15	2	21	10.5	6.089	.00798	3.25-j.1620	.309-j.015
11	20	11.1	140-j42	2	21	10.5	6.089	.01064	4.22-j.6202	.402-j.059

TABLE C-1 Antenna Constants

TABLE C-2 Unnormalized experimental data (Refer to Table C-1 for the numbering scheme and antenna constants).

z cms	Antenna #1 Mag	Antenna #1 Phase	Antenna #2 Mag	Antenna #2 Phase	Antenna #3 Mag	Antenna #3 Phase
0.1	-	-	38	-50	-	-
0.2	130.0	30.4	-	-	-	-
0.3	100.0	30.2	31.5	-48.8	-	-
0.5	-	-	-	-	-	-
0.6	-	-	25.5	-47.9	-	-
0.8	-	-	22.0	-47.5	-	-
1.0	77.0	30	20.5	-47.2	82.5	-
1.5	-	-	16	-47.0	57.0	-
2.0	49.0	30	13	-46.6	44	-169.2
3.0	33.0	30	9.1	-46.4	28.5	-178
4.0	23.0	30	6.4	-46.5	19.0	-182
5.0	17.0	30	4.7	-46.5	13.5	-184
6.0	12.5	30	3.5	-46.5	10.0	-185
7.0	9.25	30	2.65	-46.5	7.7	-185
8.0	7.0	30	2.0	-46.5	6.2	-185
9.0	5.3	30	1.45	-46.8	5.6	-183.5
10.0	4.0	30	1.0	-47	?	?
11.0	3.30	30.5	.8	-47.5	3.1	-184
12.0	2.65	30.6	.63	-48.0	2.35	-185.5
13.0	1.95	30.6	.51	-48.5	1.85	-186
14.0	1.75	30.6	.41	-49	1.45	-186
15.0	1.45	31.2	.34	-50.2	1.20	-186
16.0	1.20	31.6	.285	-51.0	1.02	-186
17.0	.9	32.8	.240	-52	.86	-186
18.0	.75	32.6	.205	-52	.70	-186
19.0	.62	33.0	.175	-52	.59	-186
20.0	.51	33.6	.140	-52	.50	-186
21.0	.42	35			.41	-187
22.0	.36	38.2			.35	-186
23.0	.31	38			.30	-186.5
24.0	.27	38			.26	-188.5
25.0	.22	38			.23	-188
26.0	.19	38			.205	-190

TABLE C-2 (Continued)

z	Antenna #4		Antenna #5		Antenna #6		Antenna #7	
cms	Mag	Phase	Mag	Phase	Mag	Phase	Mag	Phase
.1	-	-	16.0	-129.2	33	-130	5.7	-70
.3	-	-	14.5	-129.2	30.5	-130.2	5.3	-70.2
.5	4.0	-130	13.5	-129.3	28.5	-130.2	4.9	-70.4
1.0	3.5	-130.4	12.0	-129.3	25.5	-130.4	4.5	-70.8
1.5	3.2	-130.4	11.0	-129.4	23.5	-130.5	4.2	-71.2
2.0	3.05	-130.4	10.5	-129.4	22.0	-130.6	3.7	-71.4
2.5	2.85	-130.4	9.8	-129.4	20.5	-130.7	3.5	-71.6
3.0	2.70	-130.2	9.3	-129.5	19.5	-130.8	3.3	-71.8
3.5	2.55	-130.1	8.7	-129.5	18.5	-130.9	3.15	-72.0
4.0	2.45	-130	8.3	-129.6	17.5	-131	3.0	-72.2
4.5	2.30	-130	7.9	-129.6	16.5	-131.0	-	-
5.0	2.15	-130	7.5	-129.6	15.5	-131.2	2.9	-72.2
5.5	2.05	-129.9	7.1	-129.6	15	-131.2	-	-
6.0	1.95	-129.9	6.8	-129.6	14	-131.3	2.75	-72.5
6.5	1.85	-129.8	6.5	-129.7	13.5	-131.4	-	-
7.0	1.80	-129.7	6.2	-129.7	13	-131.4	2.50	-72.8
7.5	-		5.9	-129.7	-	-	-	-
8.0	1.65	-129.7	5.7	-129.7	12	-131.5	2.30	-73.2
9.0	1.50	-129.7	5.2	-129.8	11	-131.6	2.05	-73.6
10	1.37	-129.6	4.7	-129.8	10	-131.7	1.9	-73.8
11	1.25	-129.6	4.3	-129.8	9.2	-131.8	1.75	-74
12	1.15	-129.7	4.0	-129.8	8.5	-131.9	1.60	-74.2
13	1.05	-129.6	3.60	-129.8	7.8	-132.0	1.48	-74.5
14	.99	-129.7	3.30	-129.8	7.1	-132.0	1.35	-74.6
15	.89	-129.5	3.05	-129.9	6.5	-132.1	1.20	-74.6
16	.81	-129.5	2.75	-130	5.9	-132.2	1.08	-74.6
17	.74	-130.0	2.5	-130	5.3	-132.2	1.00	-74.6
18	.66	-129.5	2.2	-130	4.8	-132.2	.89	-75
19	.59	-129.5	2.0	-130	4.2	-132.3	.80	-75
20	.52	-129.3	1.75	-130	3.8	-132.2	.71	-75
21	.46	-129.5	1.55	-130	3.3	-132.3	.66	-75
22	.39	-129.2	1.3	-130	2.9	-132.4	.54	-75
23	.33	-129.2	1.1	-130	2.4	-132.4	.45	-75
24	.26	-129.2	.9	-130	2.0	-132.5	.37	-75

TABLE C-2 (Continued)

z	Antenna #8		Antenna #9		Antenna #10		Antenna #11	
cms	Mag	Phase	Mag	Phase	Mag	Phase	Mag	Phase
.1	6.3	-60	4.4	-50	89	-80	175	-100
.5	5.7	-62.8	3.8	-51.8	84	-79.5	170	-99.2
1	5.4	-64.6	3.3	-53	78	-79	158	-98.4
2	4.8	-66.8	2.8	-54	71.5	-78.2	145	-97.2
3	4.3	-68	2.5	-54.6	66	-77.8	135	-96.5
4	4.0	-68.6	2.23	-55	60	-77.5	125	-96
5	3.7	-69.1	2.05	-55.2	56	-77.2	115	-95.7
6	3.5	-69.4	1.86	-56	52	-77.2	110	-95.4
7	3.2	-69.8	1.72	-56.2	49	-77	105	-95
8	3.05	-70	1.60	-56.3	46	-77	99	-94.6
9	2.90	-70	1.50	-56.4	43	-76.8	93	-94.4
10	2.75	-70	1.40	-56.4	40	-76.8	87	-94.2
11	2.56	-69.4	1.30	-56.4	37	-76.7	80	-94.0
12	2.40	-68.8	1.20	-56.4	35	-76.6	75	-93.7
13	2.25	-68.0	1.15	-56.3	32	-76.6	69	-93.6
14	2.10	-68.2	1.09	-56.1	30	-76.5	64	-93.3
15	1.96	-68.2	1.01	-55.7	28	-76.4	60	-93.3
16	1.85	-68.3	.95	-55.6	26.2	-76.4	55	-93.3
17	1.70	-68	.90	-55.0	24.2	-76.4	51	-93.2
18	1.60	-67.8	.84	-54.8	22	-76.4	47	-93
19	1.5	-67.4	.79	-54.6	20	-76.3	42	-93.0
20	1.36	-67	.73	-54.4	18	-76.3	38	-92.8
21	1.26	-66.5	.67	-54	16.2	-76.2	33	-92.8
22	1.15	-65.6	.62	-53.6	14	-76.2	29	-92.7
23	1.05	-64.6	.56	-53	12	-76.2	25	-92.6
24	.94	-63	.50	-52.2	10	-76.2	20.5	-92.7

COMPUTER PROGRAMS USED TO SOLVE THE COUPLED INTEGRAL EQUATIONS (86a,b):

```
FORTRAN IV G LEVEL  21          MAIN            DATE = 75205      14/42/31

                C     THIS PROGRAM COMPUTES THE AXIAL MAGNETIC AND AZIMUTHAL ELECTRIC
                C     CURRENTS ON A FINITE CIRCULAR LOOP ANTENNA DRIVEN BY A LOOP CARR-
                C     YING CONSTANT CURRENT.
                C
                C     SOLUTION BY THE MOMENT METHOD FOR THE COUPLED
                C     INTEGRAL EQNS # 2,82 OF CHAPTER 2.
                C
                      IMPLICIT COMPLEX*8 (C)
                      DIMENSION CG(20),CK(20,20),CT(10),AA(40,40),CB(10,10),CX(20)
                     2 ,CR1(10,10),CM1T(10),CK2(10,10),CK2T(10),CB2(10,10),CM2T(10)
                      COMMON TAKO,CMUR,TPY,TA,CK1,CAK1,TH,T,TKOT,TK3,IPS
                      INTEGER P
                      EXTERNAL FK11R,FK11I,FK12I,FCTK,FM11R,FM11I,FM12I,
                     2FCTM1,FK2T1R,FK2T1I,FK2T2I,FCTK2,FM21R,FM21I, FM22I,FCTM2
                    1 READ (5,10) TAKO,CMUR,TMDA,TF,CFP
                      IF (TAKO.GT.0.5) GO TO 150
                   10 FORMAT (F9.5,1X,(F10.5,1X))
                      TPY=3.14159265
                      TMUO=4.*TPY*1.E-07
                      TPSUO= (1./(36.*TPY))*1.E-09
                      TKO=TPY*TF/150.
                      TA=TAKO/TKO
                      CK1=TKO*CSQRT(CMUR*CFP)
                      CAK1=CK1*TA
                      WRITE (6,15) TAKO,CMUR,TMDA,TF,CFP
                   15 FORMAT (1H1,5X,'AXIAL MAGNETIC AND TRANSVERSE ELECTRIC CURRENTS',
                     2' ON A FINITE CIRCULAR ANTENNA',//,5X,' AKO = ',F10.5,4X,' MUR = ',
                     3F10.5,' ET ',F10.5,4X,' H/A = ',F10.5,//,5X,'FREQ = ',F4.2,' MHZ '
                     4,//,'IPS = ',F10.5,' ET ',F10.5,//,19X,'(2*PY*A) EPHI(Z)',38X,'IP
                     5HI(Z)',//,6X,'Z/H',8X,'MAG',5X,'PHASE',6X,'REAL',6X,'IMAG',12X,'MA
                     6G',5X,'PHASE',6X,'REAL',6X,'IMAG',//)
                C
                C     COMPUTE THE CONSTANTS IN THE TWO INTEGRAL EQNS. CG IS THE ONLY
                C     UNKNOWN CONSTANT WHICH IS DETERMINED AS A COMPONENT OF MATRIX
                C     SOLUTION.
                C
                      C1=(0.,-.6)*TPY*TF/(TA**2)
                      C2=(0.,-.5)*TPY*TPY/TAKO
                      C3=1./(TAKO*TA*CMUR)
                      C4=2.*C1
                      C10=-1./TA
                C
                C     DIVISION INTO PANELS
                C
                      N=2
                   16 CCALL NOD
                      NP1=N+1
                      TH=TMDA*TAKO/TKO
                      T =TH/(2.*FLOAT(N))
                      TKOT=TKO*T
                C
                C     COMPUTING THE RIGHT HAND SIDE
                C
```

```
            DO 20 I=1,NP1
            T(I)=FLOAT(I) -1.
   20       CG(I)=CZ*SIN(2.*T(I)*TKOT)
            N2=2*NP1
            NP2=NP1+1
            DO 10 I=NP2,N2
   10       CG(I)=(0.,0.)
            I=1
   22       WRITE (6,21) I,CG(I)
   21       FORMAT (5X,'CG(',I2,') = ',F20.5,2X,F20.5)
            I=I+1
            IF (I.LE.N2) GO TO 22
      C
      C     COMPUTING THE ELEMENTS OF REGION I.
      C
      C     COMPUTING K(1,1) BY 10 POINT GAUSS QUADRATURE.
            CALL QG10(0.,50.,FKI1R,YR)
            CALL QG10(0.,50.,FKI1I,YI)
            CK(1,1)=CMPLX(YR,YI)
      C
      C     COMPUTING K(I,1) FOR I=2,N+1
      C
            DO 25 I=2,NP1
            J=1
            CALL QGI10(I,J,FKI1,TR,TI)
            CT(I)=CMPLX(TR,TI)
   25       CK(I,1)=CK(1,1)*.5+CT(I)
      C
      C     COMPUTING K(I,J) FOR I=1,N+1 AND J=I+1,N+1
      C
            DO 30 I=1,NP1
            DO 30 J=I+1,NP1
            CALL QGI10(I,J,FCIK,TR,TI)
            CK(I,J)=CMPLX(TR,TI)
   30       CK(J,I)=CK(I,J)
      C
      C     MODIFYING THE LOWER TRIANGLE ELEMENTS TO OBTAIN THE
      C     KRAW ELEMENTS. THE FIRST COLUMN ELEMENTS ARE HALVED.
      C
            DO 40 I=1,NP1
   40       CK(I,1) =.5*CK(I,1)
            DO 45 I=2,NP1
            IIP2=2*I-2
            DO 45 P=1,IIP2
   45       AA(I,P) = (1./TKOT)*(COS(TKOT*(2*I-P-2))-COS(TKOT*(2*I-P-1)))
      C
      C     COMPUTING B(I,J)FROM THE SERIES
      C
            DO 48 I=1,NP1
            DO 48 J=1,NP1
            CALL SERIES(I,J,(BC)
```

```
   46   CM(I,J)=CBC
C       THE FIRST COLUMN ELEMENTS
        DO 50 I=2,NP1
   50   CK(I,1) =CK(I,1)-AA(I,1)*C3
C       THE DIAGONAL ELEMENTS
C
        DO 55 I=2,N
   55   CK(I,I) =CK(I,I)-AA(I,(2*I-2))*C3
C       THE ELEMENTS IN THE LOWER TRIANGLE BUT NOT IN THE FIRST
C       COLUMN OR THE DIAGONAL.
C
        DO 60 I=3,NP1
        IM1=I-1
        DO 60 J=2,IM1
   60   CK(I,J) =CK(I,J)- C3*(AA(I,2*J-2)+AA(I,2*J-1))
C
C       COMPUTING K1(I,J) ELEMENTS.
C
        DO 62 I=1,NP1
        DO 62 J=1,NP1
   62   CK(I,J)=CK(I,J)+CB(I,J)
C
C       BY NOW ALL THE ELEMENTS IN REGION I ARE COMPUTED.
C
C       COMPUTING ELEMENTS OF REGION II.
C
        CALL QG10(0.,50.,FM1I1R,YR)
        CALL QG10(0.,50.,FM1I1I,YI)
        CM1(1,1)=CMPLX(YR,YI)
        DO 65 I=2,N
        J=1
        CALL QGL10(I,J,FM1I,TR,TI)
        CM1T(I)=CMPLX(TR,TI)
   65   CM1(I,1)=CM1(I,1)*.5+CM1T(I)
        DO 70 I=1,NP1
        IP1=I+1
        DO 70 J=IP1,N
        CALL QGL10(I,J,FC(IF),TR,TI)
        CM1(I,J)=CMPLX(TR,TI)
   70   CM1(J,I)=CM1(I,J)
        DO 75 I=1,NP1
   75   CM1(1,I)=0.5*CM1(2,1)
C
C       BY NOW ALL THE ELEMENTS IN REGION II ARE COMPUTED.
C
C       COMPUTING ELEMENTS IN REGION III.
C
        CALL QG10(0.,50.,FK2I1R,YR)
        CALL QG10(0.,50.,FK2I1I,YI)
        CK2(1,1)=CMPLX(YR,YI)
        DO 80 I=2,NP1
        J=1
        CALL QGL10(I,J,FK2I,TR,TI)
```

```
0097          CK2T(I)=CMPLX(TR,TI)
0098     80   CK2(I,I)=CK2(I,I)+.5*CK2T(I)
0099          DO 85 I=1,NP1
0100          IP1=I+1
0101          DO 85 J=IP1,NP1
0102          CALL OGLIO(I,J,FCTK2,TR,TI)
0103          CK2(I,J)=CMPLX(TR,TI)
0104     85   CK2(J,I)=CK2(I,J)
0105          DO 90 I=1,NP1
0106     90   CK2(I,I)=0.5*CK2(I,I)
        C
        C     BY NOW ALL THE ELEMENTS IN REGION III ARE COMPUTED.
        C
        C     COMPUTING ELEMENTS OF REGION IV.
        C
0107          CALL OGLIO(0.,50.,FM2I1,YR,YI)
0108          CALL OGLIO(0.,50.,FM2I1,YI)
0109          CM2(1,1)=CMPLX(YR,YI)
0110          DO 95 I=2,N
0111          J=1
0112          CALL OGLIO(I,J,FM2I1,TR,TI)
0113          CM2T(I)=CMPLX(TR,TI)
0114     95   CM2(I,I)=CM2(I,I)+.5*CM2T(I)
0115          DO 100 I=1,NP1
0116          IP1=I+1
0117          DO 100 J=IP1,N
0118          CALL OGLIO(I,J,FCTM2,TR,TI)
0119          CM2(I,J)=CMPLX(TR,TI)
0120    100   CM2(J,I)=CM2(I,J)
0121          DO 105 I=1,NP1
0122    105   CM2(I,I)=0.5*CM2(I,I)
        C
        C     BY NOW ALL THE ELEMENTS IN REGION IV ARE COMPUTED.
        C
        C     COMPUTING ELEMENTS OF REGION V
        C
0123          N2P2=2*N+2
0124          DO 110 I=1,NP1
0125    110   CK(2,N2P2)=-COS(TKOI*(2*I-2))
        C
        C     COMPUTING ELEMENTS OF REGION VI.
        C
0126          NP2=N+2
0127          DO 115 I=NP2,N2P2
0128    115   CK(1,N2P2)=(0.,0.)
        C
        C     BY NOW ALL THE ELEMENTS IN REGION V AND VI ARE DONE.
        C
        C     SETTING UP THE FINAL MATRIX CON
        C
0129          N2P1=2*N+1
0130          DO 120 I=1,NP1
0131          DO 120 J=NP2,N2P1
```

```
  120 CK(I,J)=CK1(I,J-NP1)
C
      DO 125 I=NP2,N2P2
      DO 125 J=1,NP1
  125 CK(I,J)=CK2(I-NP1,J)
C
      DO 130 I=NP2,N2P1
      DO 130 J=NP2,N2P1
  130 CK(I,J)=CM2(I-NP1,J-NP1)
C
C
      DO 72 I=1,N2P2
   72 CK(I,NP1)=0.5*CK(I,NP1)
C     BY NOW STEP, THE ENTIRE MATRIX IS COMPUTED. NEXT WE
C     PROCEDE TO SOLVE THE LINEAR SYSTEM OF EQUATIONS.
C
C
      N=N2
      CALL DECOMP(N,CK,CUL)
      CALL SOLVE(N,CUL,CG,CX)
      WRITE (6,66) (CX(I),I=1,N2)
   66 FORMAT (12F10.5)
      CALL IMPRUV(N,CK,CUL,CG,CX,DIGITS)
      WRITE (6,66) (CX(I),I=1,N2)
      CX(N2)=(0.,0.)
C     CONVERT FROM (Z) TO I*(Z)
      INCEM=( 2.*TPY*TAKO/TKO)
      DO 67 I=1,NP1
   67 CX(I)=CX(I)*INCEM
C
C     PRINTOUT OF THE SOLUTION.
C
      I=1
   71 TER=REAL(CX(I))
      TEI=AIMAG(CX(I))
      TIR=REAL(CX(I+N+1))
      TII=AIMAG(CX(I+N+1))
      ZCP=(FLOAT(I)-1.)/(FLOAT(N))
      TEM=CABS(CX(I))
      TEP=ANGLE(TER,TEI)
      TIM=CABS(CX(I+N+1))
      TIP=ANGLE(TIR,TII)
      WRITE (6,73) X,TEM,TEP,TER,TEI,TIM,TIP,TIR,TII
   73 FORMAT (//,5X,F4.2,6X,4(F6.2,3X),4X,4(F6.2,3X))
      I=I+1
      IF (I.LE.NP1) GO TO 71
      CYSTAR=CX(1)
      CZSTAR=1./CYSTAR
      WRITE (6,69) CYSTAR,CZSTAR
   69 FORMAT (5X,//,'ZSTAR = ',2F9.5,5X,'YSTAR = ',2F9.5)
C
C
      GO TO 2
  150 CONTINUE
      END
```

```
      SUBROUTINE  BSLSML(NORD,XYO,XYL)
C     SUBROUTINE 'BSLSML'
C     'BSLSML'  COMPUTES BESSEL  J FUNCTION WITH COMPLEX ARGUMENTS
C     AND ORDERO AND 1. ACCURACY UPTO 6TH DECIMAL PLACE OR MORE IS
C     OBTAINED FOR ABS(Z) LESS THAN 20.
      IMPLICIT COMPLEX*16(D), REAL*8(T)
      COMPLEX  XYO,XYL
      DZZ=XYO
      N=NORD
      TX=REAL(DZZ)
      TY=AIMAG(DZZ)
      X=TX
      Y=TY
      TX=D.5D0*TX
      TY=D.5D0*TY
      TR=TX*TX-TY*TY
      TF=2.D0*TX*TY
      R=N
      ETC=10.C
      L=(SQRT(R*R+10.0*(X*X+Y*Y))+R)+ETC
      TFR=1.D0
      TFI=0.D0
      II=(L+1)*(N+L+1)
      JJ=-(2*L+N+2)
      DO 400 K=1,L
      TF=II*(JJ+K)+K
      TGR=TR/TF
      TGI=TI/TF
      TC=TFR
      TFR=1.D0-TGR*TFR+TGI*TFI
  400 TFI=-(TGR*TFI+TGI*TC)
      IF (N.EQ.0)-GO TO 401
      IF (N.GT.0) GO TO 402
  401 CONTINUE
      DCOSLJ=DCMPLX(TFR,TFI)
      XYL=DCOSLJ
      RETURN
  402 TGR=1.D0
      TGI=0.DC
      NN=N
  403 TC=TGR
      TGR=TGR*TX-TGI*TY
      TGI=TC*TY+TGI*TX
      NN=NN-1
      IF (NN.GT.0) GO TO 403
      TN=1.DC
      DO 404 M=1,N
      TMP=TN
  404 TN=TN*TMP
      TGR=TGR/TN
      TGI=TGI/TN
      TC=TFR
      TFR=TFR*TGR-TFI*TGI
      TFI=TC*TGI+TFI*TGR
      GO TO 401
      END
```

```
      SUBROUTINE BESH(XYO,N,KIND,XYL,IER)
C  SUBROUTINE  'BESH'
C  'BESH' COMPUTES HANKEL FUNCTION WITH COMPLEX ARGUEMENTS.
      IMPLICIT COMPLEX*16(D),REAL*8(T)
      COMPLEX XYO,XYL
      DIMENSION DT(12),DTT(6),DTX(6)
      DX=XYO
      IF(N.EQ.0.AND.KIND.EQ.1) GO TO 300
      IF(N.EQ.0.AND.KIND.EQ.2) GO TO 400
      IF(N.EQ.1.AND.KIND.EQ.1) GO TO 300
      IF(N.EQ.1.AND.KIND.EQ.2) GO TO 400
  300 DX=DX*DCMPLX(0.D0,-1.D0)
      GO TO 500
  400 DX=DX*DCMPLX(0.D0,1.D0)
      GO TO 500
  500 TRX=REAL(DX)
      TIX=AIMAG(DX)
      TMAG=DSQRT(TRX**2+TIX**2)
      DBK=DCMPLX(0.D0,0.D0)
      TPI=3.14159265
      IF(N) 10,20,20
   10 IER=1
      RETURN
   20 IF (TMAG-170.D0) 22,22,21
   21 IER=3
      RETURN
   22 IER=0
      IF (TMAG-1.D0) 36,36,25
   25 DA=CDEXP(-DX)
      DB=1.D0/DX
      DC=CDSQRT(DB)
      IF(REAL(DC))100,101,101
  100 DC=-DC
  101 CONTINUE
      DT(1)=DB
      DO 26 L=2,12
   26 DT(L)=DT(L-1)*DB
      DTT(1)=(DX/3.7500)**2
      DO 600 LL=2,6
  600 DTT(LL)=DTT(LL-1)*DTT(1)
      DTX(1)=(DX/2.D0)**2
      DO 605 LLL=2,6
  605 DTX(LLL)=DTX(LLL-1)*DTX(1)
      IF(N-1) 627,270,627
  627 IF(TMAG-2.0D0) 610,610,27
C     COMPUTE IO AND THEN KO
  610 DIO=1.D0+3.5156229D0*DTT(1)+3.0899424D0*DTT(2)
     1+1.2067492D0*DTT(3)+.2659732D0*DTT(4)+.0360768D0*DTT(5)
     2+.0045813D0*DTT(6)
      DQO=-CDLOG(DX/2.D0)*DIO-.57721566D0+.42278420D0*DTX(1)
     1+.23069756D0*DTX(2)+.03488590D0*DTX(3)+.00262698D0*DTX(4)
     2+.00010750D0*DTX(5)+.0000074D0*DTX(6)
      IF(N) 20,628,629
  628 DBK=DQO
      GO TO 200
C
C     COMPUTE KO USING POLYNOMIAL APPROXIMATION
C
   27 DQO=DA*(1.25331414D0-.15666418D0*DT(1)+.08811128D0*DT(2)
     2-.09139095D0*DT(3)+.13445962D0*DT(4)-.22998503D0*DT(5)
     3+.37924097D0*DT(6)-.52472773D0*DT(7)+.55753684D0*DT(8)
     4-.42626329D0*DT(9)+.21845181D0*DT(10)-.06680977D0*DT(11)
```

```
     5+.00918938300*DT(12))*DC
      IF(N)20,28,29
  28  DBK=DGO
      GO TO 200
C     COMPUTE J1 AND THEN K1
 270  IF(IMAG-2.00D0)-629,629,29
 629  DI1=DX*(.5D0+.8789059*D0*DTT(1)+.51498869D0*DTT(2)
     1+.15084934D0*DTT(3)+.02658733D0*DTT(4)+.00301532D0*DTT(5)
     2+.00032411D0*DTT(6))
      DG1=CDLOG(DX/2.D0)*DI1+(1.D0/DX)*(1.D0+.15443144D0*DTX(1)
     1+.67278579D0*DTX(2)+.18156897D0*DTX(3)+.01919402D0*DTX(4)
     2+.00110404D0*DTX(5)+.00004686D0*DTX(6))
      IF (N-1) 20,630,31
 630  DBK=DG1
      GO TO 200
C
C     COMPUTE K1 USING POLYNOMIAL APPROXIMATION
C
  29  DG1=DA*(1.2533141D0+.4699927D0*DT(1)+.1468583D0*DT(2)
     2+.12804266D0*DT(3)+.01736431D0*DT(4)+.2847618ID0*DT(5)
     3+.45943421D0*DT(6)+.62833807D0*DT(7)+.66322954D0*DT(8)
     4+.50502386D0*DT(9)+.25813038D0*DT(10)+.07880012D0*DT(11)
     5+.01082417D0*DT(12))*DC
      IF(N-1)20,30,31
  30  DBK=DG1
      GO TO 200
C
C     FROM K0,K1 COMPUTE KN USING RECURRENCE RELATION
C
  31  DO 35 J=2,N
      DGJ=2.D0*(FLOAT(J)-1.D0)*DG1/DX+DG0
      IF(CDABS(DGJ)-1.D70) 33,33,32
  32  IER=4
      GO TO 34
  33  DGO=DG1
  35  DG1=DGJ
  34  DBK=DGJ
      GO TO 200
  36  DB=DX/2.D0
      IF (REAL(DB)) 70,71,70
  71  IF (AIMAG(DB)) 72,70,73
  72  TANG=-TPI/2.D0
      GO TO 75
  73  TANG=TPI/2.D0
  75  TABS=CDABS(DB)
      TAR=0.57721660D0+DLOG(TABS)
      DA=DCMPLX(TAR,TANG)
      GO TO 76
  70  DA=0.5772156600+CDLOG(DB)
  76  DC=DB*DB
      IF(N-1)37,43,37
C
C     COMPUTE K0 USING SERIES EXPANSION
C
  37  DGO=-DA
      DX2J=DCMPLX(1.D0,0.D0)
      TFACT=1.D0
      THJ=0.D0
      DO 40 J=1,6
      TRJ=1.D0/FLOAT(J)
      DX2J=DX2J*DC
      TFACT=TFACT*TRJ*TRJ
      THJ=THJ+TRJ
```

```
      40 DGO=DGO+DX2J*TFACT*(THJ-DA)
         IF(N)43,42,43
      42 DBK=DGO
         GO TO 200
C
C     COMPUTE K1 USING SERIES EXPANSION
C
      43 DX2J=DB
         TFACT=1.DO
         THJ=1.DC
         DG1=1.DC/DX+DX2J*(.5DO*DA-THJ)
         DO 50 J=2,8
         DX2J=DX2J*DC
         TRJ=1.DO/FLOAT(J)
         TFACT=TFACT*TRJ*TRJ
         THJ=THJ+TRJ
      50 DG1=DG1+DX2J*TFACT*(.5DO*(DA-THJ)+FLOAT(J))
         IF(N-1)31,52,31
      52 DBK=DG1
C
C     COMPUTE HANKEL FUNCTION USING K0 AND K1
C
      200 IF(N.EQ.0.AND.KIND.EQ.1) GO TO 110
          IF(N.EQ.0.AND.KIND.EQ.2) GO TO 115
          IF(N.EQ.1.AND.KIND.EQ.1) GO TO 120
          IF(N.EQ.1.AND.KIND.EQ.2) GO TO 120
      110 DBK=-2.DO*DCMPLX(0.DO,1.DO)*DBK/TPI
          GO TO 130
      115 DBK=2.DO*DCMPLX(0.DO,1.DO)*DBK/TPI
          GO TO 130
      120 DBK=-2.DO*DBK/TPI
      130 CONTINUE
          XYL=DBK
          RETURN
          END
```

```
      SUBROUTINE GG10(XL,XU,F,Y)
      A=.5*(XU+XL)
      B=XU-XL
      C=.4869533*B
      Y=.03333567*(F(A+C)+F(A-C))
      C=.4325317*B
      Y=Y+.07472567*(F(A+C)+F(A-C))
      C=.3397048*B
      Y=Y+.1095432*(F(A+C)+F(A-C))
      C=.2166977*B
      Y=Y+.1346334*(F(A+C)+F(A-C))
      C=.0744371?*B
      Y=B*(Y+.1477621*(F(A+C)+F(A-C)))
      RETURN
      END
```

```
FORTRAN IV G LEVEL  21          FKII          DATE = 75205      14/42/31

0001          SUBROUTINE FKII(MI,MJ,X,TR,TI)
0002          IMPLICIT COMPLEX*8(C),REAL*4(T)
0003          COMMON TAKO,CMUR,TPY,TA,CK1,CAK1,TH,T,TKOT,TKO,IPS
0004          CKOT=(0.,1.)*TKOT
0005          CY=1.+(0.,1.)*(X/TKOT)
0006          CY2=CY**2
0007          CV=TAKO*CSQRT(1.-CY2)
0008          CALL WSLSHL(0,CV,CJ)
0009          CJ2=CJ**2
0010          I4=4*MI-4
0011          TI4=FLOAT(I4)
0012          CF=CEXP(CKOT*TI4)
0013          CIP=CEXP(CKOT)
0014          CIM=CEXP(-CKOT)
0015          I44=4*MI-4
0016          TI4=FLOAT(I44)
0017          I46=4*MI-6
0018          TI6=FLOAT(I46)
0019          TI11=EXP(-X*TI4)
0020          TI12=EXP(-X*TI6)
0021          CFX=CF*CJ2*(CIP*TI11-CIM*TI12)/(CKOT*CV)
0022          TR=REAL(CFX)
0023          TI=AIMAG(CFX)
0024          RETURN
0025          END
```

```
FORTRAN IV G LEVEL  21          FMII          DATE = 75205      14/42/31

0001          SUBROUTINE FMII(MI,MJ,X,TM,TI)
0002          IMPLICIT COMPLEX*8(C),REAL*4(T)
0003          COMMON TAKO,CMUR,TPY,TA,CK1,CAK1,TH,T,TKOT,TKO,IPS
0004          CKOT=(0.,1.)*TKOT
0005          CY=1.+(0.,1.)*(X/TKOT)
0006          CY2=CY**2
0007          CV=TAKO*CSQRT(1.-CY2)
0008          CALL WSLSHL(0,CV,CJ)
0009          CJ2=CJ**2
0010          I4=4*MI-4
0011          TI4=FLOAT(I4)
0012          CF=CEXP(CKOT*TI4)
0013          CIP=CEXP(CKOT)
0014          CIM=CEXP(-CKOT)
0015          I44=4*MI-4
0016          TI4=FLOAT(I44)
0017          I46=4*MI-6
0018          TI6=FLOAT(I46)
0019          TI11=EXP(-X*TI4)
0020          TI12=EXP(-X*TI6)
0021          CFX=CF*CJ2*(CIP*TI11-CIM*TI12)/(CKOT*CV)
0022          CFX=CFX*TA*TA/CV
0023          TM=REAL(CFX)
0024          TI=AIMAG(CFX)
0025          RETURN
0026          END
```

```
FORTRAN IV G LEVEL 21                FK211                DATE = 75205

0001          SUBROUTINE FK211(MI,MJ,X,TR,TI)
0002          IMPLICIT COMPLEX*8(C),REAL*4(T)
0003          COMMON TAKO,CHUR,TPY,TA,CK1,CAK1,TH,T,TKOT,TKO,IPS
0004          CKOT=(0.,1.)*TKOT
0005          CY=1.+(0.,1.)*(X/TKOT)
0006          CY2=CY**2
0007          CV=TAKO*CSQRT(1.-CY2)
0008          CALL BESSHL(0,CV,CJ)
0009          CJ2=CJ**2
0010          I4=4*MI-4
0011          TI4=FLOAT(I4)
0012          CF=CEXP(CKOT*TI4)
0013          CIP=CEXP(CKOT)
0014          CIM=CEXP(-CKOT)
0015          I44=4*MI-4
0016          TI4=FLOAT(I44)
0017          I46=4*MI-6
0018          TI6=FLOAT(I46)
0019          TI1=EXP(-X*TI4)
0020          TI2=EXP(-X*TI6)
0021          CFX=CF*CJ2*(CIP*TI1I-CIM*TI12)/(CKOT*CV)
0022          CFX=CFX/(TA*CV)
0023          TR=REAL(CFX)
0024          TI=AIMAG(CFX)
0025          RETURN
0026          END
```

```
FORTRAN IV G LEVEL 21                FK211                DATE = 75205

0001          SUBROUTINE FK211(MI,MJ,X,TR,TI)
0002          IMPLICIT COMPLEX*8(C),REAL*4(T)
0003          COMMON TAKO,CHUR,TPY,TA,CK1,CAK1,TH,T,TKOT,TKO,IPS
0004          CKOT=(0.,1.)*TKOT
0005          CY=1.+(0.,1.)*(X/TKOT)
0006          CY2=CY**2
0007          CV=TAKO*CSQRT(1.-CY2)
0008          CALL BESSHL(0,CV,CJ)
0009          CJ2=CJ**2
0010          I4=4*MI-4
0011          TI4=FLOAT(I4)
0012          CF=CEXP(CKOT*TI4)
0013          CIP=CEXP(CKOT)
0014          CIM=CEXP(-CKOT)
0015          I44=4*MI-4
0016          TI4=FLOAT(I44)
0017          I46=4*MI-6
0018          TI6=FLOAT(I46)
0019          TI1=EXP(-X*TI4)
0020          TI2=EXP(-X*TI6)
0021          CFX=CF*CJ2*(CIP*TI1I-CIM*TI12)/(CKOT*CV)
0022          CFX=-CFX*TA*TPY
0023          TR=REAL(CFX)
0024          TI=AIMAG(CFX)
0025          RETURN
0026          END
```

```
FORTRAN IV G LEVEL  21                  FKIIR                   DATE = 75205

0001              FUNCTION FKIIR(YE)
0002              IMPLICIT COMPLEX*8(C),REAL*4(T)
0003              COMMON TAKO,CMUR,TPY,TA,CK1,CAK1,TH,T,TKOT,TKO,IPS
0004              YE2=YE**2
0005              CU=TAKO*CSQRT((1.-YE2)*(1.,0.))
0006              CU1=CU
0007              CALL BSLSML(0,CU,CJ)
0008              CALL BESH(CU1,0,1,CH,IER)
0009              CF=(0.,4.)*CJ*CH*SIN(TKOT*YE)/YE
0010              FKIIR= REAL(CF)
0011              RETURN
0012              END

FORTRAN IV G LEVEL  21                  FKIII                   DATE = 75205

0001              FUNCTION FKIII(YE)
0002              IMPLICIT COMPLEX*8(C),REAL*4(T)
0003              COMMON TAKO,CMUR,TPY,TA,CK1,CAK1,TH,T,TKOT,TKO,IPS
0004              YE2=YE**2
0005              CU=TAKO*CSQRT((1.-YE2)*(1.,0.))
0006              CU1=CU
0007              CALL BSLSML(0,CU,CJ)
0008              CALL BESH(CU1,0,1,CH,IER)
0009              CF=(0.,4.)*CJ*CH*SIN(TKOT*YE)/YE
0010              FKIII=AIMAG(CF)
0011              RETURN
0012              END

FORTRAN IV G LEVEL  21                  FMIIII                  DATE = 75205

0001              FUNCTION FMIIII(YE)
0002              IMPLICIT COMPLEX*8(C),REAL*4(T)
0003              COMMON TAKO,CMUR,TPY,TA,CK1,CAK1,TH,T,TKOT,TKO,IPS
0004              YE2=YE**2
0005              CU=TAKO*CSQRT((1.-YE2)*(1.,0.))
0006              CU1=CU
0007              CALL BSLSML(1,CU,CJ)
0008              CALL BESH(CU1,0,1,CH,IER)
0009              CF=(0.,4.)*TA*CJ*CH*SIN(TKOT*YE)/(YE*(1.-YE2)*TKO)
0010              FMIIII=AIMAG(CF)
0011              RETURN
0012              END

FORTRAN IV G LEVEL  21                  FMIIIR                  DATE = 75205

0001              FUNCTION FMIIIR(YE)
0002              IMPLICIT COMPLEX*8(C),REAL*4(T)
0003              COMMON TAKO,CMUR,TPY,TA,CK1,CAK1,TH,T,TKOT,TKO,IPS
0004              YE2=YE**2
0005              CU=TAKO*CSQRT((1.-YE2)*(1.,0.))
0006              CU1=CU
0007              CALL BSLSML(1,CU,CJ)
0008              CALL BESH(CU1,0,1,CH,IER)
0009              CF=(0.,4.)*TA*CJ*CH*SIN(TKOT*YE)/(YE*(1.-YE2)*TKO)
0010              FMIIIR=REAL(CF)
0011              RETURN
0012              END
```

```
FORTRAN IV G LEVEL  21                  FK211R                  DATE = 75205

0001              FUNCTION FK211R(YE)
0002              IMPLICIT COMPLEX*8(C),REAL*4(T)
0003              COMMON TAKO,CMUR,TPY,TA,CK1,CAK1,TH,T,TKOT,TKO,IPS
0004              YE2=YE**2
0005              CU=TAKO*CSQRT((1.-YE2)*(1.,0.))
0006              CU1=CU
0007              CALL RSLSML(0,CU,CJ)
0008              CALL RESH(CU1,1.,1,CH,TFR)
0009              CE=(0.,-4.)*TKO*(1.-YE2)*CJ*CH*SIN(TKOT*YE)/YE
0010              FK211R=REAL(CE)
0011              RETURN
0012              END

FORTRAN IV G LEVEL  21                  FK211I                  DATE = 75205

0001              FUNCTION FK211I(YE)
0002              IMPLICIT COMPLEX*8(C),REAL*4(T)
0003              COMMON TAKO,CMUR,TPY,TA,CK1,CAK1,TH,T,TKOT,TKO,IPS
0004              YE2=YE**2
0005              CU=TAKO*CSQRT((1.-YE2)*(1.,0.))
0006              CU1=CU
0007              CALL RSLSML(0,CU,CJ)
0008              CALL RESH(CU1,1.,1,CH,TFR)
0009              CE=(0.,-4.)*TKO*(1.-YE2)*CJ*CH*SIN(TKOT*YE)/YE
0010              FK211I=AIMAG(CE)
0011              RETURN
0012              END

FORTRAN IV G LEVEL  21                  FK211R                  DATE = 75205

0001              FUNCTION FK211R(YE)
0002              COMMON TAKO,CMUR,TPY,TA,CK1,CAK1,TH,T,TKOT,TKO,IPS
0003              IMPLICIT COMPLEX*8(C),REAL*4(T)
0004              YE2=YE**2
0005              CU=TAKO*CSQRT((1.-YE2)*(1.,0.))
0006              CU1=CU
0007              CALL RSLSML(1,CU,CJ)
0008              CALL RESH(CU1,1.,1,CH,TFR)
0009              CE=(0.,4.)*TA*CJ*CH*SIN(TKOT*YE)/YE
0010              FK211R=REAL(CE)
0011              RETURN
0012              END

FORTRAN IV G LEVEL  21                  FK211I                  DATE = 75205

0001              FUNCTION FK211I(YE)
0002              IMPLICIT COMPLEX*8(C),REAL*4(T)
0003              COMMON TAKO,CMUR,TPY,TA,CK1,CAK1,TH,T,TKOT,TKO,IPS
0004              YE2=YE**2
0005              CU=TAKO*CSQRT((1.-YE2)*(1.,0.))
0006              CU1=CU
0007              CALL RSLSML(1,CU,CJ)
0008              CALL RESH(CU1,1.,1,CH,TFR)
0009              CE=(0.,4.)*TA*CJ*CH*SIN(TKOT*YE)/YE
0010              FK211I=AIMAG(CE)
0011              RETURN
0012              END
```

```
FORTRAN IV G LEVEL 21                FCTK                DATE = 75205

0001          SUBROUTINE FCTK(MI,MJ,X,TR,TI)
0002          IMPLICIT COMPLEX*8(C),REAL*4(T)
0003          COMMON TAKO,CMUR,TPY,TA,CK1,CAK1,TH,T,TKOT,TKO,IPS
0004          CY=1.+(0.,1.)*(X/TKOT)
0005          CY2=CY**2
0006          CV=TAKO*CSQRT(1.-CY2)
0007          CALL BSLSPL(0,CV,CJ)
0008          CJ2=CJ**2
0009          I2=2*MI-2
0010          FI2=FLOAT(I2)
0011          TKOZ=TKOT*FI2
0012          CKOZ=(0.,1.)*TKOZ
0013          CF=CEXP(CKOZ)
0014          CALL AUX(MI,MJ,X,TR,TI)
0015          C1=CMPLX(TR,TI)
0016          CFX=CF*CJ2*C1/(CKOT*CY)
0017          TR=REAL(CFX)
0018          TI=AIMAG(CFX)
0019          RETURN
0020          END


FORTRAN IV G LEVEL 21                FCTMI               DATE = 75205

0001          SUBROUTINE FCTMI(MI,MJ,X,TR,TI)
0002          IMPLICIT COMPLEX*8(C),REAL*4(T)
0003          COMMON TAKO,CMUR,TPY,TA,CK1,CAK1,TH,T,TKOT,TKO,IPS
0004          CY=1.+(0.,1.)*(X/TKOT)
0005          CY2=CY**2
0006          CV=TAKO*CSQRT(1.-CY2)
0007          CV1=CV
0008          CVG=CV
0009          CALL BSLSPL(0,CVG,CJ0)
0010          CALL BSLSPL(1,CV1,CJ1)
0011          CJ2=CJ0*CJ1
0012          I2=2*MI-2
0013          FI2=FLOAT(I2)
0014          TKOZ=TKOT*FI2
0015          CKOZ=(0.,1.)*TKOZ
0016          CF=CEXP(CKOZ)
0017          CALL AUX(MI,MJ,X,TR,TI)
0018          C1=CMPLX(TR,TI)
0019          CFX=CF*CJ2*C1*TA*TA/((0.,1.)*TKOT*CV*CV)
0020          TR=REAL(CFX)
0021          TI=AIMAG(CFX)
0022          RETURN
0023          END
```

```
FORTRAN IV G LEVEL  21                  FCTK2                   DATE = 75205

0001          SUBROUTINE FCTK2(MI,MJ,X,TR,TI)
0002          IMPLICIT COMPLEX*8(C),REAL*4(T)
0003          COMMON TAKO,CMUR,TPY,TA,CK1,CAK1,TH,T,TKOT,TKO,IPS
0004          CY=1.+(0.,1.)*(X/TKOT)
0005          CY2=CY**2
0006          CV=TAKO*CSQRT(1.-CY2)
0007          CV1=CV
0008          CV0=CV
0009          CALL BSLSML(0,CV0,CJ0)
0010          CALL BSLSML(1,CV1,CJ1)
0011          CJ2=CJ0*CJ1
0012          I2=2*MI-2
0013          TI2=FLOAT(I2)
0014          TKO7=TKOT*TI2
0015          CKOZ=(0.,1.)*TKOZ
0016          CF=CEXP(CKOZ)
0017          CALL AUX(MI,MJ,X,TR,TI)
0018          C1=CMPLX(TR,TI)
0019          CFX=-CF*CJ2*CV*C1*4./(TA*TKOT*CY)
0020          TR=REAL(CFX)
0021          TI=AIMAG(CFX)
0022          RETURN
0023          END
```

```
FORTRAN IV G LEVEL  21                  FCTM2                   DATE = 75205

0001          SUBROUTINE FCTM2(MI,MJ,X,TR,TI)
0002          IMPLICIT COMPLEX*8(C),REAL*4(T)
0003          COMMON TAKO,CMUR,TPY,TA,CK1,CAK1,TH,T,TKOT,TKO,IPS
0004          CY=1.+(0.,1.)*(X/TKOT)
0005          CY2=CY**2
0006          CV=TAKO*CSQRT(1.-CY2)
0007          CALL BSLSML(1,CV,CJ1)
0008          CJ2=CJ1**2
0009          I2=2*MI-2
0010          TI2=FLOAT(I2)
0011          TKO7=TKOT*TI2
0012          CKO7=(0.,1.)*TKO7
0013          CF=CEXP(CKO7)
0014          CALL AUX(MI,MJ,X,TR,TI)
0015          C1=CMPLX(TR,TI)
0016          CFX=-4.*CF*CJ2*C1/(TKOT*CY)
0017          TR=REAL(CFX)
0018          TI=AIMAG(CFX)
0019          RETURN
0020          END
```

```
FORTRAN IV G LEVEL  21                  DECOMP                  DATE = 75195

0001                  SUBROUTINE  DECOMP(NN, A, UL)
0002                  DIMENSION SCALES(35),IPS(35)
0003                  COMPLEX A(35,35),UL(35,35),PIVOT,EM
0004                  COMMON TAKO,TPY,TKOT,IPS
0005                  N=NN
                C
                C     INITIALIZE  IPS,UL AND SCALES
0006                  DO 5 I=1,N
0007                  IPS(I)=I
0008                     ROWNRM=0.0
0009                     DO 2  J=1,N
0010                       UL(I,J)= A(I,J)
0011                  IF(ROWNRM-CABS(UL(I,J))) 1,2,2
0012               1  ROWNRM= CABS(UL(I,J))
0013               2   CONTINUE
0014                  IF(ROWNRM) 3,4,3
0015               3  SCALES(I)=1.0/ROWNRM
0016                  GO TO 5
0017               4  CALL  SING(1)
0018                  SCALES(I)=0.0
0019               5  CONTINUE
                C
                C     GAUSSIAN ELIMINATION WITH PARTIAL PIVOTING
0020                  NM1=N-1
0021                  DO  17  K=1,NM1
0022                  BIG=0.0
0023                  DO  11  I=K,N
0024                  IP=IPS(I)
0025                  SIZE= CABS(UL(IP,K))*SCALES(IP)
0026                  IF(SIZE-BIG) 11,11,10
0027              10  BIG=SIZE
0028                  IDXPIV=I
0029              11   CONTINUE
0030                  IF(BIG) 13,12,13
0031              12   CALL  SING(2)
0032                  GO TO 17
0033              13   IF(IDXPIV-K) 14,15,14
0034              14   J=IPS(K)
0035                  IPS(K)=IPS(IDXPIV)
0036                  IPS(IDXPIV)=J
0037              15  KP = IPS(K)
0038                  PIVOT=UL(KP,K)
0039                  KP1=K+1
0040                  DO 16  I=KP1,N
0041                  IP=IPS(I)
0042                  EM=-UL(IP,K)/PIVOT
0043                  UL(IP,K)=-EM
0044                  DO  16  J=KP1,N
0045                  UL(IP,J)=UL(IP,J)+EM*UL(KP,J)
                C     INNER LOOP.
0046              16   CONTINUE
0047              17   CONTINUE
0048                  KP=IPS(N)
0049                  IF(CABS(UL(KP,N))) 19,18,19
0050              18   CALL  SING(2)
0051              19   RETURN
0052                  END
```

```
FORTRAN IV G LEVEL  21                SOLVE                DATE = 75195

0001                  SUBROUTINE SOLVE(NN,UL,B,X)
0002                  DIMENSION IPS(35)
0003                  COMPLEX UL(35,35),B(35),X(35),SUM
0004                  COMMON TAKO,TPY,TKOT,IPS
0005                  N=NN
0006                  NP1= N+1
                C
0007                  IP=IPS(1)
0008                  X(1) =B(IP)
0009                  DO 2  I=2,N
0010                  IP=IPS(I)
0011                  IM1=I-1
0012                  SUM=(0.,0.)
0013                  DO  1  J=1,IM1
0014              1   SUM=SUM+UL(IP,J)*X(J)
0015              2   X(I)=B(IP)-SUM
                C
0016                  IP=IPS(N)
0017                  X(N)= X(N)/UL(IP,N)
0018                  DO  4  IBACK=2,N
0019                  I=NP1-IBACK
                C   I  GOES (N-1),....,1
0020                  IP=IPS(I)
0021                  IP1=I+1
0022                  SUM=(0.,0.)
0023                  DO  3  J=IP1,N
0024              3    SUM=SUM+UL(IP,J)*X(J)
0025              4   X(I)=(X(I)-SUM)/UL(IP,I)
0026                  RETURN
0027                  END

FORTRAN IV G LEVEL  21                ANGLE                DATE = 75195

0001                  FUNCTION ANGLE(X,Y)
0002                  COEFT=57.29577951
0003                  IF(X)550,500,450
0004            500   IF(Y) 350,300,250
0005            300   ANGLE =0.0
0006                  RETURN
0007            350   ANGLE=270.0
0008                  RETURN
0009            250   ANGLE =90.0
0010                  RETURN
0011            450   IF(Y) 455,454,453
0012            454   ANGLE=0.0
0013                  RETURN
0014            453   ANGLE=COEFT*ATAN(Y/X)
0015                  RETURN
0016            455   ANGLE=-COEFT*ATAN(-Y/X)+360.0
0017                  RETURN
0018            550   XN=-X
0019                  IF(Y)554,553,552
0020            553   ANGLE=180.0
0021                  RETURN
0022            552   ANGLE=180.0-COEFT*ATAN(Y/XN)
0023                  RETURN
0024            554   ANGLE=180.0+COEFT*ATAN(-Y/XN)
0025                  RETURN
0026                  END
```

FORTRAN IV G LEVEL 21 IMPRUV DATE = 75195

```
0001            SUBROUTINE IMPRUV(NN,A,UL,B,X,DIGITS)
0002            COMMON TAKO,TPY,TKOT,IPS
0003            COMPLEX A(35,35),UL(35,35),B(35),X(35),R(35),DX(35),T
0004            COMPLEX*16  SUM,AIJ,XJ
              C USES  ABS(),AMAX1(),ALOG10()
0005            N=NN
              C
0006            EPS=1.0E-8
0007            ITMAX=16
              C  **EPS AND ITMAX ARE MACHINE DEPENDENT.
              C
0008            XNORM=0.0
0009            DO 1  I=1,N
0010          1 XNORM=AMAX1(XNORM,CABS(X(I)))
0011            IF(XNORM) 3 ,2,3
0012          2 DIGITS = -ALOG10(EPS)
0013            GO TO 10
              C
0014          3 DO 9  ITER=1,ITMAX
0015            DO 5 I=1,N
0016            SUM=0.0
0017            DO  4  J=1,N
0018            AIJ=A(I,J)
0019            XJ=X(J)
0020          4 SUM=SUM+AIJ*XJ
0021            SUM=B(I)-SUM
0022          5 R(I)=SUM
              C  **IT IS ESSENTIAL THAT A(I,J)*X(J) YIELD A DOUBLE PRECISION
              C   RESULT AND THAT THE ABOVE + AND - BE DOUBLE PRECISION.**
0023            CALL  SOLVE(N,UL,R,DX)
0024            DXNORM=0.0
0025            DO 6 I=1,N
0026            T=X(I)
0027            X(I)=X(I) +DX(I)
0028            DXNORM=AMAX1(DXNORM, CABS(X(I)-T))
0029          6 CONTINUE
0030            IF(ITER-1) 8,7,8
0031          7   DIGITS=-ALOG10(AMAX1(DXNORM/XNORM,EPS))
0032          8 IF(DXNORM-EPS*XNORM) 10,10,9
0033          9 CONTINUE
              C  ITERATION DID NOT CONVERGE
0034            CALL SING(3)
0035         10 RETURN
0036            END
```

```
      SUBROUTINE SERIES(MI,MJ,C8)
      IMPLICIT COMPLEX*8(C),REAL*4(T)
      DIMENSION CSUM(30)
      COMMON TAKO,CMUR,TPY,TA,CK1,CAK1,TH,T,TKOT,TKO,IPS
      TI1=FLOAT(MI)-1.
      TJ1=FLOAT(MJ)*2.-1.
      TJ3=FLOAT(MJ)*2.-3.
      K=2
      CSUM(K-1)=(0.,0.)
      CCON=-4./(TPY*CMUR)
      TN=0.
    5 TP=(TN+.5)*(TPY/TH)
      CS=1.-((TP/CK1)**2)
      CZ=CAK1*CSQRT(CS)
      CZ1=CZ
      CZO=CZ
      CALL BSLSML(0,CZO,CJ0)
      CALL BSLSML(1,CZ1,CJ1)
      TAP=TA*TP
      COEFT=(CJ0*CZ/CJ1)-TAP-0.5
      TC1=COS(2.*TP*TI1)
      TC2=COS(2.*TKOT*TI1)
      TS1=SIN(TPT*TJ1)
      TS2=SIN(TPT*TJ3)
      TDR=(TN+0.5)*(TAKO**2-TAP**2)
      TF=((TC1-TC2)*(TS1-TS2))/TDR
      CSUM(K)=CSUM(K-1)+COEFT*TF
      T1=CABS(CSUM(K))
      T2=CABS(CSUM(K-1))
      ERR=ABS((T1-T2)/T1)
      IF (ERR.LE.1.E-03) GO TO 20
      K=K+1
      TN=TN+1
      IF (K.LE.26) GO TO 15
      WRITE (6,16)
   16 FORMAT (5X,'ERROR CRITERION UNSATISFIED IN 25 TERMS',///)
      C8=(0.,0.)
      RETURN
   15 GO TO 5
   20 C8=CCON*CSUM(K)
      RETURN
      END
```

```
      SUBROUTINE AUX(MI,MJ,X,TR,TI)
      IMPLICIT COMPLEX*8(C),REAL*4(T)
      COMMON TAKO,CMUR,TPY,TA,CK1,CAK1,TH,T,TKOT,TKO,IPS
      J1=2*MJ-1
      TJ1=FLOAT(J1)
      J3=2*MJ-3
      TJ3=FLOAT(J3)
      CKOT=(0.,1.)*TKOT
      MIJ4=4*MI+2*MJ-4
      TE1=FLOAT(MIJ4)
      IJ=MI-MJ
      TIJ=FLOAT(IJ)
      TE2=ABS(TIJ)+2.
      MIJ6=2*MI+2*MJ-6
      TE3=FLOAT(MIJ6)
      TE4=TE2-2.
      T1=EXP(-X*TE1)
      T2=EXP(-X*TE2)
      T3=EXP(-X*TE3)
      T4=EXP(-X*TE4)
      C1=CEXP(CKOT*TJ1)
      C2=CEXP(-CKOT*TJ3)
      C3=CEXP(CKOT*TJ3)
      C4=CEXP(-CKOT*TJ1)
      CFX=(C1*T1+C2*T2-C3*T3-C4*T4)
      TR=REAL(CFX)
      TI=AIMAG(CFX)
      RETURN
      END
```

```
      SUBROUTINE GGL10(I,J,FCT,TYR,TYI)
      IMPLICIT COMPLEX*8(C),REAL*4(T)
C
C     10 POINT GAUSS-LAGUERRE QUADRATURE FORMULA OF S.S.P. (IBM)
      TX=29.92070
      CALL  FCT(I,J,TX,TGR,TGI)
      TYR =.9911827E-12* TGR
      TYI=.9911827E-12 *TGI
      TX=21.99659
      CALL  FCT(I,J,TX,TGR,TGI)
      TYR=TYR+.1839565E-8 *  TGR
      TYI=TYI+.1839565E-8  *TGI
      TX=16.27966
      CALL  FCT(I,J,TX,TGR,TGI)
      TYR=TYR+.4249314E-6  * TGR
      TYI=TYI+.4249314E-6 *TGI
      TX=11.84379
      CALL  FCT(I,J,TX,TGR,TGI)
      TYR=TYR+.2825923E-4  *  TGR
      TYI=TYI+.2825923E-4  *  TGI
      TX=8.330159
      CALL  FCT(I,J,TX,TGR,TGI)
      TYR=TYR+.7530084E-3  *  TGR
      TYI=TYI+.7530084E-3  *  TGI
      TX=5.562496
      CALL  FCT(I,J,TX,TGR,TGI)
      TYR=TYR+.009501517  *   TGR
      TYI=TYI+.009501517  *TGI
      TX=3.401434
      CALL  FCT(I,J,TX,TGR,TGI)
      TYR=TYR+.06208746   *   TGR
      TYI=TYI+.06208746   *   TGI
      TX=1.808343
      CALL  FCT(I,J,TX,TGR,TGI)
      TYR=TYR+.2180683  *     TGR
      TYI=TYI+.2180683    *   TGI
      TX=.7299545
      CALL  FCT(I,J,TX,TGR,TGI)
      TYR=TYR+.4011199    *   TGR
      TYI=TYI+.4011199    *   TGI
      TX=.1377935
      CALL  FCT(I,J,TX,TGR,TGI)
      TYR=TYR+.3084411    *   TGR
      TYI=TYI+.3084411    *   TGI
      RETURN
      END
```

```
      SUBROUTINE SING(IWHY)
   11 FORMAT (54HOMATRIX WITH 0 POW IN DECOMPOSE
   12 FORMAT (54HOSINGULAR MATRIX IN DECOMPOSE.  ZERO DIVIDE IN SOLVE )
   13 FORMAT (54HONO CONVERGENCE IN IMPROV. MATRIX IS NEARLY SINGULAR. )
      GO TO (1,2,3),IWHY
    1 WRITE (6,11)
      GO TO 10
    2 WRITE (6,12)
      GO TO 10
    3 WRITE (6,13)
   10 RETURN
      END
```

APPENDIX D

BASIS FOR MORE ACCURATE COMPARISON OF THEORETICAL AND EXPERIMENTAL RESULTS

With reference to Fig. 8, the voltage V(z) induced in the receiving loop is proportional to the tangential electric field, viz.,

$$V(z) = \int \dot{B}_z \, dS = -2\pi a E_\phi(a,z)$$

This relation, however, assumes that there is azimuthal symmetry and that the current in the receiving loop is negligible. These assumptions are investigated in detail.

Azimuthal Symmetry. The value of ak_0 for the eleven cases studied in the experiment ranges from .00133 to .01662, whereas $|ak_1|$ has values between .02 to about .41. It is well known that a loop in free space has nearly constant current if $ak_0 \leq .1$. If this criterion is applied, all of the eleven cases are rotationally symmetric. However, if $|ak_1| \leq .1$ is the criterion, rotational symmetry is clearly absent in some of the cases. Because of the unique location of the driving loop on the surface $\rho = a$, a simple analytical criterion on the radius is not possible to ensure rotational symmetry. For this reason, rotational symmetry was ensured experimentally.

As shown in Fig. D-1, a shielded loop of 3/16 in. diameter was fabricated and used to measure the voltage induced by the radial magnetic field as a function of azimuthal coordinate for eight of the eleven cases. The largest deviation from a constant value was found to be less than 5%. The three antennas not tested had lower values of $|ak_1|$ than those tested. The experimental measurements established rotational symmetry conclusively for all of the cases considered in the experimental study.

Measurements were then made of the total axial magnetic current on a

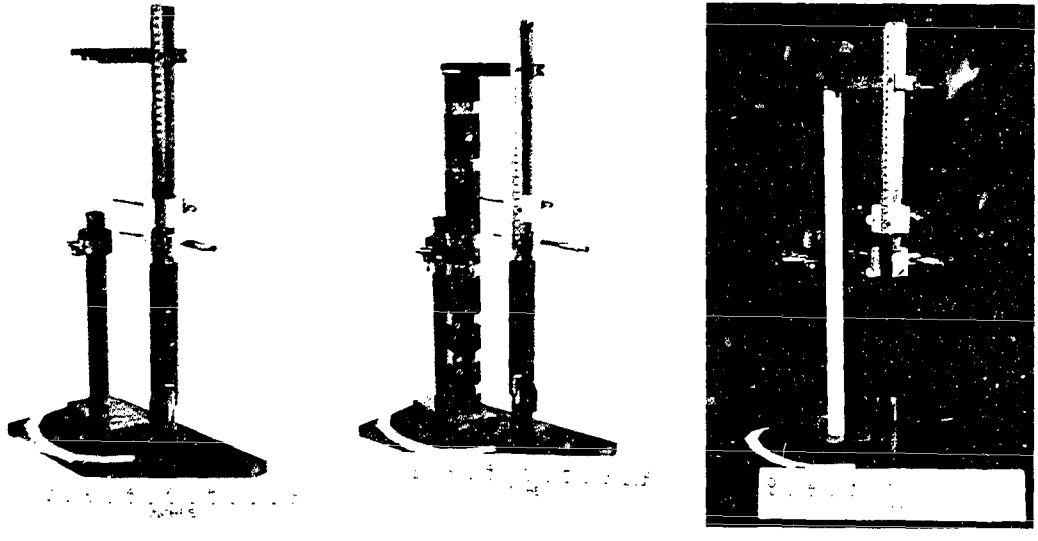

(a) (b) (c)

FIG D-1 PHOTOGRAPH SHOWING THE DRIVEN LOOP AND THE TWO RECEIVING LOOPS. c) AIR CORE b) LARGEST RADIUS FERRITE CORE c) TEFLON CORE.

dielectric rod made of Teflon, as shown in Fig. D-1(c). The experimental parameters are summarized below:

Diameter of the driven loop = 1.0^{+} inch

Diameter of the Teflon rod = 1.0 inch

Diameter of loop for axial measurements = 1.0 inch

Diameter of loop for radial measurements = 3/16 inch

Frequency = 20 MHz

The axial magnetic current distribution was measured with and without the Teflon rod present. The results are tabulated in Table D-1 and plotted in Fig. D-2. As one might expect, the dielectric rod ($\varepsilon_r \simeq 2.2$) has very little effect, and the measurements taken with it present do not differ significantly from those taken with it absent. In both cases, rotational symmetry was confirmed experimentally. The characteristics of the Teflon rod antenna are similar to those of the air-core antenna because the loop used in the experiment was small enough to act as a magnetic dipole.

Correction to Experimental Data. An answer was then sought to the important question, what is the voltage V(z) induced at the terminals of the receiving loop? The receiving loop is loaded by the vector voltmeter which has a nominal impedance of 100 K-ohms shunted by a 2.5 pf capacitor. The frequency in this experiment varies from 5 to 150 MHz so that the vector voltmeter impedance has a range of values. An analysis based on circuit theory can be carried out to determine accurately the voltage $V_R(z)$ measured by the vector voltmeter. A diagram of the two coupled circuits is in Fig. D-3. The various quantities shown in the figure are:

$Ve^{-i\omega t}$ = Oscillator voltage

TABLE D-1: Unnormalized experimental data of total axial magnetic current with an air core and also a teflon rod. (This data is plotted in Figure D-2).

Z cms	Air Core ak_o=.00532		Teflon, ε_r=2.2, ak_o=.00792	
	Mag	Phase	Mag	Phase
0.3	11.0	35	11.0	40
0.5	8.4	35	8.5	40
1.0	4.5	35	4.35	40
1.5	2.4	35	2.58	40.1
2.0	1.5	35	1.60	40.2
2.5	.98	35.4	1.02	40.3
3.0	.65	35.5	.695	40.4
3.5	.45	35.6	.500	40.6
4.0	.33	35.6	.365	40.7
4.5	.245	36	.265	40.7
5.0	.18	36	.205	40.7
5.5	.15	36	.155	40.7
6.0	.135	36.2	.130	40.8
6.5	.105	36.2	.10	41
7.0	.085	36	.083	41
7.5	.07	36	.067	41
8.0	.06	36	.056	41
8.5	.05	36	.048	41
9.0	.04	36	.041	41
10.0	.03	36	.03	41

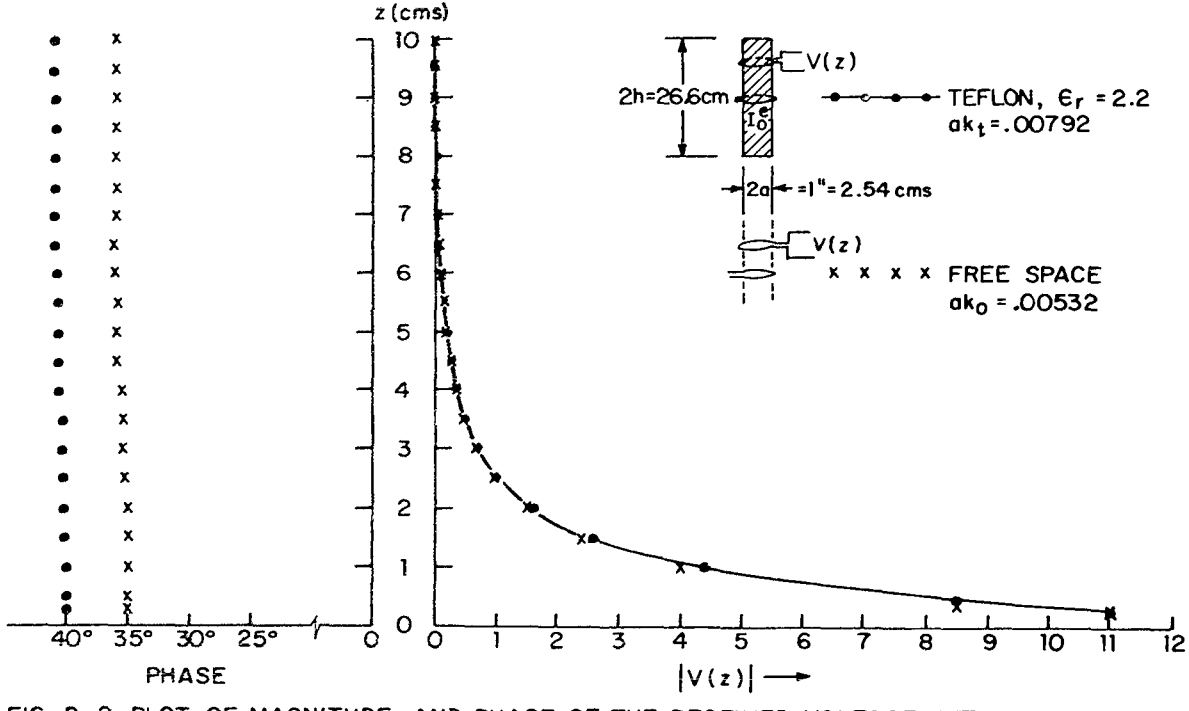

FIG. D-2 PLOT OF MAGNITUDE AND PHASE OF THE RECEIVED VOLTAGE WITH AND WITHOUT A DIELECTRIC ROD. (THE DATA IS IN TABLE D-1)

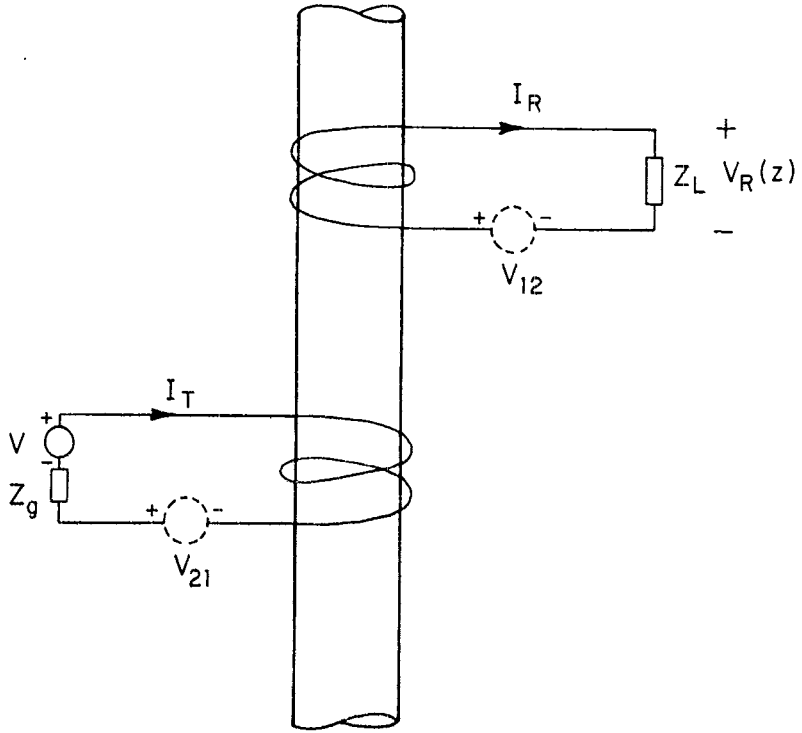

FIG. D-3 THE TWO COUPLED CIRCUITS

Z_g = Generator impedance

I_T = Current in the transmitting loop

$V_{21} = V_{12}$ = Fictitious generator due to coupling

I_R = Current in the receiving loop

Z_L = Vector voltmeter impedance

The two mesh equations can be written as

$$V = I_T(Z_s + Z_g) - I_R Z_M \tag{D-1}$$

$$0 = I_T(-Z_M) + I_R(Z_s + Z_L) \tag{D-2}$$

where Z_M is the mutual impedance, Z_s the self-impedance of the two loops. From (D-1),

$$I_T = (V + I_R Z_M)/(Z_s + Z_g)$$

Substituting this into (D-2) gives

$$0 = \frac{(V + I_R Z_M)(-Z_M)}{(Z_s + Z_g)} + I_R(Z_s + Z_L)$$

or

$$I_R = \frac{VZ_M}{(Z_s + Z_g)} \frac{1}{[(Z_s + Z_L) - Z_M^2/(Z_s + Z_g)]}$$

The measured voltage $V_R(z) = I_R Z_L$ in Fig. D-3 is, therefore,

$$V_R(z) = \frac{VZ_M Z_L}{(Z_s + Z_g)} \frac{1}{[(Z_s + Z_L) - Z_M^2/(Z_s + Z_g)]}$$

$$= \frac{VZ_M}{Z_s}\left(\frac{1}{1 + Z_g/Z_s}\right)\left(\frac{1}{1 + Z_s/Z_L}\right)\left[\frac{1}{1 - Z_M^2/(Z_s + Z_g)(Z_s + Z_L)}\right] \tag{D-3}$$

The theoretical computations from the integral equation account only for the mutual coupling and ignore the generator impedance Z_g, the loading of the receiver by the vector voltmeter impedance Z_L, and the change in the current in the transmitting loop due to the nearness of the receiving loop. The correction terms can be identified in (D-3) as follows:

$$V_R(z)\Big|_{\text{measured}} = V_R(z)\Big|_{\text{calculated}} \times C_1 \times C_2 \times C_3(z) \qquad \text{(D-4)}$$

where

C_1 = Correction due to generator impedance.

C_2 = Correction due to the loading of the vector voltmeter.

$C_3(z)$ = Correction due to secondary coupling (Lenz's Law).

It is observed that the correction terms C_1 and C_2 are independent of the separation between the two loops. Since the measured $V_R(z)$ is only relative in the present study, $C_3(z)$ is the only correction factor which is significant. It is [from the right-hand term in (D-3)]:

$$C_3(z) = \left[\frac{1}{1 - Z_M^2(z)/(Z_s + Z_g)(Z_s + Z_L)}\right] \qquad \text{(D-5)}$$

As a first approximation the generator impedance Z_g is set equal to zero. Z_L is the impedance of the vector voltmeter transferred to the gap in the receiving loop. The impedance of the vector voltmeter is composed of a 100 k-ohm resistor shunted by a 2.5 pf capacitance, viz.,

$$Z_{VVM} = R/(1 + j\omega CR)$$

with $R = 10^5$ ohms and $C = 2.5 \times 10^{-12}$ farads. Z_L can be calculated using

$$Z_L = R_c\left(\frac{Z_{VVM} + jR_c \tan \beta d}{R_c + jZ_{VVM} \tan \beta d}\right) \qquad \text{(D-6)}$$

where

R_c = 50 ohms = Characteristic impedance of the line

$\beta = \beta_0 \epsilon_{rt}^{1/2}$

ϵ_{rt} = Dielectric constant of Teflon FEP

d = Distance from the vector voltmeter output terminals to the gap in the receiving loop

An approximate value for $C_3(z)$ can now be computed using (D-5) with Z_g set equal to zero. However, Z_M - the mutual impedance between two loops that are in the near zone of one another - is still unknown. An excellent analysis of the mutual impedance of two loops in air is available [8]. In the present case, however, the mutual impedance is required when the ferrite is present. If the permeability μ_0 in King's analysis [8] is replaced by the permeability μ_1 of the ferrite, an approximate value for the mutual impedance is obtained, viz.,

$$Z_M(z) = (j\omega\mu_1 a^2/2)\{[4/(z^2 + 4a^2)^{1/2}][(2/\Lambda^2 - 1)K(\pi/2,\alpha) - (2/\Lambda^2)F(\pi/2,\alpha)] - j\pi a^2 k_1^3/3\} \qquad (D\text{-}7)$$

where

ω = Angular frequency; k_1 = Propagation Constant in the ferrite = $\omega\sqrt{\mu_1\epsilon_1}$

μ_1 = Permeability of the ferrite; ϵ_1 = Permittivity of the ferrite

a = Radius of the two loops

z = Distance separating the two loops

$\Lambda^2 = \sin^2\alpha = 4a^2/(z^2 + 4a^2)$

$K(\pi/2,\alpha) = \int_0^{\pi/2} \frac{d\psi}{(1 - \sin^2\alpha \sin^2\psi)^{1/2}}$ = Elliptic integral of the first kind

and

$$F(\pi/2,\alpha) = \int_0^{\pi/2} (1 - \sin^2 \alpha \sin^2 \psi)^{1/2} \, d\psi = \text{Elliptic integral of the second kind}$$

Fortran IV computer programs for computing the elliptic functions were available in the Scientific Subroutine Packa of IBM 360. Thus, the correction factor $C_3(z)$ was computed as a function of the separation distance z using equations (D-5), (D-6) and (D-7). This factor was then used to correct the experimental data for a comparison with the theoretical results. A typical comparison of the theory with corrected and uncorrected experimental data is shown in Fig. D-4 for the specific case of antenna #6. The uncorrected experimental data depart from the theoretical curve near the driving point, $0 \leq z/h \leq .25$. The vector voltmeter impedance Z_L at the gap for the antenna configuration under consideration (antenna #6) is $Z_L = 2.88 - j534.7$ ohms. The corrected experimental data obtained when this value of Z_L is used to compute the correction factor are plotted in Fig. D-4 and are seen to deviate less from the theory than the uncorrected values. The correction factor does not account for the entire discrepancy, however. This is in part because of the approximations made in computing the correction factor and in part because of the lack of an accurate value for Z_L. For this reason, the correction factor was also computed for a range of real and imaginary parts of Z_L. Two representative cases are shown in Fig. D-4. They illustrate that a precise knowledge of Z_L could improve the accuracy of the correction factor applied to the experimental data and, thus, minimize the discrepancy with theory near the driving point. Away from the driving point ($z/h \geq .25$) the agreement is seen to be very good.

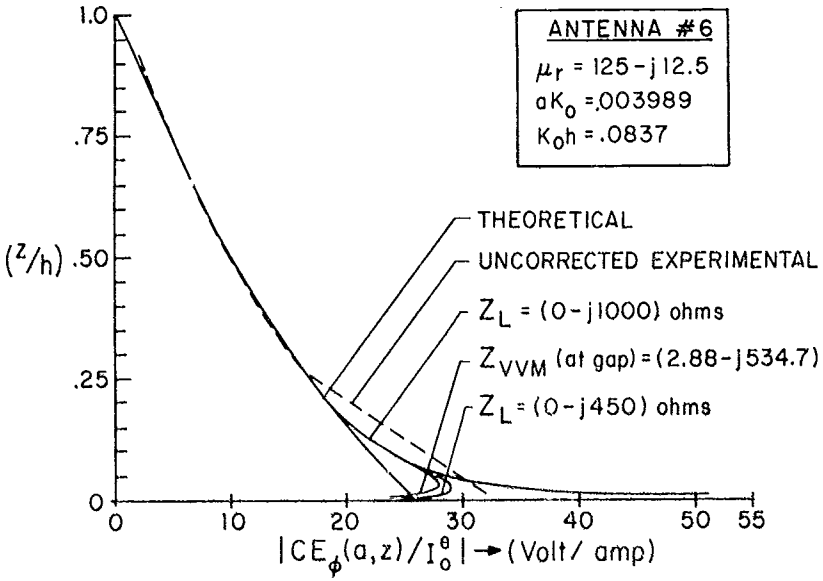

FIG. D-4 MAGNITUDE OF THE VOLTAGE RECEIVED BY THE MEASURING LOOP

ACKNOWLEDGMENT

The authors wish to thank Dr. G. S. Smith and Mr. Neal Whitman for their help in the design and construction of the experimental apparatus. Thanks are also due Dr. D. H. Preis for painstakingly reading the manuscript and Ms. Margaret Owens for her assistance in the preparation of this report.

REFERENCES

[1] R. W. P. King and C. W. Harrison, Jr., Antennas and Waves: A Modern Approach. Cambridge, Mass.: M.I.T. Press, 1969, pp. 143-149.

[2] D. V. Giri, "Electrically Small Loop Antenna Loaded by a Homogeneous and Isotropic Ferrite Cylinder - Part I," Technical Report No. 646, Division of Engineering and Applied Physics, Harvard University, Cambridge, Mass., July 1973.

[3] R. W. P. King and T. T. Wu, "The Imperfectly Conducting Cylindrical Transmitting Antenna," IEEE Trans. Antennas Propagat., vol. AP-14, No. 5, pp. 524-534, May 1966.

[4] R. W. P. King, C. W. Harrison, Jr., and E. A. Aronson, "The Imperfectly Conducting Cylindrical Transmitting Antenna; Numerical Results," IEEE Trans. Antennas Propagat., vol. AP-14, No. 5, pp. 535-542, May 1966.

[5] A. Sommerfeld, Electrodynamics. New York, N.Y.: Academic Press, 1966, pp. 177-185, 3rd Edition.

[6] G. E. Forsyth and C. B. Moler, Computer Solution of Linear Algebraic Systems. New York: Prentice-Hall, 1967.

[7] H. A. Dropkin, E. Metzger, and J. C. Cacheris, "VHF Ferrite Antenna Radiation Measurements," Diamond Ordnance Fuze Laboratories, Washington, D.C., Tech. Report No. TR-484, July 1957.

[8] R. W. P. King, Fundamental Electromagnetic Theory. New York: Dover Publications, 1963, Ch. VI, Secs. 13 and 14.

JSEP REPORTS DISTRIBUTION LIST

Director
National Security Agency
ATTN: Dr. [illegible]
Fort George G. Meade, MD 20755

Defense Documentation Center
ATTN: DDC-TCA [illegible]
Cameron Station
Alexandria, VA 22314

Asst. Dir.
Office of Director of Defense
Research and Engineering
The Pentagon
Washington, DC [illegible]

Defense Advanced Research
Projects Agency
ATTN: [illegible]
1400 Wilson Boulevard
Arlington VA [illegible]

Commandant
US Army Air Defense School
ATTN: [illegible]
Fort Bliss, TX [illegible]

Commander
US Army Armament R&D Command
ATTN: [illegible]
Dover, NJ [illegible]

Commander
US Army Ballistic Research Lab.
ATTN: [illegible]
Aberdeen Proving Ground
Aberdeen, MD [illegible]

HQDA [illegible]
Washington, DC 20310

Commander
US Army Electronics Command
Fort Monmouth, NJ 07703
ATTN: [illegible]

COL Robert [illegible]
Senior Standardization Representative
US Army Standardization Group, Canada
Canadian Force Headquarters
Ottawa, Ontario, Canada [illegible]

Director
Night Vision Laboratory
ATTN: [illegible]
Fort Belvoir, VA [illegible]

Commander
Picatinny Arsenal
ATTN: [illegible]
Dover, NJ 07801

Mr. [illegible]
Technical Director
[illegible]
Frankford Arsenal
Philadelphia, PA 19137

Mr. [illegible] (ISCP)
Rome Air Development Center
Griffiss AFB, NY 13441

LTC [illegible]
Air Force Office of Scientific
Research
(AFSC) AFOSR/NP
Bolling Air Force Base, DC 20332

LTC [illegible]
Air Force Office of Scientific
Research
(AFSC) AFOSR/NM
Bolling Air Force Base, DC 20332

Dr. [illegible]
Naval Surface Weapons Center
Code [illegible]
White Oak
Silver Spring, MD 20910

Naval Weapons Center
ATTN: Code [illegible]
China Lake, CA 93555

Dr. [illegible]
Technical Director
Naval Undersea Center
San Diego, CA 92152

Naval Research Laboratory
4555 Overlook Avenue, SW
Washington, DC 20375
ATTN: Code [illegible]

Naval Undersea Center
ATTN: Technical Library
San Diego, CA 92152

Naval Underwater Systems Center
ATTN: Technical Library
Newport, RI 02840

Office of Naval Research
Electronic & Solid State Sciences
Program (Code [illegible])
800 North Quincy Street
Arlington, VA 22217

Office of Naval Research
Mathematics Program (Code [illegible])
800 North Quincy Street
Arlington, VA 22217

Office of Naval Research
Naval Systems Division
Code [illegible]
800 North Quincy Street
Arlington, VA 22217

Director
Office of Naval Research
New York Area Office
715 Broadway, 5th Floor
New York, NY 10003

Office of Naval Research
San Francisco Area Office
One Hallidie Plaza - Suite 601
San Francisco, CA 94102

Los Alamos Scientific Laboratory
ATTN: Reports Library
P.O. Box 1663
Los Alamos, NM 87544

Dr. [illegible]
Program Director
Solid-State Physics
Division of Materials Research
National Science Foundation
1800 G Street
Washington, DC 20550

Mr. [illegible]
National Aeronautics and Space
Administration
Washington, DC 20546

[illegible]
Deputy Director, Institute for
Computer Sciences and Technology
National Bureau of Standards
Washington, DC [illegible]

Director
Columbia Radiation Laboratory
Columbia University
538 West 120th Street
New York, NY 10027

Director
Coordinated Science Laboratory
University of Illinois
Urbana, IL 61801

Director of Laboratories
Division of Applied Sciences
Harvard University
Pierce Hall
Cambridge, MA 02138

[illegible]